MULTIAREA SYSTEM RELIABILITY: THE ECONOMIC EVALUATION OF
SYSTEM SECURITY CRITERIA

BY

TEOMAN GULER

B.S., Bogazici University, 1999
M.S., Rensselaer Polytechnic Institute, 2001

DISSERTATION

Submitted in partial fulfillment of the requirements
for the degree of Doctor of Philosophy in Electrical and Computer Engineering
in the Graduate College of the
University of Illinois at Urbana-Champaign, 2009

Urbana, Illinois

Doctoral Committee:

      Professor George Gross
      Professor Peter W. Sauer
      Professor Thomas J. Overbye
      Professor M. A. Pai
      Associate Professor George Deltas
      Assistant Professor Uday V. Shanbhag
      Dr. Eugene Litvinov, ISO New England Inc

ABSTRACT

In this dissertation, we construct models and develop tools for security assessment studies and the quantification of the economics of secure power system operations in the restructured electricity industry. We illustrate the capabilities of the proposed tools with a set of applications on the large-scale ISO New England system. These studies serve to indicate the practical nature of the capabilities that the tools provide for dealing with a wide range of problems in the area of power system security and the economics of secure operations in the competitive market environment.

The advent of competitive electricity markets has resulted in the operation of the system very near its security limits over increasingly longer periods. A particular need for system security assessment studies is the rapid assessment of the impacts of multiple-line outages in the power grid so as to be able to effectively deal with the situations of cascading outages, including cases resulting in system separation into one or more islands. In this dissertation, we develop an analytic expression for the generalized line outage distribution factors (GLODFs) which we use to assess whether the post-outage flows violate any line flow limits under multiple-line outages. The GLODFs are particularly useful to analyze the complications arising from the multiple-line outages, such as detection of island formation. Our proposed approach to detect island formation combines the graph-theoretic connectivity characterization with the algebraic expressions for the GLODFs. The approach can be used to identify the subset of outaged lines that results in system separation. A particularly noteworthy aspect is the numerical efficiency of the approach due to its low computational requirements – a function simply of the

number of outaged lines and *not* of the size of the system. The approach's computational efficiency enables its effective application to the formulation of appropriate preventive/corrective control actions in multiple-line outage contingencies, particularly those that involve the *domino effect* of cascading outages.

The maintenance of secure system operations is a highly challenging task that became even more complex with the prominence of electricity markets. We use the insights we gained into the tight coupling between market and system operations under restructuring to characterize analytically the interrelationships between the secure power system operations and the performance of the electricity markets. Such a characterization allows the development of an integrated analysis approach to quantify the economics of secure power system operations. This approach permits the quantification of the market performance as a function of security criterion and provides, for the first time, the means to provide an economic justification for a modification the security criterion. Furthermore, the approach is useful for the cost/benefit analysis of network improvements to mitigate the market performance impacts of a set of contingencies and their associated security control actions. An important application is to the assessment of the impacts of specific behavioral changes in market participants on system security. The generalization of the approach is made by its extension to quantitatively characterize the linkages between the real-time system operations and the day-ahead markets (DAMs) and their associated real-time markets (RTMs) for use in a multi-settlement environment. The extended approach provides the ability to explicitly show that the auction surplus attained in the multi-settlement system is equivalent to the sum of the auction surpluses attained in

each RTM. Therefore, the mere presence of the DAMs results in surplus transfers among market participants. Furthermore, the extended approach provides a very useful tool to analyze the nature of the DAM-RTM price deviations and the impacts of financial entities on near-real-time system security.

We illustrate the application of the proposed approaches on the large-scale ISO New England system in a number of studies. The results provide useful insights into the multi-faceted nature of issues that arise in the today's tightly coupled market and system operations. In fact, the studies on the economics of the system security provide important insights into the role of price-responsive demand and that of specific selected security control actions measured by the economic efficiency of the electricity markets. A key result is that this efficiency need not decrease when a power system is operated under a stricter criterion, as long as there is effective price-responsive demand and appropriate utilization of the corrective control capabilities of the resources. Furthermore, the ISO New England application study in the multi-settlement environment indicates that financial entity participation not only results in reduced DAM-RTM price deviations but also leads to DAM dispatch results that are "closer" to those of their associated RTMs. Therefore, financial player participation improves the ability of the system operator to ensure system security.

The GLODF-based models for security assessment and the quantification approaches for the economics of secure power system operations provide practical tools for the study of system security and the economic quantification of security. They constitute significant contributions to the state of the art in the power system security domain.

To My Love, Ozlem

ACKNOWLEDGMENTS

I would like to thank my advisor, Professor George Gross, for the guidance and support he provided throughout my doctoral studies. His kind consideration and patient help in both my work and my life are greatly appreciated. This work would not be possible without his endless help.

I also want to thank all the professors, students and staff in the power group for their encouragement, advice and friendship. I would like to acknowledge Professor Pete Sauer and Professor Tom Overbye for their inspiring lectures on various aspects of power systems courses that I had the opportunity to take. I also would like to thank Pablo Ruiz and Zeb Tate for their continuous support and friendship. I would like to use this opportunity to thank Dr. Eugene Litvinov and Ron Coutu for their invaluable insights and incomparable help during my internships at the ISO New England. Their contributions to this work are greatly appreciated.

This list would be incomplete without appreciating my family, especially my wife. Her unconditional love and support throughout my doctoral studies is the source of my inspiration and strength to accomplish this work.

TABLE OF CONTENTS

LIST OF FIGURES

LIST OF TABLES

CHAPTER 1

INTRODUCTION

In this chapter, we describe the nature of the problems considered in this dissertation, review the relevant literature and discuss the scope and the key contributions of the dissertation. We provide the nature of the the problems discussed in this dissertation in Section 1.1. Our lterature survey in Section 1.2 reviews the state of the art and the progress to date on the solution of these problems. We discuss in Section 1.3 the scope of the dissertation and highlight the key contributions. We end in Section 1.4 with an outline of the chapter-by-chapter contents of this dissertation.

1.1 The Nature of the Problems Discussed in This Dissertation

The advent of competitive electricity markets brings about a key need to thoroughly understand the nature of the interactions between the market environment and the way we operate the power system. Specifically, we need to quantify the impacts of market operations on the ability of the system to continue operating without interrupting the supply of electricity to the consumers as well as the impacts of system operations on market performance. Such assessments allow us to quantify the economics of power system operations and to make the appropriate decision-making trade-offs between market and system performance. In this section, we discuss such needs in a comprehensive manner and lay out the motivation of this dissertation.

Since 1996 the US electricity industry has undergone a profound restructuring that is still continuing to this day. The vast array of changes was begun by the advent of

competitive markets in electricity and was accompanied by regulatory initiatives spearheaded by the watershed Federal Energy Regulatory Commission's (FERC) Order Nos. 888/889, 2000 and subsequent decisions. The restructuring has resulted in the creation of fertile grounds for innovation, not seen by the industry in many decades, in the entry of many new players and in the implementation of changes in nearly every sector of the industry, including the planning, operations and investment domains. The increasingly competitive environment in electricity has changed both the nature and scope of system operations and planning, led to more decentralized decision making, resulted in increased number of transactions and growth in the volume of trades, and established new centralized entities, such as the Independent System Operators (ISOs) and the Regional Transmission Organizations (RTOs) in North America. A number of troubling warning signs have appeared in the current implementation of the designs in use in various jurisdictions, bringing into focus specific issues that must be addressed in order to bring about FERC's vision of "vibrant competitive markets" [1].

Secure system operations is a highly challenging task that became even more complex with the prominence of electricity markets [1], [2]. The advent of the competitive environment in which today's power system operations take place results in highly *stressed* networks due to the utilization of the transmission system in a manner very different than that for which it was planned, the frequent changes in the nature and the points of origin/destination of the various transactions, and the growing frequency of system congestion situations. The increased system congestion combined with the fact

that power systems are continually subject to various disturbances[1] necessitates the extensive use of effective control actions to ensure secure power system operations. In fact, the recent experience of the August 2003 mega-blackout reinforces the need to develop security assessment tools and schemes for the formulation and the deployment of appropriate security control actions that can effectively deal with the cases that involve the *domino effect* of cascading outages. However, in the market environment, the deployment of security actions has economic consequences that also need to be evaluated so as to allow ISOs/RTOs to make decisions that fully take into account the economics of system security.

Under the ideal conditions in a transmission-unconstrained electricity market, each market participant is able to consummate its desired transaction(s). Taking into account the system operational constraints, be they of a physical, an engineering or a policy nature, the system operators must deploy security control actions to ensure that the dispatch of the desired transactions does not violate the imposed constraints. In some cases, one or more transactions unwilling or unable to pay sufficiently high congestion charges may need to be partially or fully curtailed. Such curtailments may, consequently, adversely impact the economics of electricity markets. The evaluation of such impacts resulting from the deployment of security control actions must take into account the *willingness of* the sellers (buyers) to sell (pay for) the MWh commodity.

In the restructured environment, the independent entity in charge of system operations – be it an ISO or an RTO – must ensure secure power system operations using market-

---

[1] These disturbances include sudden changes in the loads and the outages of one or more components, such as lines, transformers and generating units. In security assessment studies, we refer to such disturbances as *contingencies*. System operators dispatch security control actions to ensure that, in case such contingencies occur, the power system can be operated without violating any operational and engineering constraints imposed on system operations [3].

based schemes. We refer to this independent entity by the generic name of *independent grid operator* or IGO in this dissertation. While there are different market design implementations in the various jurisdictions around the world, we concentrate on the typical market structure widely adopted in North American markets based on the design that the same MWh commodity is traded in a sequence of markets run at different lead times – such as the day-ahead markets (DAMs) and their associated real-time markets (RTMs) – using the uniform price auction mechanism coexisting side-by-side with bilateral transactions [1], [2]. For a given snapshot of the power system, the IGO collects the information on the willingness of each seller and buyer to sell and pay for the MWh commodity, respectively, as well as the transmission service requests for the bilateral transactions. The IGO then clears the market by solving a security-constrained optimization problem with the objective to maximize the so-called auction surplus [4], [5]. In a highly competitive market environment and a uniform price auction mechanism, the market participants tend to reveal their true marginal costs and benefits [6]. Under such conditions, the auction surplus becomes a good proxy for the social welfare and, therefore, an appropriate approximation of the economic efficiency of the markets [6]. The market clearing provides the MWh quantities and the prices at each node. The corresponding dispatch results ensure secure system operations [7]. It is evident from the formulation and the solution of this problem that the system operations impact market outcomes and that market operations influenced by the participants' behaviors impact system security. Therefore, the tight coupling between system and market operations is a key consideration in the evaluation of the economics of secure power system operations.

The interactions between system and market operations are further complicated by the

4

design and implementation of electricity markets resulting in two or more interrelated markets that trade the same MWh commodity that is physically produced and consumed only in real time. Such a design is commonly referred to as a multi-settlement system to underline the fact that there are multiple markets, at different points in time, for the same commodity and that may result in distinct prices [8], [9]. These prices reflect the system and market conditions under which the electricity commodity is cleared by each market. In fact, the security management task is further complicated in the multi-settlement environment since not every player has physical resources or loads and the markets are strongly interrelated over time.

In the restructured environment, the improvement of system security as well as that of the economic efficiency of electricity markets has been the focus of recent policy initiatives [1], [2]. Central to these efforts is the need to improve the characterization of the tight coupling between market and system operations. In particular, we need to go beyond the qualitative description and to quantify the coupling in economic terms. In this way, we can evaluate the economics of secure power system operations. Such quantification enables us to appropriately *value* the trade-offs between system security and market performance: in particular, we can determine what economic impacts arise due to a specified level of security.

The research on the quantification of the economics of secure power system operations is still in the very early stages. The growing awareness of the important role that system security plays in competitive electricity markets requires a better understanding of the problem and the development of an analytic approach for its

evaluation. The analytic approach requires the development of models that appropriately represent secure power system operations and the characterization of all relevant aspects of the commodity markets. Such an approach provides a practical tool for the quantification of the economics of secure power system operations and has numerous practical applications. These are the type of topics that we explicitly consider in this dissertation. But before we discuss them in more detail, we first review the state of the art in the area.

1.2 Review of the State of the Art

We briefly review the literature on system security and the economics of maintaining it in a market environment. We start out with a review of system security assessment and the appropriate tools under competition. We discuss the economics of power system security in a multi-settlement market environment and evaluate the state of the art in the field.

Power system reliability is evaluated in terms of the adequacy and the security of the power network [10], [11]. Adequacy is the ability of the electric system to supply the aggregate electrical demand and energy requirements of all the end-use customers at all times, taking into account scheduled and reasonably expected unscheduled outages of system elements [12] - [14]. Security, on the other hand, is the ability of the system to withstand unexpected disturbances and continue operating without interruption of supply to meet the customers' demand [12] - [14]. Security is an instantaneous and so a time-dependent phenomenon and is a function of the robustness of the system with respect to imminent disturbances – the so-called contingencies. A pragmatic definition of the

system security is the ability of the interconnected system to provide electricity supply to all the customers with the appropriate quality under both the normal and the contingency conditions [3]. The IGO must maintain and ensure the security of the multiarea system on its geographic footprint by effectively balancing the interconnected areas' generation and demand while maintaining the frequency of the system within acceptable bounds, the voltages within the required ranges and the operation of each component within its appropriate rating under both the base case and the contingency case conditions for each postulated contingency in the list of specified contingencies. Security assessment is carried out for the operating state at the specified time, i.e., the state of the snapshot of the system at that time. For a given time t, security assessment analyzes whether the occurrence of a postulated contingency results in the violation of any operational constraints, and the ability of the system to remove or "attenuate" such violations by dispatching appropriate preventive and/or corrective security control actions [3]. A preventive control action associated with a postulated contingency entails the modification of the precontingency, i.e., the base case state, so as to eliminate any potential violation, were that contingency to occur. On the other hand, an associated corrective control action involves the deployment of generation redispatch/load curtailment to modify the postcontingency state only *after* the contingency actually occurs. For certain contingencies, such as a generator outage or a sudden change in load, the IGO can use only corrective control actions.

Security assessments are, typically, based on some deterministic criterion, such as ($n -$ 1) or ($n - 2$) security. We associate with each security criterion a specific contingency list and a specified control action for every contingency on that list. For example, the

contingency list of the ($n-1$) criterion consists of all the single element contingencies while that of the ($n-2$) criterion considers all the double element contingencies in addition to the single element contingencies. Since all the contingencies on the ($n-1$) list are also included in the ($n-2$) contingency list, the ($n-2$) is considered to be a *stricter* criterion. Virtually every system operator uses, at the very least, some modified ($n-1$) list of single line outages and associated preventive control actions to deal with their impacts. But, in many instances, a stricter criterion is imposed, such as a modified version of the ($n-2$) criterion with only a subset of all the double element contingencies considered on the list of specified contingencies. The elements of this subset are carefully selected to include contingencies that are particularly critical for the multiarea structure of the system, such as the outages of pairs of tie lines interconnecting an export and an import area. In this dissertation, we consider a broad range of security criteria, which are representative of the practices of some actual IGOs.

The advent of competitive electricity markets has resulted in the operation of the system very near its security limits over increasingly longer periods. Thus, the need for rapid methods to assess security is evident [16], [17]. The need is particularly acute given the large number of contingency cases that are considered even in moderate size systems. A key issue in security analysis and control is the appropriate representation of the operational limits in the network under each postulated contingency. The power flow equations used to model the steady state behavior of the power system are nonlinear and their solution represents a computationally demanding task, especially for large-scale power systems [18] - [20]. Security assessment is performed around the clock and so the computing burden is simply too large in the market environment. For market

applications, such detailed modeling and extensive computing may be unnecessary and impractical. Rather, models based on the linearization of the AC power flow representation, i.e., those under DC power flow assumptions, are typically used [21].

A widely used analytic tool in the analysis of power networks in system security studies is the family of distribution factors. A distribution factor is a linear approximation of the sensitivity of various system variables with respect to a change in nodal injection and withdrawal [21] - [23]. The computation and the deployment of different types of distribution factors have been explored in a wide range of applications [22] - [30].

The basic distribution factors are typically developed under the DC power flow assumptions and are used in studies in which the real power flows are considered. The impacts of the reactive power flows are, therefore, ignored. To overcome these limitations, distribution factors providing the sensitivity-based relationships of the reactive power flows and the nodal voltage magnitudes to the net nodal injections and withdrawals are proposed [23]. In an alternative approach, the nodal voltage magnitude and reactive power limits are "converted" into real power line flow limits imposed on the corresponding lines and interfaces [30]. By exploring the relationship between the real and the complex power flows in a transmission line, yet another study provided a scheme to "translate" the thermal limit of a transmission line into the corresponding real power line flow limit for use in the available transfer capability evaluation [31]. These modified factors enable the inclusion of the impacts of reactive power flows in the representation of the power system.

Distribution factors play a key role in many system security analysis and market

applications. The well-known injection shift factors (ISFs) [26] serve as the basic building blocks for the evaluation of the other distribution factors. For example, the impact of a line outage on the postoutage flow on another line may be evaluated by the line outage distribution factors (LODFs) which may be computed using the ISFs. While the line outage distribution factors (LODFs) are conceptually well understood [18], their evaluation under multiple line outages has received little attention.

Under certain conditions, a particular complication of the multiple line outages may result in the formation of islands, a fact that leads to complications in power network computations. These complications prevent the use of the tools based on distribution factors in their standard form. Rather, their application to the connected subnetworks that result is possible in these cases. Indeed, the detection of island formation in power networks is a prerequisite for the study of security analysis and control. Power systems are continuously subject to various disturbances such as changes in the loads and in the availability of system components. The detection/identification of island formation provides the information needed to be able to deal effectively with the computational complications that arise. These complications all stem from the singularity of the Jacobian matrix in the Newton power flow [32] - [34] due to system separation into disconnected subnetworks. Under such conditions, the solution of power flow equations for each subnetwork is required. Moreover, separation into two or more islands requires the deployment of different control strategies to ensure system security. For off-line steady-state security analysis studies, involving the study of numerous *what if* cases, the line outages that lead to island formation are regarded as "most problematic" [35] - [37]. Therefore, situations with multiple line outages may require extensive corrective control

efforts, ranging from redispatch to load shedding – a last resort.

For both real-time, as well as off-line applications, the rapid detection of island formation and the identification of the causal factors are required to deal with the complications cited above. In cases with several lines outaged and no island formation, additional network analysis is needed to identify which additional line outage(s) result in system separation into two or more islands. There exist various methods to detect island formation [32], [38] - [44]. We may classify these methods into three major categories – linked list approaches, numerical techniques and graph theoretic schemes. The pioneering works on real-time island detection are based on the use of linked list tables [38], [39]. Several numerical schemes to determine system connectivity use the node-to-node connectivity matrix with different exponent values [40], LU decomposition for detecting Jacobian singularity [32], and eigen-system evaluation of the nodal susceptance matrix [41]. The graph theoretic schemes include breadth-first search [42], [43] and path finding approaches [44]. The *generic* graph theoretic approaches such as the node fusion [45] and two-stage processes [46], may also be used to study the connectivity in power system networks. The underlying notion in the graph theoretic approaches is the determination of paths between node pairs in the system. These topological approaches use the in/out status of each line to determine the system connectivity. When multiple line outages are involved, the topological approaches may not be the most appropriate tools because any change in the topology requires a repeat of the application of the topological algorithm for the modified network. The analysis of a cascading situation requires the repeated application of the topology-based scheme to each outage condition in the sequence; therefore, the consideration of a sequence of outages without utilizing the information on

any subset of the outages requires the repeated application of the topology-based scheme resulting in a task that is computationally burdensome, particularly for large-scale systems. While computational considerations are critical in on-line studies, the numerous off-line studies of an extensive list of *what if* cases may also be unfavorably impacted by the heavy computational requirements.

In the competitive market environment, the improvement of system security together with the economic efficiency of electricity markets has become the focus of recent efforts [1], [2]. Central to these efforts is the better understanding of the nature of the tight coupling between market and system operations. An important aspect of this coupling is the dependence of the market outcomes on the way the system is operated. As system and market operations strongly interact, any change in the system security impacts the economics and vice-versa. While the nature of these interactions is well understood on a qualitative basis, the quantification of the economics of secure power system operations is typically not performed. We next review the literature on the economic aspects of secure power system operations.

A commonly used metric to assess the performance of electricity markets is the economic efficiency of the electricity market as measured by the social welfare [3], [7]. The social welfare is defined as the total consumption benefits of the demands minus the total production costs of the suppliers [47]. Various allocation schemes have been proposed to distribute the social welfare among the market participants and to price the scarce and severely constrained transmission transfer capabilities in the network [48] - [59]. In some schemes, the electricity trading and transmission service scheduling are

treated as independent tasks that are performed sequentially [60], [61]. First, electricity trading is assessed in terms of transactions between the selling and buying entities with each system operational constraint ignored. The solution provides the so-called preferred schedule. Next, these preferred schedules are submitted to the IGO to assess the capability of the system to provide the required transmission services. When the transmission network is unable to accommodate all these preferred schedules taking into account the base and the contingency case conditions, the IGO dispatches control actions to ensure system security. As such, some of the preferred transactions become modified.

The NERC transmission loading relief (TLR) scheme used in the Eastern Interconnection is a purely reliability-centered procedure performed by the so-called security coordinators. Under the TLR scheme, each transaction is assigned a priority for transmission service and curtailment as a function of its *firmness*. A non-firm transaction is curtailed ahead of any firm transactions. Each transaction is curtailed by an amount proportional to its contribution to the flow on the overloaded line(s). The TLR scheme completely ignores the economic aspects of transactions since, in effect, each curtailed MW is treated as equal to any other curtailed MW [62]. Note that, unlike the market-based schemes under which transactions may override curtailments by submitting a higher willingness-to-pay for congestion, no economic considerations are taken into account in the TLR scheme. Consequently, the transmission schedules resulting from this command and control scheme need not be efficient in an economic sense [62], [63].

An alternative approach that explicitly incorporates market economics is the market clearing that simultaneously determines the energy market outcomes and the allocation of

transmission services. This approach essentially integrates secure power system operations with the clearing of the IGO-operated market [3], [9], [64] - [66]. The bilateral transactions request the desired transmission services from the IGO, and these requests are considered side-by-side with the willingness-to-buy bids of the buyers and the willingness-to-sell offers of the sellers. The market outcomes are determined as the optimal solution of a security constrained optimal power flow (SCOPF) problem formulation [33], [36] with the objective to maximize the auction surplus while ensuring that secure power system operations comply with the specific security criterion. We note that the auction surplus equals the social welfare for the case that market participants submit their true marginal costs and benefits. A by-product of the SCOPF solution is the locational marginal price, or LMP, at each network node computed as the dual variable of the nodal real power balance equation at that node. The LMPs play a very important role in the assessment of the market outcomes. Each seller (buyer) at a given node is paid (pays) the LMP at that node for every MWh of electricity sold to (bought from) the IGO. Each bilateral transaction pays the congestion charges to the IGO equal to the product of the transaction amount and the LMP difference between the delivery and receipt nodes of the transaction. In the absence of congestion, the LMP at each node in a lossless network has the identical value. However, in the presence of congestion, the LMP differences are nonzero and, consequently, there are congestion charges collected by the IGO for transmission usage. In addition, the LMP differences result in a nonnegative IGO surplus contribution – the so-called congestion rents [50] – which are computed as the difference between the payments made by the buyers and the revenues paid to the sellers.

The LMP-based approach was implemented by PJM [67], [68] and its success

prompted FERC to cast the LMP-based market as a fundamental aspect of its vision for standard market design [1]. In a highly competitive, LMP-based market environment, the market participants tend to reveal their true marginal costs and benefits. Under such conditions, the auction surplus becomes a good proxy for the social welfare and, therefore, an appropriate approximation of the economic efficiency of the markets. Therefore, an attractive feature of the LMP-based scheme is the ability to attain high economic efficiency in electricity markets by explicitly maximizing the auction surplus with system security taken into account explicitly.

The economic performance of electricity markets with constrained system operations explicitly taken into account may be analyzed in various contexts by empirical and analytical methods. The empirical studies focus on the adverse impacts of market participants' behavior on the outcome of the markets [69] - [72]. The analytical studies, on the other hand, focus on the impacts of constrained system operations on markets to determine the unavoidable losses in market efficiency [73], [74]. A number of papers analyze the interactions between the system security criterion and the associated economics. These papers may be classified into two distinct categories – the marginal costing aspects of system security and the evaluation of total system security costs. The studies in [75] - [79] explore the notion of the security pricing using marginal cost information for a specified period using snapshots of the system, with each snapshot representing the system over a subperiod of the specified period. The willingness of the market participants to provide security control capability for each postulated contingency is explicitly incorporated into the market clearing process in the optimization process. A by-product is the evaluation of the so-called security prices. Another approach defines

system security for a given base case as a function of overloads in each line under each postulated contingency case [80]. A decrease in overloads in response to injections at a node is regarded as an improvement in security, and marginal cost of security is defined in terms of the incremental cost of improving security. The total system security costs papers [81] - [83] evaluate system security costs using probabilistic techniques, taking explicitly into account the random nature of the outages. These papers may be viewed as applying the notion of "value of reliability" [84] to study the system security over the period of interest. A particularly useful application is to operational planning with a horizon typically in the range of one or two years [85]. The study in [81] evaluates the "expected cost of security" by computing the outage costs associated with specific operating states with the explicit representation of the security control actions. The study in [82] uses Monte Carlo simulation for a given system snapshot to evaluate the "value of system security" and is extended to a longer period in [83] making use of the corrective control capabilities in the demand side. The two Monte Carlo studies conclude that the security criterion to use may be set on the basis of cost/benefit analysis taking into account the costs of operating the system and the expected outage costs.

The studies [69] - [83] analyze a single aspect of the problem by focusing on either the economic efficiency of the markets or the system security costs. Therefore, they fail to provide an integrated analysis approach to quantify the interdependence between the market performance and the way the power systems are operated to ensure security.

Competitive electricity markets in the U.S. share some salient market design features with those in other jurisdictions. Typically, electricity markets are held at different points

in time ranging from a year- and a month-ahead – the so-called forward markets – to a day- and hour-ahead – the so-called spot markets – and to a five-minutes-ahead – the so-called real-time markets [86], [87]. Each market, be it an hourly day-ahead market (DAM) or one of the real-time markets (RTMs) associated with that hour, trades the identical MWh commodity at prices that may differ, reflecting the information on the system and market conditions available at the time the MWh commodity is cleared [8]. As these conditions are subject to continual changes in real time, RTMs are cleared at a higher frequency, typically every 5 minutes, than the hourly DAMs, which are cleared once a day. The 24 DAMs' outcomes reflect the lower resolution with which the imperfect information on the real-time conditions in the next day is known. Although the DAMs are financial markets in contrast to the purely physical RTMs, both markets are cleared using the same SCOPF tool. A salient difference between these markets is the nature of the participants. While financial entities may participate[2] in the DAMs, only players with physical resources or loads are permitted to participate in the RTMs. In addition, while the demand may be price-responsive in the DAMs, it is typically, fixed in the RTMs. Such a market design with different lead times and clearing frequencies is commonly referred to as a *multi-settlement system* [8], [9], [52], [86].

The economic benefits of multi-settlement systems are analyzed in several studies. The duopoly model in a simple two-node network shows that for low probabilities of congestion, multi-settlement systems enhance the social welfare when compared to single-settlement market designs [87]. In a subsequent study, the social-welfare enhancing role of a multi-settlement system is found to be highly sensitive to the

---

[2] Financial entity participation is enabled through the so-called "virtual bidding" in the DAMs [8]. Often, the terms *financial entity participation* and *virtual bidding* are used interchangeably in the literature.

presence of real-time congestion [88]. The findings of the empirical analysis of the PJM and NY-ISO market data provide added emphasis to this social welfare [89].

In a multi-settlement system, the hour *h* DAM clearing uses the available information and forecasts for the next day to provide the market outcomes and associated system states for the real-time conditions for that hour. In a way, these forecasts provide *ex-ante* real-time price discovery for the secure power system operations in hour *h* of the next day. The role of the DAMs in providing incentives for accurate real-time market forecasts and in facilitating trades through *ex-ante* price discovery is discussed in [86]. In case the DAM clearing *fails* to appropriately forecast real-time conditions, system security may be adversely impacted. Under these conditions, the IGO may need to undertake *excessive* real-time security control actions. Therefore, the ability to ensure real-time system security is greatly dependent on by how well the DAMs forecast the real-time system conditions for the next day.

As financial entities may participate in the DAMs, their presence impacts the ability to forecast the actual real-time conditions for the hours of the next day. Much of the analysis of the role of financial entities has a focus on the economic impacts of these entities [89] - [92]. These studies show specifically that the financial entity participation results in DAM-RTM price convergence and, therefore, the DAMs provide improved *ex-ante* price discovery over that in the case of no financial entities. As a concrete example, the ISO-NE study [91] concludes that the introduction of financial entity participation in the DAMs led to the convergence of the DAM and the RTM prices. Convergence implies an improvement in market efficiency as temporal arbitrage opportunities diminish [92].

Moreover, financial entity participation not only leads to price convergence, but results in lower average price of electricity. Indeed, multi-settlement systems provide appropriate price signals to financial entities to undertake profitable transactions that may lead to price convergence [93]. The discussion of the impacts of the behavior of the financial entities driven by such price signals on the real-time system security is absent in the literature.

We next describe the motivation for and the scope of the work undertaken, and the key contributions that this dissertation makes.

1.3 Scope and Contributions of This Dissertation

The identification of the issues requiring further attention serves to provide the motivation for the work presented in this dissertation. Our review in Section 1.2 pinpoints the specific needs in better understanding and quantifying of the tight coupling between system and market operations. A particular need for system security assessment studies is the rapid assessment of the impacts of multiple line outages on the power system, in order to cope with cascading outages as well as system separation into one or more islands. Given the usefulness of LODFs in the study of security when multiple line outages – as in the case of cascading outages occurring in blackouts – are considered, there is a need for analytic, closed-form expressions for and the computationally efficient evaluation of, LODFs under multiple line outages. Under such multiple line outage conditions, an additional need is the rapid identification of island formation in a computationally efficient way in which we can make effective use of the connectivity information of the set of outaged lines.

In the field of the economics of secure power system operations, an important need is an integrated analysis approach to quantify the interdependence between the market performance and the way the power systems are operated to ensure security that appropriately reflects the actual IGO operations. Furthermore, such a need has to take into account the multi-settlement environment. Specifically, there is a clear need to analyze whether the behavior of financial entities driven by price signals can impact, in some measurable way, system security. We address these and other related issues in the analysis and economics of power system security in the competitive environment by proposing a set of appropriate approaches and tools that are effective for the analysis and quantification of a wide range of issues for large-scale networks that we encounter in actual power systems. We illustrate a number of representative applications on the large-scale ISO-NE system and discuss the insights we obtain from our studies. We next describe the specific contributions of this dissertation.

We address the need in security applications for the rapid assessment of multiple line outage impacts by developing the *generalized* LODF (GLODF) to evaluate the impacts of multiple line outages on the postoutage network flows. A salient characteristic of the GLODF is its closed-form analytic expression in terms of the preoutage network parameters of the outaged lines. In this way, the GLODF avoids the need to determine the postoutage network state, and, thus, significantly reduces the computational efforts required in security analysis for cascading outages. In fact, the low computing requirement makes the GLODF an effective tool for the formulation of appropriate security control actions to prevent cascading outages.

The GLODFs are particularly useful to analyze the complications arising from the multiple line outages, such as detection of island formation. We develop the approach to detect island formation by combining the graph-theoretic connectivity characterization with the algebraic expressions for the GLODFs. The approach can be used to identify the subset of outaged lines that results in system separation. A noteworthy aspect of the approach is its computational efficiency due to its low computational requirements – a function simply of the number of outaged lines and not of the size of the system. The approach's computational efficiency enables its effective application to the formulation of appropriate preventive/corrective control actions in multiple line outage contingencies, particularly those that involve the *domino effect* of cascading outages. The development of the expressions for the GLODFs and the construction of the numerically efficient approach to detect island formation for security assessment studies constitute an important contribution of this dissertation.

The highly challenging task of security management becomes even more complex in the competitive market environment. We used the insights we developed into the tight coupling between market and system operations under restructuring to characterize analytically the interrelationships between the way the power systems are operated and the performance of the electricity markets. Such characterization led us to the development of a systematic approach that quantifies the market performance as a function of security criterion under diverse system and market conditions. This approach permits the quantification of the market performance impacts arising from a change from a given to another security criterion. The approach provides, for the first time, an economic justification for the IGO decision to modify the security criterion. Furthermore,

the approach can be used in the cost/benefit analysis of network improvements to mitigate the market performance impacts of a set of contingencies or their associated security control actions. Another application of the approach is to the assessment of the impacts of specific behavioral changes in market participants on system security. In fact, the large-scale ISO-NE application study provides important insights into the role of price-responsive demand and selected security control actions by demonstrating that the economic efficiency of the electricity markets need not decrease when a power system is operated under a stricter criterion, as long as there is effective price-responsive demand and appropriate utilization of the corrective control capabilities of the resources. Thus, the proposed approach allows the effective quantification of the system security impacts on the overall economics of electricity markets.

We extend this approach to quantitatively characterize the linkages between the real-time system operations and the DAMs and their associated RTMs for a multi-settlement environment, where electricity is traded in a sequence of markets that are cleared at different frequencies and with different lead times. We explicitly show with the extended approach that the auction surplus attained in the multi-settlement system is equivalent to the sum of the auction surpluses attained in each RTM. Therefore, the mere presence of the DAMs results in surplus transfers among market participants. Furthermore, the extended approach provides a very useful tool to analyze the nature of the DAM-RTM price deviations and the impacts of financial entities on real-time system security. Indeed, the ISO-NE application study indicates that financial entity participation not only results in reduced DAM-RTM price deviations but also leads to DAM dispatch results that are "closer" to those of their associated RTMs. Therefore, financial player participation

improves the ability of the IGO to ensure system security.

The GLODF-based models for security assessment and the quantification approaches for the economics of secure power system operations provide solid tools for the study of system security and the economic quantification of security. They constitute significant contributions to the state of the art in the power system security domain.

1.4 Dissertation Outline

This dissertation contains seven additional chapters. In Chapter 2, we review the basic models for the analysis of multiarea power system networks and their security management framework. We focus on the representation of the operational constraints, making extensive use of distribution factors. We present their extension to develop an analytic expression for the GLODFs, which we use to assess whether the postoutage flows violate any line flow limits under multiple line and cascading outages. We make use of the GLODF-based models of this chapter in the analysis of system security in the subsequent chapters.

We review in Chapter 3 some key graph-theoretic notions to describe the connectivity of power system networks. We use these notions together with the distribution factors to characterize the power system connectivity. We extend the characterization of system connectivity to the study of multiple line outages and to construct the island detection scheme by effectively deploying the GLODFs. We analyze the computational complexity of the proposed scheme and illustrate its application to the IEEE 118-bus system.

We provide a brief review of the basic structure of electricity markets for the MWh

commodity in Chapter 4 and present the decision making problem of the IGO for clearing the markets. For the latter, we introduce the market-snapshot problem formulation and solution. We discuss the metrics of interest for use in the quantification of the impacts of secure power system operations on the performance of electricity markets.

In Chapter 5, we use the market-snapshot formulation and present the quantification of the market performance as a function of security criterion for a single system snapshot using the set of economic and resource dispatch metrics. We focus on the DAMs in a given period and extend the snapshot assessment to cover that period and discuss various applications of the multiple snapshot approach.

We describe in Chapter 6 the nature of the multi-settlement problem and the market performance quantification for a DAM and its associated RTMs. We prove analytically that the auction surplus attained through a multi-settlement system equals the total auction surplus attained in the RTMs. We also extend the multiple snapshot approach developed in Chapter 5 to a multi-settlement system and quantify the impacts of financial entities on the near-real-time system security.

We present in Chapter 7 a set of applications of the proposed methodologies developed in this dissertation to various studies on the large-scale ISO-NE system and markets. These studies effectively illustrate the capabilities of the island detection scheme, and the multiple snapshot approach in a single- and in a multi-settlement environment. We discuss the results of these studies and provide important insights into the role of price-responsive demand and the financial entities.

In the final chapter, we provide concluding remarks together with a summary of the work presented and discuss directions for future research to extend the results in this dissertation.

The dissertation has two appendices. In Appendix A, we provide the proofs of the theorems stated in Chapter 3. In Appendix B, we provide the statement and the characterization of the optimal solution of the market-snapshot problem formulation discussed in Chapter 4.

CHAPTER 2

MULTIAREA POWER SYSTEM SECURITY ANALYSIS

In this chapter, we discuss the modeling aspects of the multiarea network and the nature of the operational constraints, including those that restrict the transfer capabilities between the constituent areas of the interconnection. We review the basic notions of, and the framework for, the management of system security in order to construct the appropriate model to represent the physical network. Our interest is in the explicit representation of the postulated contingencies for the study of the steady-state system security of the interconnected network. Our basic approach is based on the system snapshot analysis and we make extensive use of the distribution factors [21] - [26] to ensure computational tractability. These factors are linear approximations of the sensitivities of variables of interest with respect to changes in injections at specified nodes. We extend the formulation of line outage distribution factors to the general case of multiple line outages whose impacts are evaluated in security assessment. We develop what we call the *generalized line outage distribution factors* (GLODFs) that we deploy to assess system security under the specified contingencies including cascading outages. These GLODFs are essential building elements in the construction of the procedures to evaluate multiple line outage impacts on the interconnected power system. The GLODF results constitute an important contribution of this dissertation.

This chapter consists of four sections. In Sections 2.1 and 2.2, we review the basic models of the multiarea power system network and the security management framework, respectively. In Section 2.3, we focus on the representation of the operational constraints,

26

making extensive use of distribution factors. We present the development of the GLODFs and incorporate them into the security assessment framework. The GLODF-based models serve well in a wide range of security assessment applications. We summarize this chapter's results in Section 2.4.

2.1 Multiarea Power System Model

We consider a power system with $(N+1)$ buses and L lines. We denote by $\mathcal{N} \triangleq \{0,1,2,\cdots,N\}$ the set of buses, with the bus 0 being the slack bus, and by $\mathcal{L} \triangleq \{\ell_1, \ell_2, \cdots, \ell_L\}$ the set of transmission lines and transformers that connect the buses in the set $\mathcal{N}$. We associate with each line $\ell_r \in \mathcal{L}$ the *ordered* pair $\ell_r = (i_r, j_r)$, with the convention that the direction of the flow in line ℓ_r is *from* the node i_r to the node j_r.

The modeling of the large-scale interconnected system operated by the IGO requires the explicit representation of all areas that constitute the system, as well as the tie lines that interconnect them. We consider the power system network to consist of K interconnected areas and denoted by $\mathcal{A} = \{\mathcal{A}^k : k = 1, \cdots, K\}$ the set of K areas. Each area $\mathcal{A}^k$ has the node set $\mathcal{N}^k \in \mathcal{N}$ and the set of transmission lines $\mathcal{L}^k$, which has L^k elements. We assume that the system slack bus is in area $\mathcal{A}^1$. We define the ordered pair

$$c^{k,m} \triangleq \left(\mathcal{A}^k, \mathcal{A}^m \right)$$

to denote an interconnection between areas $\mathcal{A}^k$ and $\mathcal{A}^m$ with the convention that the

interconnection is defined to be from area $\mathcal{A}^k$ to area $\mathcal{A}^m$. For each $c^{k,m}$, we define a subset of transmission lines

$$\mathcal{L}^{k,m} \triangleq \left\{ \ell_r = (i_r, j_r) : i_r \in \mathcal{N}^k, j_r \in \mathcal{N}^m \right\}$$

constituting the tie lines interconnecting areas $\mathcal{A}^k$ and $\mathcal{A}^m$.

We denote the augmented branch-to-node incidence matrix of the system by

$$\underline{\tilde{A}} \triangleq \begin{bmatrix} \underline{A}^1 & \underline{0} & \underline{0} & \underline{0} \\ \underline{0} & \underline{A}^2 & \underline{0} & \underline{0} \\ \underline{0} & \underline{0} & \ddots & \underline{0} \\ \underline{0} & \underline{0} & \underline{0} & \underline{A}^K \\ & \underline{A}^C & \end{bmatrix}^T , \qquad (2.1)$$

where $\underline{A}^k$ is the branch-to-node incidence matrix of the area $\mathcal{A}^k \in \boldsymbol{\mathcal{A}}$ for all the intra-area transmission lines. By definition, $\underline{A}^k$ does not include any interconnection to other areas. $\underline{A}^C \in \mathbb{R}^{L_C \times N+1}$ is the branch-to-node incidence matrix of the interconnections between the areas. L_C denotes the total number of interconnecting lines between the areas.

Note that a column of $\underline{A}^1$ includes entries corresponding to the slack bus 0. As such, the algebraic sum of the columns of $\underline{\tilde{A}}$ vanishes:

$$\underline{\tilde{A}} \, \mathbf{1}^{N+1} = \underline{0} , \qquad (2.2)$$

where $\mathbf{1}^{N+1} = [1,1,\cdots,1]^T \in \mathbb{R}^{N+1}$. For each area $\mathcal{A}^k$, we denote the L^k diagonal branch susceptance matrix by

$$\underline{\boldsymbol{B}}_d^k \triangleq diag\left\{b_{\ell_r} : \ell_r \in \mathcal{L}^k\right\}. \tag{2.3}$$

Furthermore, we define the tie line diagonal branch susceptance matrix by

$$\underline{\boldsymbol{B}}_d^C \triangleq diag\left\{b_{\ell_r} : \ell_r \in \mathcal{L}^{k,m}\right\}, \tag{2.4}$$

using the ordering as for the rows of $\underline{\boldsymbol{A}}^C$. We construct from the $\underline{\boldsymbol{B}}_d^k$ and the $\underline{\boldsymbol{B}}_d^C$ arrays the interconnected system L-dimensional diagonal branch susceptance matrix

$$\underline{\boldsymbol{B}}_d = \begin{bmatrix} \underline{\boldsymbol{B}}_d^1 & \boldsymbol{0} & \cdots & \boldsymbol{0} & \boldsymbol{0} \\ \boldsymbol{0} & \boldsymbol{B}_d^2 & \cdots & \boldsymbol{0} & \boldsymbol{0} \\ \vdots & \vdots & \ddots & \vdots & \vdots \\ \boldsymbol{0} & \boldsymbol{0} & \cdots & \underline{\boldsymbol{B}}_d^K & \boldsymbol{0} \\ \boldsymbol{0} & \boldsymbol{0} & \cdots & \boldsymbol{0} & \underline{\boldsymbol{B}}_d^C \end{bmatrix}. \tag{2.5}$$

The augmented nodal susceptance matrix of the system is

$$\tilde{\underline{\boldsymbol{B}}} = \tilde{\underline{\boldsymbol{A}}}^T \underline{\boldsymbol{B}}_d \tilde{\underline{\boldsymbol{A}}} \tag{2.6}$$

and $\tilde{\underline{\boldsymbol{B}}}$ is singular since

$$\tilde{\underline{\boldsymbol{B}}} \mathbf{1}^{N+1} = \tilde{\underline{\boldsymbol{A}}}^T \underline{\boldsymbol{B}}_d \tilde{\underline{\boldsymbol{A}}} \mathbf{1}^{N+1} = \boldsymbol{0}, \tag{2.7}$$

29

which follows from (2.2).

Next, we obtain the reduced incidence matrix $\underline{A}$ from $\tilde{\underline{A}}$ by removing the row corresponding to the slack node. We also partition $\tilde{\underline{B}}$

$$\tilde{\underline{B}} = \begin{bmatrix} b_{00} & \underline{b}_0^T \\ \underline{b}_0 & \underline{B} \end{bmatrix}. \tag{2.8}$$

The reduced nodal susceptance matrix $\underline{B}$ is then

$$\underline{B} \triangleq \underline{A}^T \underline{B}_d \underline{A} \in \mathbb{R}^{N \times N}. \tag{2.9}$$

Clearly, $\underline{B}$ is a symmetric and positive definite matrix since $\underline{A}$ is full rank and $\underline{B}_d$ is a diagonal matrix with the elements corresponding to inductive elements of transmission lines.

For a node i in area $\mathcal{A}^k$, the real power injection $p_{g_i}^k$ and the real power withdrawal $p_{d_i}^k$ determine the net real power injection p_i^k with

$$p_i^k \triangleq p_{g_i}^k - p_{d_i}^k, \ i \in \mathcal{N}^k. \tag{2.10}$$

We construct the area k net real power injection vector $\underline{p}^k$ using (2.10). The systemwide net real power injection vector $\underline{p}$ is then constructed as

$$\underline{p} \triangleq \left[\left(\underline{p}^1 \right)^T, \left(\underline{p}^2 \right)^T, \cdots, \left(\underline{p}^K \right)^T \right]^T. \tag{2.11}$$

2.2 The Security Assessment Framework

We devote this section to the discussion of the concept of system security, to the security analysis framework and to the summary of the security assessment methodology. We also provide a brief summary of the so-called security control actions deployed by the IGO to ensure the secure power system operations in a multiarea system.

The basic elements of power systems operations are system security and economy. The reliability criteria under which planning is done have corresponding security criteria that are enforced in system operations. The planning and operating criteria aim to forestall the onset of cascading outages.

Power system security is defined as the ability of the interconnection to provide electricity with the appropriate quality under normal and disturbance conditions [15]. Security is a time-dependent phenomenon and is a function of the robustness of the system with respect to imminent disturbances. We refer to such disturbances as *contingencies*. For a given operating state, we analyze the security to determine whether the occurrence of each postulated contingency results in no violation of any operational constraints or, in case of such a violation, whether appropriate control actions maybe deployed to prevent it. The security is defined with respect to the postulated set of contingencies. We note, therefore, that the notion of power system security is always relative to the set of contingencies considered.

The security assessment utilizes the security framework developed by Dy Liacco [3]. In this framework, a given operating point of the power system – referred to as the base

case – is classified into one of three possible states – normal, emergency or restorative. The system is deemed to be in *normal state* when the demand is supplied without any operational constraint violations. An *emergency state* implies that the demand is supplied with one or more constraint violations. A *restorative state* indicates that there is a loss of load but with no operational constraint violations. A normal state is further categorized as *secure normal* or *insecure normal* to capture the impacts of each postulated contingency. A secure normal state indicates that the system is in normal state under the base case and each postulated contingency case. On the other hand, an insecure normal state refers to an operating state that is normal under the base case but in an emergency state for one or more postulated contingencies. As power systems are continuously subject to disturbances, the nature of the operating state may change instantaneously due to the impacts of such disturbances. In fact, if the IGO fails to deploy appropriate *security control actions*, the system may collapse. Such actions refer to the deployment of preventive, corrective, emergency or restorative control [3]. The notions of power system security are effectively summarized in the security framework depicted in Figure 2.1.
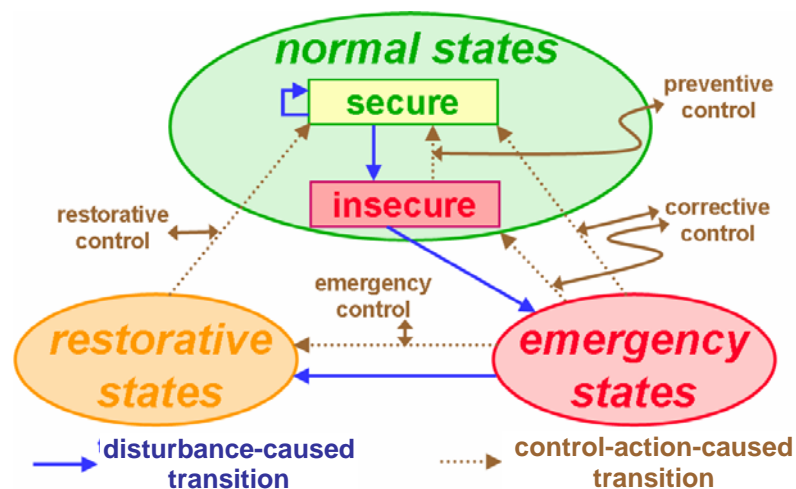
Figure 2.1 Security assessment framework

The objective of the security management is to keep the system operating state in the normal secure classification, making use of the deployment of appropriate security control actions. For an insecure normal state, the IGO may deploy either the preventive or corrective control actions. A preventive control action associated with a postulated contingency entails the modification of the precontingency – base case – state, to eliminate any potential violation, were that contingency to occur. A corrective control action involves the deployment of generation redispatch/load curtailment to modify the postcontingency state only after the contingency actually occurs. Note that for certain contingencies, such as a generator outage or a sudden change in load, the IGO may deploy only corrective control actions.

Security assessments are typically based on a deterministic criterion, such as $(n-1)$ or $(n-2)$ security. We associate with a security criterion $\mathcal{C}$ a specified contingency set. We denote by $\mathcal{J}_e = \{1, \cdots, J_e\}$ the associated index set for the postulated contingencies – each index $j \in \mathcal{J}_e$ refers to a contingency case – and a specified control action for every contingency on that list. For example, the contingency set of the $(n-1)$ security criterion consists of all single element contingency cases while that of the $(n-2)$ criterion considers all the double element contingency cases *in addition to* the single element contingencies. Since all the contingencies in the $(n-1)$ set are also included in the $(n-2)$ contingency set, the $(n-2)$ criterion is considered to be stricter than the $(n-1)$ criterion. Virtually every system operator uses, at the very least, some modified $(n-1)$ criterion list of single line outages and the set of appropriate preventive control actions to avoid their impacts. But in many instances a stricter criterion is imposed, such as a modified version of the $(n-2)$ criterion with only a subset of all the possible double element contingencies

considered. The elements in this subset are carefully selected to include contingencies that are particularly critical for the multiarea structure of the system, such as the outages of pairs of tie lines interconnecting an export and an import area. In this dissertation, we consider a representative range of security criteria in use by various IGOs.

2.3 The Applications of Distribution Factors to Security Assessment Models

A basic requirement in the operation of the electric power system is to ensure and maintain system security under a specified criterion $\mathcal{C}$. For system security, the system operating point must satisfy certain restrictions under both the base case and a pre-defined set of contingency cases. When a contingency occurs, the parameter and/or structure of the network may change, and, consequently, each disturbance results in formulation/modification of the snapshot description summarized in Section 2.1.

We define the index set $\{0\} \cup \mathcal{J}_\mathcal{C}$ to refer to both the base and the contingency cases with the base case denoted by the index 0. We use the superscript (j) to denote the values associated with a particular case with $j \in \{0\} \cup \mathcal{J}_\mathcal{C}$. For example, $\underline{\textbf{B}}^{(j)}$ refers to the nodal susceptance matrix corresponding to the network structure when contingency case j is considered. Analogously, for each contingency case represented by the index $j \in \mathcal{J}_\mathcal{C}$, we have the power flow equations [18] - [20] and the expressions for the real power line flows. There may be additional constraints such as system stability limits. In this dissertation, we limit our consideration to two operational constraint types: real power flow line limits and generation output limits.

We denote by f_{ℓ_r} the real power flow on line $\ell_r \in \mathcal{L}$. The real power line flow constraint on $\ell_r \in \mathcal{L}$ has the form

$$\left(f_{\ell_r}^{min} \right)^{(j)} \leq f_{\ell_r}^{(j)} \leq \left(f_{\ell_r}^{max} \right)^{(j)}, \ j \in \{0\} \cup \mathcal{J}_e \tag{2.12}$$

where $\left(f_{\ell_r}^{max} \right)^{(j)}$ and $\left(f_{\ell_r}^{min} \right)^{(j)}$ are the maximum and the minimum real power flow allowed on line $\ell_r \in \mathcal{L}$ under case $j \in \{0\} \cup \mathcal{J}_e$. We note that the real power flow limits of a line may be different under various contingencies due to factors such as reactive power flow patterns. The generating unit real power output limits are

$$\left(p_{g_n}^k \right)^{min} \leq \left(p_{g_n}^k \right)^{(j)} \leq \left(p_{g_n}^k \right)^{max}, \quad j \in \{0\} \cup \mathcal{J}_e, \quad k = 1, \cdots, K \tag{2.13}$$

where $\mathcal{A}^k \in \boldsymbol{a}$ and $n \in \mathcal{N}^k$.

For a given injection and withdrawal, the security assessment analyzes whether the given operating point is in normal state. For an insecure normal state, the IGO may deploy a specific security control action associated with each contingency case. Such an action may entail a redispatch of resources for the base case with a change from $\underline{p}^{(0)}$ to $\underline{\tilde{p}}^{(0)}$. For a contingency case $j \in \mathcal{J}_e$ associated with preventive action, the IGO ensures

$$\left(p_{g_n}^k \right)^{(j)} = \left(\tilde{p}_{g_n}^k \right)^{(0)}, \quad \left(p_{d_n}^k \right)^{(j)} = \left(\tilde{p}_{d_n}^k \right)^{(0)}. \tag{2.14}$$

When the IGO chooses a corrective action which is deployed once a contingency j has actually occurred, the adjustment is made on the postcontingency dispatches $\left(p_{g_n}^k \right)^{(j)}$:

35

$$\left| \left(p_{g_n}^k \right)^{(j)} - \left(p_{g_n}^k \right)^{(0)} \right| \leq \Delta p_{g_n}^k , \quad \left| \left(p_{d_n}^k \right)^{(j)} - \left(p_{d_n}^k \right)^{(0)} \right| \leq \Delta p_{d_n}^k . \quad (2.15)$$

Here, Δp's are the allowed modifications in the generating units' dispatch in the postcontingency system. Since the dynamics of the generation resources do not allow instantaneous changes, the relationships in (2.15) involve implicitly the time variable.

The associated power flow equations are nonlinear and constitute a large-scale system [18] - [31]. Consequently, modeling the power system network for each contingency may be cumbersome and the solution of the power flow equations and the specified constraints is computationally demanding. Given the frequent occurrences of such disturbances, the use of the nonlinear AC power flow modeling approach may not be practical. We introduce some reasonable assumptions to simplify the modeling and consider the impacts of contingencies making use of the so-called *distribution factors.* Distribution factors are linear approximations of the sensitivities of various system variables with respect to changes in nodal injections and withdrawals [22] - [26]. Under certain assumptions, the distribution factors are useful in modeling the impacts of line outages on system parameters. We introduce the assumptions under which we use the distribution factors:

- The nodal voltages are maintained close to 1.0 p.u.

- The angle difference between the terminal nodes of line ℓ_r is very small, so that

  $\sin\left(\theta_{i_r} - \theta_{j_r} \right) \approx \theta_{i_r} - \theta_{j_r}$ and $\cos\left(\theta_{i_r} - \theta_{j_r} \right) \approx 1$.

- $\left| g_{\ell_r} \right| \ll \left| b_{\ell_r} \right|$ so that the losses on the lines are negligible.

These are the assumptions under which the derivation of DC power flow models is obtained [18]. We replace under these conditions the nonlinear AC real power flow equations by the following set of linear equations:

$$\underline{p} \; = \; \underline{B}\,\underline{\theta}\,, \tag{2.16}$$

and

$$\underline{f} \; = \; \underline{B}_d\,\underline{A}\,\underline{\theta}\,. \tag{2.17}$$

We rewrite (2.17) using distribution factors known as the injection shift factors (ISFs), which are basic elements in the evaluation of the other distribution factors. The ISF $\psi^i_{\ell_r}$ of line ℓ_r is the (approximate) sensitivity of the change in the line ℓ_r real power flow f_{ℓ_r} with respect to a change in the injection p_i at a node $i \in \mathcal{N}$ and the withdrawal of an amount equal to the injection change at the slack bus. Under lossless conditions and the assumptions above, we construct the ISF matrix [26]

$$\underline{\Psi} \; \triangleq \; \underline{B}_d\,\underline{A}\,\underline{B}^{-1}$$

and rewrite (2.17) as

$$\underline{f} \; = \; \underline{\Psi}\,\underline{p}\,. \tag{2.18}$$

As $\underline{\Psi}$ is solely determined by the network topology/parameters, it is independent of the withdrawal and the injection amounts. However, each ISF $\psi^i_{\ell_r}$ explicitly depends on the node selected to be the slack bus. Change of the slack bus may lead to a change in the ISF

value. The notion of the ISF may be extended to include the slack bus 0. Since the injection and withdrawal buses are identical in this case, $\psi_{\ell_r}^0 = 0$ for each $\ell_r \in \mathcal{L}$. Note that each $\psi_{\ell_r}^i$ has flow direction information on the line $\ell_r = (i_r, j_r)$ definition. A positive (negative) $\psi_{\ell_r}^i$ value indicates that the injection at node i and withdrawal at node 0 result in the flows from i_r to j_r (j_r to i_r).

In security applications, we are interested in the evaluation of the impacts on the real power flows on lines of interest of a change in the injection amount at a specific node and an equal change in withdrawal at another node. For such purposes, we use the power transfer distribution factors (PTDFs). We introduce notation for transactions in discussing the PTDFs. The impact of a Δt-MW transaction from node i to node j is denoted by the *ordered* triplet

$$w \triangleq \{i,\ j,\ \Delta t\}.$$

We consider the impacts $\Delta f_{\ell_r}^w$ of such a transaction on f_{ℓ_r} is, and use

$$\Delta f_{\ell_r}^w = \varphi_{\ell_r}^w \Delta t \qquad\qquad (2.19)$$

to determine its value. Here, we write the PTDF $\varphi_{\ell_r}^w$ with

$$\varphi_{\ell_r}^w \triangleq \psi_{\ell_r}^i - \psi_{\ell_r}^j. \qquad\qquad (2.20)$$

The PTDF $\varphi_{\ell_r}^w$ is therefore not dependent on the choice of slack bus.

For the line $\tilde{\ell}_m$ outage, we evaluate its impact $\Delta f_{\ell_r}^{(\tilde{\ell}_m)}$ on the flow f_{ℓ_r} on line ℓ_r using the line outage distribution factor (LODF) $\varsigma_{\ell_r}^{(\tilde{\ell}_m)}$, which specifies the fraction of the preoutage real power flow on the line $\tilde{\ell}_m$ redistributed to the line ℓ_r and is evaluated from

$$\varsigma_{\ell_r}^{(\tilde{\ell}_m)} \triangleq \frac{\Delta f_{\ell_r}^{(\tilde{\ell}_m)}}{f_{\tilde{\ell}_m}} = \frac{\varphi_{\ell_r}^{w(\tilde{\ell}_m)}}{\left[1 - \varphi_{\tilde{\ell}_m}^{w(\tilde{\ell}_m)}\right]}, \quad \ell_r \neq \tilde{\ell}_m, \quad \varphi_{\tilde{\ell}_m}^{w(\tilde{\ell}_m)} \neq 1, \tag{2.21}$$

with

$$w(\tilde{\ell}_m) \triangleq \{\tilde{i}_m, \tilde{j}_m, \Delta t\}$$

denoting the unit transaction between the terminal nodes of $\tilde{\ell}_m = (\tilde{i}_m, \tilde{j}_m)$. As long as $\varphi_{\tilde{\ell}_m}^{w(\tilde{\ell}_m)} \neq 1$, $\varsigma_{\ell_r}^{(\tilde{\ell}_m)}$ is defined. The line $\tilde{\ell}_m$ outage results in a topology change and requires the re-evaluation of the postoutage network ISFs and PTDFs.

We use the notation $(\tau)^{(\tilde{\ell}_m)}$ to denote the value of a variable τ with the line $\tilde{\ell}_m$ outaged, as in (2.21). The pre- and postoutage ISFs, $\psi_{\ell_r}^i$ and $\left(\psi_{\ell_r}^i\right)^{(\tilde{\ell}_m)}$, respectively, are related through the relationship

$$\left(\psi_{\ell_r}^i\right)^{(\tilde{\ell}_m)} \triangleq \psi_{\ell_r}^i + \varsigma_{\ell_r}^{(\tilde{\ell}_m)} \psi_{\tilde{\ell}_m}^i. \tag{2.22}$$

Similarly, the pre- and postoutage PTDFs, $\varphi_{\ell_r}^w$ and $\left(\varphi_{\ell_r}^w\right)^{(\tilde{\ell}_m)}$, respectively, are related

through

$$\left(\varphi_{\ell_r}^w\right)^{(\tilde{\ell}_m)} \triangleq \varphi_{\ell_r}^w + \varsigma_{\ell_r}^{(\tilde{\ell}_m)} \varphi_{\tilde{\ell}_m}^w .$$ (2.23)

The LODFs are very useful in the study of security with many outaged lines, such as under blackouts which impact large geographic regions. We focus on the fast evaluation of LODFs under multiple line outages. We refer to such LODFs as generalized LODFs or GLODFs. We next present an analytic, closed-form expression for, and the computationally efficient evaluation of, GLODFs.

We first revisit the single-line outage case and examine how the outage impacts may be simulated by net injection and withdrawal changes. The line $\tilde{\ell}_1 = (\tilde{i}_1, \tilde{j}_1)$ outage changes the real power flow in the postoutage network on each line connected to $\tilde{i}_1$ by the fraction of $f_{\tilde{\ell}_1}$. We simulate this impact by introducing $w(\tilde{\ell}_1) = \{\tilde{i}_1, \tilde{j}_1, \Delta t(\tilde{\ell}_1)\}$ in the preoutage network. The injection $\Delta t(\tilde{\ell}_1)$ adds a change $\varphi_{\tilde{\ell}_1}^{w(\tilde{\ell}_1)} \Delta t(\tilde{\ell}_1)$ on the line $\tilde{\ell}_1$ flow and a net flow change of $\left(1 - \varphi_{\tilde{\ell}_1}^{w(\tilde{\ell}_1)}\right) \Delta t(\tilde{\ell}_1)$ on all the other lines but $\tilde{\ell}_1$ that are connected to node $\tilde{i}_1$. By selecting $\Delta t(\tilde{\ell}_1)$ to satisfy

$$\left(1 - \varphi_{\tilde{\ell}_1}^{w(\tilde{\ell}_1)}\right) \Delta t(\tilde{\ell}_1) = f_{\tilde{\ell}_1},$$ (2.24)

the transaction $w(\tilde{\ell}_1)$ changes the flow f_{ℓ_k}, $\ell_k \neq \tilde{\ell}_1$, by

$$\Delta f_{\ell_k}^{w(\tilde{\ell}_1)} = \varphi_{\ell_k}^{w(\tilde{\ell}_1)} \Delta t(\tilde{\ell}_1) = \left[\varphi_{\ell_k}^{w(\tilde{\ell}_1)}\left(1 - \varphi_{\tilde{\ell}_1}^{w(\tilde{\ell}_1)}\right)^{-1}\right] f_{\tilde{\ell}_1} .$$ (2.25)

In terms of (2.21), the bracketed term in (2.25) is $\varsigma_{\ell_k}^{(\tilde{\ell}_1)}$, and so $w(\tilde{\ell}_1)$ with $\Delta t(\tilde{\ell}_1)$ given by (2.25) simulates the line $\tilde{\ell}_1$ outage impacts.

We proceed with the generalization for multiple line outages by next considering the case of the outages of the two lines $\tilde{\ell}_1$ and $\tilde{\ell}_2$. We simulate the impacts on f_{ℓ_k} by introducing $w(\tilde{\ell}_1)$ and $w(\tilde{\ell}_2)$, taking explicitly into account the interactions between these two transactions in specifying $\Delta t(\tilde{\ell}_1)$ and $\Delta t(\tilde{\ell}_2)$, as shown in Figure 2.2. We set $\Delta t(\tilde{\ell}_1)$ to satisfy

$$\left[1 - \left(\varphi_{\tilde{\ell}_1}^{w(\tilde{\ell}_1)} \right)^{(\tilde{\ell}_2)} \right] \Delta t(\tilde{\ell}_1) = \left(f_{\tilde{\ell}_1} \right)^{(\tilde{\ell}_2)}. \tag{2.26}$$

Analogously, we select $\Delta t(\tilde{\ell}_2)$ to satisfy

$$\left[1 - \left(\varphi_{\tilde{\ell}_2}^{w(\tilde{\ell}_2)} \right)^{(\tilde{\ell}_1)} \right] \Delta t(\tilde{\ell}_2) = \left(f_{\tilde{\ell}_2} \right)^{(\tilde{\ell}_1)}. \tag{2.27}$$

We rewrite (2.26) and (2.27) using the relations in (2.21) and (2.22) as

$$\left[\boldsymbol{I} - \begin{bmatrix} \varphi_{\tilde{\ell}_1}^{w(\tilde{\ell}_1)} & \varphi_{\tilde{\ell}_1}^{w(\tilde{\ell}_2)} \\ \varphi_{\tilde{\ell}_2}^{w(\tilde{\ell}_1)} & \varphi_{\tilde{\ell}_2}^{w(\tilde{\ell}_2)} \end{bmatrix} \right] \begin{bmatrix} \Delta t(\tilde{\ell}_1) \\ \Delta t(\tilde{\ell}_2) \end{bmatrix} = \begin{bmatrix} f_{\tilde{\ell}_1} \\ f_{\tilde{\ell}_2} \end{bmatrix}. \tag{2.28}$$

As long as the matrix in (2.28) is nonsingular, we determine $\Delta t(\tilde{\ell}_1)$ and $\Delta t(\tilde{\ell}_2)$ by solving the linear system.
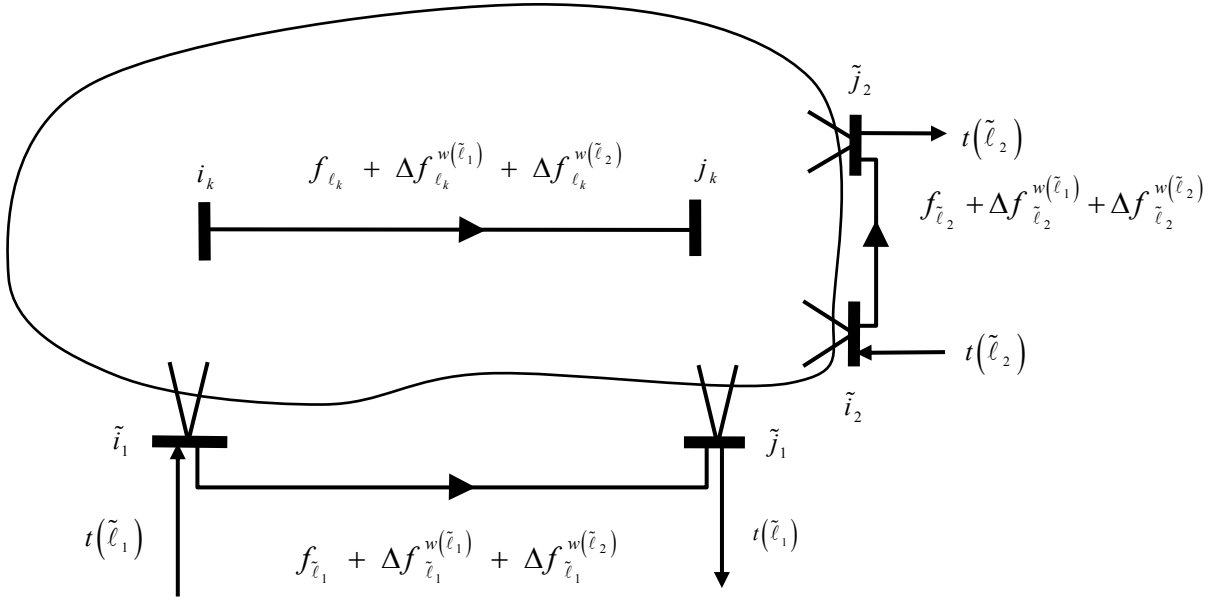
Figure 2.2 The impacts of the transactions $w(\tilde{\ell}_1)$ **and** $w(\tilde{\ell}_2)$

In the inductive process to generalize the result for the case of multiple line outages, we assume that the impacts of a set of $(\alpha - 1)$ outaged lines $\tilde{\mathcal{L}}_{(\alpha-1)} = \{\tilde{\ell}_1, \cdots, \tilde{\ell}_{\alpha-1}\}$ are simulated with $(\alpha - 1)$ transactions whose amounts are specified by

$$\left[\underline{\underline{I}} - \underline{\underline{\Phi}}_{\tilde{\mathcal{L}}_{(\alpha-1)}}\right] \underline{\Delta t}_{(\alpha-1)} = \underline{f}_{(\alpha-1)} , \tag{2.29}$$

where

$$\underline{\Delta t}_{(\alpha-1)} = \left[\Delta t(\tilde{\ell}_1), \cdots, \Delta t(\tilde{\ell}_{\alpha-1})\right]^T,$$

$$\underline{f}_{(\alpha-1)} = \left[f_{\tilde{\ell}_1}, \cdots, f_{\tilde{\ell}_{\alpha-1}}\right]^T,$$

and

42

$$
\underline{\boldsymbol{\Phi}}_{\tilde{\mathcal{L}}_{(\alpha-1)}} = \begin{bmatrix} \varphi_{\tilde{\ell}_1}^{w(\tilde{\ell}_1)} & \cdots & \varphi_{\tilde{\ell}_1}^{w(\tilde{\ell}_{\alpha-1})} \\ \vdots & \ddots & \vdots \\ \varphi_{\tilde{\ell}_{\alpha-1}}^{w(\tilde{\ell}_1)} & \cdots & \varphi_{\tilde{\ell}_{\alpha-1}}^{w(\tilde{\ell}_{\alpha-1})} \end{bmatrix},
$$

with $\left[\underline{\boldsymbol{I}} - \underline{\boldsymbol{\Phi}}_{\tilde{\mathcal{L}}_{(\alpha-1)}} \right]$ nonsingular.

We now consider the additional line $\tilde{\ell}_\alpha \notin \tilde{\mathcal{L}}_{(\alpha-1)}$ outage. The set of outaged lines is $\tilde{\mathcal{L}}_{(\alpha)} = \tilde{\mathcal{L}}_{(\alpha-1)} \cup \{\tilde{\ell}_\alpha\}$. Reasoning along the lines used in the two-line outage analysis, $\underline{\Delta t}_{(\alpha-1)}$ is given by

$$
\left[\underline{\boldsymbol{I}} - \left(\underline{\boldsymbol{\Phi}}_{\tilde{\mathcal{L}}_{(\alpha-1)}} \right)^{(\tilde{\ell}_\alpha)} \right] \underline{\Delta t}_{(\alpha-1)} = \left(\underline{\boldsymbol{f}}_{(\alpha-1)} \right)^{(\tilde{\ell}_\alpha)}. \tag{2.30}
$$

We capture the impacts of the outages of the $\tilde{\mathcal{L}}_{(\alpha-1)}$ elements on $\tilde{\ell}_\alpha$ by using the analogue of (2.27) and determine $\Delta t \left(\tilde{\ell}_\alpha \right)$ from

$$
\left[1 - \left(\varphi_{\tilde{\ell}_\alpha}^{w(\tilde{\ell}_\alpha)} \right)^{(\tilde{\mathcal{L}}_{(\alpha-1)})} \right] \Delta t \left(\tilde{\ell}_\alpha \right) = \left(f_{\tilde{\ell}_\alpha} \right)^{(\tilde{\mathcal{L}}_{(\alpha-1)})}. \tag{2.31}
$$

The superscript $\left(\tilde{\mathcal{L}}_{(\alpha-1)} \right)$ denotes the network with the elements of $\tilde{\mathcal{L}}_{(\alpha-1)}$ outaged. We define $\underline{\boldsymbol{b}} \triangleq \left[\varphi_{\tilde{\ell}_1}^{w(\tilde{\ell}_\alpha)}, \cdots, \varphi_{\tilde{\ell}_{\alpha-1}}^{w(\tilde{\ell}_\alpha)} \right]^T$ and $\underline{\boldsymbol{c}} \triangleq \left[\varphi_{\tilde{\ell}_\alpha}^{w(\tilde{\ell}_1)}, \cdots, \varphi_{\tilde{\ell}_\alpha}^{w(\tilde{\ell}_{\alpha-1})} \right]^T$ and rewrite (2.30) and (2.31) as

$$\left[\mathbf{I} - \boldsymbol{\Phi}_{\tilde{\mathcal{L}}_{(\alpha-1)}}\right]\underline{\Delta t}_{(\alpha-1)} - \underline{b}\left(1 - \varphi_{\tilde{\ell}_\alpha}^{w(\tilde{\ell}_\alpha)}\right)^{-1}\left(f_{\tilde{\ell}_\alpha} + \underline{c}^T\underline{\Delta t}_{(\alpha-1)}\right) = \underline{f}_{(\alpha-1)}$$

(2.32)

$$\left(1 - \varphi_{\tilde{\ell}_\alpha}^{w(\tilde{\ell}_\alpha)}\right)\Delta t\left(\tilde{\ell}_\alpha\right) - \underline{c}^T\left[\mathbf{I} - \boldsymbol{\Phi}_{\tilde{\mathcal{L}}_{(\alpha-1)}}\right]^{-1}\left(\underline{f}_{(\alpha-1)} + \underline{b}\,\Delta t\left(\tilde{\ell}_\alpha\right)\right) = f_{\tilde{\ell}_\alpha},$$

which may be simplified to

$$\left[\mathbf{I} - \boldsymbol{\Phi}_{\tilde{\mathcal{L}}_{(\alpha)}}\right]\underline{\Delta t}_{(\alpha)} = \underline{f}_{(\alpha)}\,, \quad \boldsymbol{\Phi}_{\tilde{\mathcal{L}}_{(\alpha)}} \triangleq \begin{bmatrix} \boldsymbol{\Phi}_{\tilde{\mathcal{L}}_{(\alpha-1)}} & \underline{b} \\[2mm] \underline{c}^T & \varphi_{\tilde{\ell}_\alpha}^{w(\tilde{\ell}_\alpha)} \end{bmatrix}.$$

(2.33)

So long as $\left[\mathbf{I} - \boldsymbol{\Phi}_{\tilde{\mathcal{L}}_{(\alpha)}}\right]$ is nonsingular, we use (2.33) to solve for $\underline{\Delta t}_{(\alpha)}$ and so simulate the impacts of the α line outages.

We use this inductive process to determine the appropriate values of the assumed transactions and thereby derive the GLODF expression. For any line $\ell_k \notin \tilde{\mathcal{L}}_{(\alpha)}$, we define $\underline{\xi}_{\ell_k}^{(\tilde{\mathcal{L}}_{(\alpha)})}$, whose elements are the GLODFs with the lines in $\tilde{\mathcal{L}}_{(\alpha)}$ outaged, with the interactions between the outaged lines fully considered. The change in the real power flow of line ℓ_k is

$$\left(\Delta f_{\ell_k}\right)^{(\tilde{\mathcal{L}}_{(\alpha)})} \triangleq \left[\underline{\xi}_{\ell_k}^{(\tilde{\mathcal{L}}_{(\alpha)})}\right]^T \underline{f}_{(\alpha)}\,, \quad \ell_k \notin \tilde{\mathcal{L}}_{(\alpha)}.$$

(2.34)

However, the combined impacts of the α transactions with the $\underline{\Delta t}_{(\alpha)}$ on the line ℓ_k determined by (2.33) are given as

$$\left(\Delta f_{\ell_k}\right)^{(\tilde{\mathcal{L}}_{(\alpha)})} = \left[\varphi_{\ell_k}^{w(\tilde{\ell}_1)}, \cdots, \varphi_{\ell_k}^{w(\tilde{\ell}_\alpha)}\right]\underline{\Delta t}_{(\alpha)}.$$

(2.35)

As long as $\left[\underline{\boldsymbol{I}} - \underline{\boldsymbol{\Phi}}_{\tilde{\mathcal{L}}_{(\alpha)}} \right]$ is nonsingular, we rewrite (2.35) as

$$\left(\Delta f_{\ell_k} \right)^{\left(\tilde{\mathcal{L}}_{(\alpha)} \right)} = \left[\varphi_{\ell_k}^{w(\tilde{\ell}_1)}, \cdots, \varphi_{\ell_k}^{w(\tilde{\ell}_\alpha)} \right] \left[\underline{\boldsymbol{I}} - \underline{\boldsymbol{\Phi}}_{\tilde{\mathcal{L}}_{(\alpha)}} \right]^{-1} \underline{\boldsymbol{f}}_{(\alpha)}. \qquad (2.36)$$

Therefore, $\underline{\boldsymbol{\xi}}_{\ell_k}^{\left(\tilde{\mathcal{L}}_{(\alpha)} \right)}$ is the solution of

$$\left[\underline{\boldsymbol{I}} - \underline{\boldsymbol{\Phi}}_{\tilde{\mathcal{L}}_{(\alpha)}} \right]^T \underline{\boldsymbol{\xi}}_{\ell_k}^{\left(\tilde{\mathcal{L}}_{(\alpha)} \right)} = \left[\varphi_{\ell_k}^{w(\tilde{\ell}_1)}, \cdots, \varphi_{\ell_k}^{w(\tilde{\ell}_\alpha)} \right]^T \qquad (2.37)$$

and is defined whenever $\left[\underline{\boldsymbol{I}} - \underline{\boldsymbol{\Phi}}_{\tilde{\mathcal{L}}_{(\alpha)}} \right]$ is nonsingular.

The singularity of $\left[\underline{\boldsymbol{I}} - \underline{\boldsymbol{\Phi}}_{\tilde{\mathcal{L}}_{(\alpha)}} \right]$, however, indicates that the outage of the α lines in $\tilde{\mathcal{L}}_{(\alpha)}$ separates the system into two or more islands. The analysis of such cases is treated in Chapter 3. In fact, a simple case is the outage of a line $\tilde{\ell}_m$ with $\varphi_{\tilde{\ell}_m}^{w(\tilde{\ell}_m)} = 1$. A special case occurs from the outage of the line $\tilde{\ell}_m$ resulting in the creation of two disconnected subsystems. When the outaged line $\tilde{\ell}_m$ is radial, its disconnection results in the isolation of the radial node.

The relation (2.37) provides an analytic, closed-form expression for the GLODFs. Since the GLODF is expressed in terms of the preoutage network parameters, we avoid the need to evaluate the postoutage network parameters. A key advantage in the deployment of GLODFs is the ability to evaluate the postoutage flows on specific lines of interest without the need to determine the postoutage network states. The proposed LODF extension permits the GLODF evaluation through a computationally efficient

procedure which involves the solution of a system of linear equations whose dimension is the number of line outages.

The postoutage network flows are determined by the appropriate GLODFs and preoutage flows on the lines to be outaged:

$$\underline{f}^{(\tilde{\mathcal{L}}_{(\alpha)})} = \underline{f} + \left[\underline{\xi}^{(\tilde{\mathcal{L}}_{(\alpha)})}\right]^{T} \underline{f}_{(\alpha)} . \tag{2.38}$$

We set the ηth component of the vector $\left(\underline{\xi}_{\tilde{\ell}_m}^{(\tilde{\mathcal{L}}_{(\alpha)})}\right)_{\eta} = -1$ and all the other components to $\left(\underline{\xi}_{\tilde{\ell}_m}^{(\tilde{\mathcal{L}}_{(\alpha)})}\right)_{\nu} = 0, \quad \nu \neq \eta$. We use (2.18) to rewrite the relationship in (2.38) as

$$\underline{f}^{(\tilde{\mathcal{L}}_{(\alpha)})} = \left[\underline{\Psi} + \left[\underline{\xi}^{(\tilde{\mathcal{L}}_{(\alpha)})}\right]^{T} \underline{\Psi}_{(\alpha)}\right] \underline{p} . \tag{2.39}$$

Here, we use $\underline{f}_{(\alpha)} = \underline{\Psi}_{(\alpha)} \underline{p}$, where $\underline{\Psi}_{(\alpha)} = \left[\underline{\psi}_{(\alpha)}^{1} \cdots \underline{\psi}_{(\alpha)}^{N}\right]$ and $\underline{\psi}_{(\alpha)}^{i} = \left[\psi_{\tilde{\ell}_1}^{i}, \cdots, \psi_{\tilde{\ell}_{\alpha}}^{i}\right]^{T}$. In fact, (2.39) allows us to explicitly determine the postoutage ISF matrix $(\underline{\Psi})^{(\tilde{\mathcal{L}}_{(\alpha)})}$ from

$$(\underline{\Psi})^{(\tilde{\mathcal{L}}_{(\alpha)})} = \underline{\Psi} + \left[\underline{\xi}^{(\tilde{\mathcal{L}}_{(\alpha)})}\right]^{T} \underline{\Psi}_{(\alpha)} . \tag{2.40}$$

Therefore, we may use GLODFs to explicitly perform security assessment to analyze whether the postoutage flows violate any line flow limits:

$$\left(\underline{f}^{min}\right)^{(\tilde{\mathcal{L}}_{(\alpha)})} \leq \underline{\Psi}^{(\tilde{\mathcal{L}}_{(\alpha)})} \underline{p} \leq \left(\underline{f}^{max}\right)^{(\tilde{\mathcal{L}}_{(\alpha)})} . \tag{2.41}$$

46

The use of this linearized model significantly reduces the computational efforts required in security analysis. However, the distribution factors are approximations of the real sensitivities and, consequently, their use may introduce errors. The errors on single line outages are investigated in detail in [24]. The results indicate the effectiveness of the model (2.41). In particular, a range of conditions over which such a model provides a reliable approximation for large power system networks is presented.

The description of the basic modeling of the multiarea network, the modeling of various operational constraints and the model used for security management are depicted in Figure 2.3. The conceptual representation also indicates that the physical operation of power systems is explicitly driven by a specified security criterion $\mathcal{C}$.
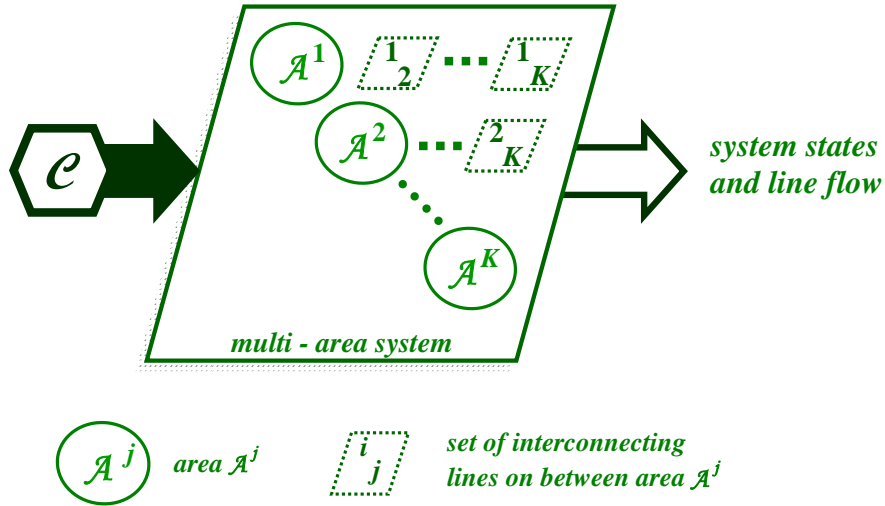
Figure 2.3 Conceptual representation of multiarea system operations under a specified security criterion

2.4 Summary

In this chapter, we discuss the modeling aspects of the multiarea network and the

operational constraints for system security assessments. Following the review of the basic system security notions and the framework used for security management, we construct the models that we use for such assessment studies. We pay special attention to the formulation of closed-form expressions for the operational constraints by making extensive use of the distribution factors. We develop an analytic expression for the GLODFs which we use to assess whether the postoutage flows violate any line flow limits under multiple line and cascading outages. Since the GLODFs are expressed in terms of the preoutage network parameters, we avoid the need to evaluate the postoutage network parameters. We view the development of the expressions for the GLODFs and the construction of the numerically efficient procedure to evaluate them as an important contribution of this dissertation.

We make use of the models of this chapter in the analysis of system security in subsequent chapters. In Chapter 3, we use the GLODFs to construct a combined graph-theoretic-algebraic approach to detect island formation in power system networks under multiple line outages. We also use the GLODFs in the formulation of the optimization problem that the IGO solves to determine the market outcomes and the associated secure system operating state.

CHAPTER 3

DETECTION OF ISLAND FORMATION UNDER MULTIPLE-LINE OUTAGES

Power systems are continually subject to various disturbances such as changes in the loads and the outages of one or more components, such as lines, transformers and generating units. There exist combinations of line outages that separate the preoutage interconnected system into two or more subnetworks resulting in the formation of islands. These line outage combinations are often regarded as "most problematic" [36] since the creation of one or more islands may disrupt "normal" system operations and also entail computational problems. In fact, the island formation may require deployment of security control actions of various types, including load shedding. On the computational side, there are numerous complications due to the singularity of the postoutage Jacobian matrix in the Newton power flow formulation [34] - [36]. Therefore, the rapid detection of island formation and the identification of the causal factors – the outages of the set of specific lines that separate the system into two or more islands – are essential to effectively deal with the complications that arise. We devote this chapter to address these issues by making detailed use of the models developed in Chapter 2.

We analyze the topological characteristics of power system interconnections to gain the necessary insights into system connectivity. With these insights, we characterize the impacts of changes in the network structure due to multiple line outages. In addition, we make use of the structural characteristics of the models describing the power system network to determine the algebraic criterion for loss of connectivity. We marry the graph theoretic and the algebraic approaches to construct an effective scheme for island

49

detection. A salient characteristic of the scheme is its low computing requirements involving the analysis of a matrix of the GLODFs of the order of the number of outaged lines. The proposed combined graph-theoretic-algebraic approach is particularly useful for large-scale systems to study the impacts of cascading outages. For illustrative purposes, we apply the proposed scheme to study island formation in the IEEE 118-bus system under multiple line outages.

This chapter contains five sections. In Section 3.1, we review the graph theoretic notions we apply to describe the connectivity of power system networks. We devote Section 3.2 to the characterization of the power system connectivity making use of the distribution factors, including GLODFs. In Section 3.3, we extend the characterization of system connectivity using GLODFs for multiple line outages and construct the proposed scheme. We also perform an analysis of the computational complexity of the developed scheme. In Section 3.4, we illustrate the application of the proposed approach to the IEEE 118-bus system. We summarize the results of this chapter in Section 3.5.

3.1 Review of the Graph Theoretic Notions

Our focus in this work is on the topological modifications of the power network due to line outages. The interest is in the connectivity information and we only consider the real power flows in the network. For these purposes, we use the linear power flow representation of the interconnected power system developed in Chapter 2, (2.16) - (2.17) . In terms of the notation developed in Chapter 2, we associate the graph $\mathcal{G} = (\mathcal{N}, \mathcal{L})$ with the power system network, with the set of vertices corresponding to set of buses $\mathcal{N}$ and the set of edges to set of lines $\mathcal{L}$. We use the terms *graph* and *network*

interchangeably in the remainder of this work.

Definition 3.1: $\mathcal{G}$ is a **connected network** if and only if there exists a path between every pair of nodes i and j, $i \neq j$.

Definition 3.2: Two connected subnetworks $\mathcal{G}_a = (\mathcal{N}_a, \mathcal{L}_a)$ and $\mathcal{G}_b = (\mathcal{N}_b, \mathcal{L}_b)$ of $\mathcal{G}$ are **disjoint** if $\mathcal{N}_a \cap \mathcal{N}_b = \varnothing$, with $\mathcal{N}_a, \mathcal{N}_b \subset \mathcal{N}$ and $\mathcal{L}_a, \mathcal{L}_b \subseteq \mathcal{L}$.

Definition 3.3: We call a subset $\bar{\mathcal{L}} \subset \mathcal{L}$ a **cutset** if and only if the removal of all the elements in $\bar{\mathcal{L}}$ from $\mathcal{L}$ partitions $\mathcal{G}$ into two disjoint connected subnetworks $\mathcal{G}_a = (\mathcal{N}_a, \mathcal{L}_a)$ and $\mathcal{G}_b = (\mathcal{N}_b, \mathcal{L}_b)$ with $\mathcal{N}_a \cup \mathcal{N}_b = \mathcal{N}$.

We refer to the separated subnetworks as the islands or the islanded subnetworks.

Definition 3.4: A cutset $\hat{\mathcal{L}} \subset \mathcal{L}$ is a **minimal cutset** if no proper subset of $\hat{\mathcal{L}}$ is a cutset.

We next make use of these definitions to describe system connectivity in the section that follows.

3.2 Power System Characterization of Minimal Cutsets

We start out our analysis of power system connectivity making use of the distribution factors (2.18) - (2.41). Consider the single line $\ell_r \in \mathcal{L}$ and consider that

$\hat{\mathcal{L}} = \{\ell_r\} = \{(i_r, j_r)\}$ constitutes a minimal cutset of the connected network

$$\mathcal{G} \triangleq (\mathcal{N}, \mathcal{L}).$$

The line ℓ_r connects the two subnetworks, $\mathcal{G}'_a$ and $\mathcal{G}'_b$, of $\mathcal{G}$ with $i_r \in \mathcal{N}'_a$ and $j_r \in \mathcal{N}'_b$.

We consider *a transaction* between the terminal nodes of ℓ_r, which we denote by

$w(\ell_r) = \{i_r, j_r, t\}$. From the definition of the PTDFs in Chapter 2, it follows that ℓ_r is

a minimal cutset if and only if

$$\varphi_{\ell_s}^{w(\ell_r)} = \begin{cases} 1, & \ell_s = \ell_r \\ 0, & \ell_s \neq \ell_r \end{cases}. \tag{3.1}$$

We infer from (3.1) that for the singleton minimal cutset $\hat{\mathcal{L}}$, the PTDFs are binary

valued for injection/withdrawal at the terminal nodes of a single element minimal cutset.

In fact, any inter- and intra-sub-network transaction, $w \triangleq \{i, j, t\}$, in $\mathcal{G}$ for which

$\{\ell_r\}$ constitutes a minimal cutset is characterized by

$$\left| \varphi_{\ell_r}^{\{i,j,t\}} \right| = \begin{cases} 1, & i \in \mathcal{N}'_a, j \in \mathcal{N}'_b \ \ or \ \ i \in \mathcal{N}'_b, j \in \mathcal{N}'_a \\ 0, & i, j \in \mathcal{N}'_a \ \ or \ \ i, j \in \mathcal{N}'_b \end{cases}. \tag{3.2}$$

In words, if the transaction terminal nodes are in the two different subnetworks with the

respective node sets $\mathcal{N}'_a$ and $\mathcal{N}'_b$, then the transaction must flow over the line ℓ_r; else

there is no net flow on the line ℓ_r when the terminal nodes of the transaction are in the

same subnetwork node set $\mathcal{N}'_a$ or $\mathcal{N}'_b$. Note that $\varphi_{\ell_r}^{w(\ell_r)} = 1$ makes $\varsigma_{\ell_s}^{(\ell_r)}$ undefined.

Consider the minimal cutset $\hat{\mathcal{L}}_{(\beta)} = \{\hat{\ell}_1, \cdots, \hat{\ell}_\beta\}^\dagger$ with β lines connecting two disjoint

connected subnetworks $\mathcal{G}_a = (\mathcal{N}_a, \mathcal{L}_a)$ and $\mathcal{G}_b = (\mathcal{N}_b, \mathcal{L}_b)$ of $\mathcal{G}$. We consider the

outages of the first β–1 elements of $\hat{\mathcal{L}}_{(\beta)}$ resulting in the modified network

$\mathcal{G}'' = (\mathcal{N}, \mathcal{L}'')$, with $\mathcal{L}'' = \mathcal{L} \setminus \{\hat{\ell}_1, \cdots, \hat{\ell}_{\beta-1}\}$. Since $\hat{\mathcal{L}}_{(\beta)}$ is a minimal cutset, $\mathcal{G}''$ is

connected. Also, $\hat{\ell}_\beta$ is a minimal cutset of $\mathcal{G}''$ connecting the two disjoint subnetworks

$\mathcal{G}_a$ and $\mathcal{G}_b$ of $\mathcal{G}''$. Therefore, (3.1) states that for this network

$$
\left(\varphi_{\ell_r}^{w(\hat{\ell}_\beta)} \right)^{\left(\hat{\mathcal{L}}_{(\beta-1)} \right)} = \begin{cases} 1, & \ell_r = \hat{\ell}_\beta \\ 0, & \ell_r \neq \hat{\ell}_\beta \end{cases}, \quad \ell_r \notin \hat{\mathcal{L}}_{(\beta-1)}. \tag{3.3}
$$

Since the terminal nodes of each minimal cutset element are in the two different

subnetworks, the discussion after (3.2) implies

$$
\left| \left(\varphi_{\hat{\ell}_\beta}^{w(\hat{\ell}_r)} \right)^{\left(\hat{\mathcal{L}}_{(\beta-1)} \right)} \right| = 1, \quad \hat{\ell}_r \in \hat{\mathcal{L}}_{(\beta)}. \tag{3.4}
$$

Thus, once all but one element of $\hat{\mathcal{L}}_{(\beta)}$ are outaged, the preoutage real power flow in

each outaged line has to flow over the minimal cutset element that is not outaged. We can

also show the case of all but two element outages of $\hat{\mathcal{L}}_{(\beta)}$:

$$
\left| \left(\varphi_{\hat{\ell}_\beta}^{w(\hat{\ell}_r)} \right)^{\hat{\mathcal{L}}_{(\beta-2)}} \right| + \left| \left(\varphi_{\hat{\ell}_{\beta-1}}^{w(\hat{\ell}_r)} \right)^{\hat{\mathcal{L}}_{(\beta-2)}} \right| = 1, \quad \hat{\ell}_r \in \hat{\mathcal{L}}_{(\beta)}. \tag{3.5}
$$

---

† While $\hat{\mathcal{L}}_{(\beta)}$ is not an ordered set we reorder the elements from 1 to β so as to allow the use of simple notation.

Then, by induction, we can rIGOrously establish that

$$\sum_{\hat{\ell}_r \in \hat{\mathcal{L}}_{(\beta)}} \left| \varphi_{\hat{\ell}_r}^{w(\hat{\ell}_s)} \right| = 1, \qquad \hat{\ell}_s \in \hat{\mathcal{L}}_{(\beta)}. \tag{3.6}$$

We use (3.6) to prove the following theorem.

Theorem 3.1: *Let* $\mathcal{G} = (\mathcal{N}, \mathcal{L})$ *be a connected power system network. The minimal cutset* $\hat{\mathcal{L}}_{(\beta)} = \{\hat{\ell}_1, \cdots, \hat{\ell}_\beta\}$ *partitions* $\mathcal{G}$ *into two subnetworks* $\mathcal{G}_a = (\mathcal{N}_a, \mathcal{L}_a)$ *and* $\mathcal{G}_b = (\mathcal{N}_b, \mathcal{L}_b)$. *Each line* $\hat{\ell}_r = (\hat{i}_r, \hat{j}_r) \in \hat{\mathcal{L}}$ *has* $\hat{i}_r \in \mathcal{N}_a$ *and* $\hat{j}_r \in \mathcal{N}_b$. *Then,*

$$(i) \qquad \varphi_{\hat{\ell}_r}^{w(\hat{\ell}_s)} > 0 \qquad\qquad \hat{\ell}_s, \hat{\ell}_r \in \hat{\mathcal{L}} \tag{3.7}$$

$$(ii) \qquad \sum_{\hat{\ell}_r \in \hat{\mathcal{L}}} \varphi_{\hat{\ell}_r}^{\{i,j,t\}} = \begin{cases} 1 & i \in \mathcal{N}_a, j \in \mathcal{N}_b \\ \\ -1 & i \in \mathcal{N}_b, j \in \mathcal{N}_a \end{cases} \tag{3.8}$$

$$(iii) \qquad \sum_{\hat{\ell}_r \in \hat{\mathcal{L}}} \varphi_{\hat{\ell}_r}^{\{i,j,t\}} = 0 \quad i, j \in \mathcal{N}_a \ \text{ or } \ i, j \in \mathcal{N}_b. \tag{3.9}$$

■

We provide the proof of Theorem 3.1 in Appendix A. This theorem states the necessary conditions of minimal cutsets. The physical intuitions behind these conditions lead us to state that the result in (*i*) of the Theorem 3.1 is a generalized restatement of (3.6). The result in (*ii*) states that any transaction between $\mathcal{N}_a$ and $\mathcal{N}_b$ results in net power flows on the minimal cutset elements; the algebraic sum of the minimal cutset flows equals the transaction amount. The result in (*iii*) states that any transaction between nodes of $\mathcal{N}_a$ ($\mathcal{N}_b$) results in *0* net power flow across the minimal cutset. Next,

54

we extend the development in this section to construct the proposed approach.

3.3 Detection of Island Formation

We consider a set of α outaged lines denoted by $\tilde{\mathcal{L}}_{(\alpha)} = \{\tilde{\ell}_1, \tilde{\ell}_2, \cdots, \tilde{\ell}_\alpha\}$ which need

not be a cutset. To determine whether $\tilde{\mathcal{L}}_{(\alpha)}$ contains one or more minimal cutsets, we

make use of the GLODFs. For line $\ell_r \notin \tilde{\mathcal{L}}_{(\alpha)}$ with all the α lines in $\tilde{\mathcal{L}}_{(\alpha)}$ outaged, the

vector $\underline{\xi}_{\ell_r}^{\tilde{\mathcal{L}}_{(\alpha)}} \in \mathbb{R}^\alpha$ is given:

$$\underline{\boldsymbol{H}}_\alpha^T \, \underline{\xi}_{\ell_r}^{\tilde{\mathcal{L}}_{(\alpha)}} = \left[\varphi_{\ell_r}^{w(\tilde{\ell}_1)}, \varphi_{\ell_r}^{w(\tilde{\ell}_2)}, \cdots, \varphi_{\ell_r}^{w(\tilde{\ell}_\alpha)} \right]^T , \tag{3.10}$$

where

$$\underline{\boldsymbol{H}}_\alpha \triangleq \left[\underline{\boldsymbol{I}} - \boldsymbol{\varPhi}_{\tilde{\mathcal{L}}_{(\alpha)}} \right] = \begin{bmatrix} 1 - \varphi_{\tilde{\ell}_1}^{w(\tilde{\ell}_1)} & \cdots & -\varphi_{\tilde{\ell}_1}^{w(\tilde{\ell}_\alpha)} \\ \vdots & \ddots & \vdots \\ -\varphi_{\tilde{\ell}_\alpha}^{w(\tilde{\ell}_1)} & \cdots & 1 - \varphi_{\tilde{\ell}_\alpha}^{w(\tilde{\ell}_\alpha)} \end{bmatrix} . \tag{3.11}$$

As long as $\underline{\boldsymbol{H}}_\alpha$ is nonsingular, (3.10) uniquely determines the LODFs for a line

$\ell_r \notin \tilde{\mathcal{L}}_{(\alpha)}$ of the outaged lines in $\tilde{\mathcal{L}}_{(\alpha)}$. $\underline{\boldsymbol{H}}_\alpha$ also possesses a key characteristic which will

be utilized in the development of the proposed approach. To present such a characteristic,

we construct the PTDF matrix for the entire set of $\mathcal{L}$:

$$\boldsymbol{\varPhi}_{\mathcal{L}} = \underline{\boldsymbol{\varPsi}} \, \underline{\boldsymbol{A}}^T = \boldsymbol{B}_d \, \underline{\boldsymbol{A}} \left(\underline{\boldsymbol{A}}^T \, \boldsymbol{B}_d \, \underline{\boldsymbol{A}} \right)^{-1} \underline{\boldsymbol{A}}^T , \tag{3.12}$$

55

an $L \times L$ matrix with the element $\varphi_{\ell_s}^{w(\ell_r)}$ in row m and column k. We use the notation $w(\ell_r) = \{i_r, j_r, t\}$, since $\varphi_{\ell_s}^{w(\ell_r)}$ is defined for the transaction between the terminal node pairs $\{i_r, j_r\}$ of ℓ_k as opposed to $\varphi_{\ell_r}^{w}$, where the transaction is defined between any node pair $\{i, j\}$. We can show that $\underline{A} \left(\underline{A}^T \underline{B}_d \underline{A} \right)^{-1} \underline{A}^T$ is symmetric positive definite. Since the diagonal elements of the diagonal matrix $\underline{B}_d$ are positive, $\underline{\Phi}_{\mathcal{L}}$ is structurally symmetric with

$$
\begin{aligned}
1 \geq \; &\varphi_{\ell_r}^{w(\ell_r)} \; > 0, \qquad \ell_r \in \mathcal{L} \\
&\varphi_{\ell_r}^{w(\ell_p)} \varphi_{\ell_s}^{w(\ell_r)} \geq 0, \qquad \ell_s, \ell_r \in \mathcal{L}.
\end{aligned}
\tag{3.13}
$$

Since $\underline{\Phi}_{\tilde{\mathcal{L}}_{(\alpha)}}$ is a submatrix of $\underline{\Phi}_{\mathcal{L}}$, its components satisfy (3.13). Consequently, the components of $\underline{H}_\alpha$ satisfy

$$
1 > h_{i,i} \geq 0 \quad , \qquad h_{i,j} h_{j,i} \geq 0 \quad i, j = 1, \cdots, \alpha . \tag{3.14}
$$

We derive an important relationship between the singularity of $\underline{H}_\alpha$ and the existence of minimal cutsets in $\tilde{\mathcal{L}}_{(\alpha)}$ in the following theorem.

Theorem 3.2: *Let* $\mathcal{G} = (\mathcal{N}, \mathcal{L})$ *be a connected power system network. For a set of* α *outaged lines* $\tilde{\mathcal{L}}_{(\alpha)} = \{\tilde{\ell}_1, \tilde{\ell}_2, \cdots, \tilde{\ell}_\alpha\}$,

$\underline{H}_\alpha$ *is singular* $\Leftrightarrow$ $\tilde{\mathcal{L}}_{(\alpha)}$ *contains one or more minimal cutsets.*

■

We provide the proof in Appendix A. The singularity of $\underline{\boldsymbol{H}}_\alpha$ is equivalent to the existence of a $\underline{\boldsymbol{u}} \in \mathbb{R}^\alpha$, such that $\underline{\boldsymbol{u}}^T \underline{\boldsymbol{H}}_\alpha = \underline{\boldsymbol{0}}^T$. By definition, $\underline{\boldsymbol{u}}$ is a (left) eigenvector corresponding to a zero eigenvalue of $\underline{\boldsymbol{H}}_\alpha$, i.e., $\underline{\boldsymbol{u}}$ is an element of the left nullspace $\mathfrak{N}\left(\underline{\boldsymbol{H}}_\alpha^T\right)$, where

$$\mathfrak{N}\left(\underline{\boldsymbol{H}}_\alpha^T\right) = \left\{\underline{\boldsymbol{x}}: \ \underline{\boldsymbol{x}}^T \underline{\boldsymbol{H}}_\alpha^T = \underline{\boldsymbol{0}}^T \ , \quad \underline{\boldsymbol{x}} \neq \underline{\boldsymbol{0}}\right\}. \tag{3.15}$$

If $\underline{\boldsymbol{H}}_\alpha$ has $\rho(\alpha)$ zero eigenvalues, we can use Theorem 3.2 and show that each zero eigenvalue has a unique (up to a scaling factor) eigenvector $\underline{\boldsymbol{u}}^i$, and is distinct, [3] $i = 1, \cdots, \rho(\alpha)$. Consequently, $\left\{\underline{\boldsymbol{u}}^i : i = 1, \cdots, \rho(\alpha)\right\}$ forms a basis for $\mathfrak{N}\left(\underline{\boldsymbol{H}}_\alpha^T\right)$.

Theorem 3.2 provides graph theoretic insights into minimal cutsets. In the realm of the rank of $\underline{\boldsymbol{H}}_\alpha$, we establish that the $rank\left(\underline{\boldsymbol{H}}_\alpha\right) = \alpha - \rho(\alpha)$ and so there is equivalence of the existence of $\rho(\alpha)$ minimal cutsets in $\tilde{\mathcal{L}}_{(\alpha)}$ with that rank. We denote each such minimal cutset by $\hat{\mathcal{L}}^i$, $i = 1, \cdots, \rho(\alpha)$. By definition, $\hat{\mathcal{L}}^i$ partitions $\mathcal{G} = (\mathcal{N}, \mathcal{L})$ into the disjoint subnetworks $\mathcal{G}_a^i = \left(\mathcal{N}_a^i, \mathcal{L}_a^i\right)$ and $\mathcal{G}_b^i = \left(\mathcal{N}_b^i, \mathcal{L}_b^i\right)$.

We next find a basis for $\rho(\alpha)$ dimensional $\mathfrak{N}\left(\underline{\boldsymbol{H}}_\alpha^T\right)$ by the *rank revealing* QR (RRQR) factorization [94] - [96], of $\underline{\boldsymbol{H}}_\alpha^T$:

$$\underline{\boldsymbol{H}}_\alpha^T \underline{\boldsymbol{P}} = \underline{\boldsymbol{Q}}\,\underline{\boldsymbol{R}} = \begin{bmatrix} \underline{\boldsymbol{Q}}_{\omega(\alpha)} & \underline{\boldsymbol{Q}}_{\rho(\alpha)} \end{bmatrix} \begin{bmatrix} \underline{\boldsymbol{R}}_{\omega(\alpha),\omega(\alpha)} & \underline{\boldsymbol{R}}_{\omega(\alpha),\rho(\alpha)} \\ \underline{\boldsymbol{0}} & \underline{\boldsymbol{R}}_{\rho(\alpha),\rho(\alpha)} \end{bmatrix}, \tag{3.16}$$

---

[3] In fact, the Jordan canonical form of $\underline{\boldsymbol{H}}_\alpha$ has Jordan submatrices that correspond to the 0 eigenvalues with "order unity" [94].

where $\omega(\alpha) \triangleq \alpha - \rho(\alpha)$. Here, $\underline{\boldsymbol{R}}_{\rho(\alpha),\rho(\alpha)} \in \mathbb{R}^{\rho(\alpha),\rho(\alpha)}$ is the submatrix with the 0 diagonal elements. The set of the columns of the $\underline{\boldsymbol{Q}}_{\rho(\alpha)}$ forms an orthonormal basis for the nullspace of $\mathfrak{N}(\underline{\boldsymbol{H}}_\alpha^T)$ [96]. We next transform this basis so as to identify the elements in each minimal cutset using the transformation matrix $\underline{\boldsymbol{T}} \in \mathbb{R}^{\rho(\alpha),\rho(\alpha)}$:

$$\left[\underline{\boldsymbol{v}}_1 \vdots \underline{\boldsymbol{v}}_2 \vdots \cdots \vdots \underline{\boldsymbol{v}}_{\rho(\alpha)} \right] \underline{\boldsymbol{T}} = \underline{\boldsymbol{Q}}_{\rho(\alpha)}. \qquad (3.17)$$

The construction of $\underline{\boldsymbol{T}}$ is detailed in the following analysis. The set of columns of $\underline{\boldsymbol{Q}}_{\rho(\alpha)}$ and $\{\underline{\boldsymbol{v}}_1, \underline{\boldsymbol{v}}_2, \cdots, \underline{\boldsymbol{v}}_{\rho(\alpha)}\}$ form a basis for $\mathfrak{N}(\underline{\boldsymbol{H}}_\alpha^T)$. Therefore, $\underline{\boldsymbol{Q}}_{\rho(\alpha)}$ and $\left[\underline{\boldsymbol{v}}_1 \vdots \underline{\boldsymbol{v}}_2 \vdots \cdots \vdots \underline{\boldsymbol{v}}_{\rho(\alpha)} \right]$ are full rank arrays. We define $\underline{\boldsymbol{T}}$ to be the matrix in $\mathbb{R}^{\rho(\alpha) \times \rho(\alpha)}$ relating the two sets of vectors: $\left[\underline{\boldsymbol{v}}_1 \vdots \underline{\boldsymbol{v}}_2 \vdots \cdots \vdots \underline{\boldsymbol{v}}_{\rho(\alpha)} \right] \underline{\boldsymbol{T}} = \underline{\boldsymbol{Q}}_{\rho(\alpha)}$. Since the components of each $\underline{\boldsymbol{v}}_i$, $i = 1, \cdots, \rho(\alpha)$, satisfy (A.13), we can reorder the rows of $\left[\underline{\boldsymbol{v}}_1 \vdots \underline{\boldsymbol{v}}_2 \vdots \cdots \vdots \underline{\boldsymbol{v}}_{\rho(\alpha)} \right]$, introduce multiplication by -1 where necessary, and perform identical operations on the corresponding rows of $\underline{\boldsymbol{Q}}_{\rho(\alpha)}$ to obtain the first $\rho(\alpha)$ elements as the identity matrix. We denote the other rows of $\left[\underline{\boldsymbol{v}}_1 \vdots \underline{\boldsymbol{v}}_2 \vdots \cdots \vdots \underline{\boldsymbol{v}}_{\rho(\alpha)} \right]$ by $\underline{\boldsymbol{V}}$.

Then the transformation that relates the rearranged rows of the two rearranged bases is

$$\begin{bmatrix} \underline{\boldsymbol{Q}}'_{\rho(\alpha)} \\ \underline{\boldsymbol{Q}}''_{\rho(\alpha)} \end{bmatrix} = \begin{bmatrix} \underline{\boldsymbol{I}}^{\rho(\alpha)} \\ \underline{\boldsymbol{V}} \end{bmatrix} \underline{\boldsymbol{T}} = \left[\hat{\underline{\boldsymbol{v}}}_1 \vdots \hat{\underline{\boldsymbol{v}}}_2 \vdots \cdots \vdots \hat{\underline{\boldsymbol{v}}}_{\rho(\alpha)} \right], \qquad (3.18)$$

where each $\hat{\underline{\boldsymbol{v}}}_i$ also satisfies (A.13). So, $\underline{\boldsymbol{T}} = \underline{\boldsymbol{Q}}'_{\rho(\alpha)}$. It follows that $\{\underline{\boldsymbol{v}}^i : i = 1, \cdots, \rho(\alpha)\}$ is a basis for $\mathfrak{N}(\underline{\boldsymbol{H}}_\alpha^T)$ with

$$|v_r^i| = \begin{cases} 1, & \tilde{\ell}_r \in \hat{\boldsymbol{\mathcal{L}}}^i \\ 0, & \tilde{\ell}_r \notin \hat{\boldsymbol{\mathcal{L}}}^i \end{cases} . \tag{3.19}$$

Each $\underline{\boldsymbol{v}}^i$, $i = 1, \cdots, \rho(\alpha)$, identifies the elements of the corresponding minimal cutset, i.e., the subset of lines without which the system separates into two islands. For two lines $\tilde{\ell}_r, \tilde{\ell}_s \in \hat{\boldsymbol{\mathcal{L}}}^i$, we check $\delta_{r,s} = sign\{ v_r^i v_s^i \}$. If $\delta_{r,s} > 0$, then both of the from terminal nodes $\tilde{i}_r$ and $\tilde{i}_s$ are in the same island, which is different than the island of those of the terminal nodes $\tilde{j}_r$ and $\tilde{j}_s$. For $\delta_{r,s} < 0$, however, $\tilde{i}_r$ and $\tilde{i}_s$ ($\tilde{j}_r$ and $\tilde{j}_s$) are in two separate islands.

The analysis of $\underline{\boldsymbol{H}}_\alpha$ provides insights into the formation of islands under multiple line outages. For detection of island formation we use Gaussian elimination, and for identification of the elements of each minimal cutset we obtain the RRQR factors of $\underline{\boldsymbol{H}}_\alpha^T$. In the Gaussian elimination of $\underline{\boldsymbol{H}}_\alpha$, a zero diagonal element at some elimination step r corresponds to

$$h_{i,i}^{(r)} = 1 - \left(\varphi_{\tilde{\ell}_i}^{w(\tilde{\ell}_i)} \right)^{\tilde{\mathcal{L}}_{(r-1)}} = 0 . \tag{3.20}$$

By Theorem 3.2, then, there exists at least one minimal cutset contained in $\tilde{\mathcal{L}}_{(\alpha)}$ and therefore the outages of the elements of $\tilde{\mathcal{L}}_{(\alpha)}$ are responsible for the formation of two or more islands. We stop the Gaussian elimination process and proceed with the RRQR factorization of $\underline{\boldsymbol{H}}_\alpha^T$. The relations in (3.16) and (3.17) establish the number of minimal

cutsets and the identity of the elements of each minimal cutset. Moreover, the sign of each pair of $\delta_{r,s}$ in each minimal cutset provides the location of the terminal nodes with respect to the formed islands.

We determine an analytic bound for the total number of multiplication/division operations required in the detection of island formation. For the outage of a set of k-lines, the construction of $\underline{\boldsymbol{H}}_r$ requires no such operations. We note that the dimension of $\underline{\boldsymbol{H}}_r$ is considerably smaller than that of the topological arrays $\underline{\boldsymbol{B}}$ and $\underline{\boldsymbol{A}}$. For this single set of k-line outages, the number of multiplication/division operations in the Gaussian elimination is $O(r^3)$ [94]. When additional line outages are considered, the factors of $\underline{\boldsymbol{H}}_k$ are used. For a single additional line, the number of multiplication/division operations is $O(r^2)$. Then for, say, q additional line outages, the number of multiplication/division operations is $O(qr^2)$. Note that these bounds represent "worst case conditions" since no computations are performed once a 0 diagonal element is detected, which may be done by inspection.

A salient feature of the proposed approach is its low computational requirements as the computations are carried out on matrices whose dimension is the number of outaged lines. These computations take advantage of the structural characteristics of the proposed method whereby a set of r-line outages serves to establish the results of any larger set of outaged lines containing this r-line set as a subset. In this way, we can directly pinpoint the impact of the interactions between the additional line outage and the r-line outages as a causal factor for island formation. For this reason, the proposed method is particularly useful in the analysis of appropriate preventive/corrective control actions in cases

involving the *domino effect* of multiple line outages to effectively mitigate the impacts of such a sequence of outages.

3.4 Illustrative Example: The IEEE 118-Bus System

The implementation of the proposed approach is straightforward. We illustrate the application of the proposed approach to the IEEE 118-bus system. In the connected IEEE 118-bus system, we select a subset of 7 of the 194 lines and study the impacts of the outages of this subset. The line definitions and the PTDFs are given in Table 3.1.

Table 3.1 The PTDF Values for a Subset of Outaged Lines

line		PTDF						
id	node pairs	$w(\tilde{\ell}_1)$	$w(\tilde{\ell}_2)$	$w(\tilde{\ell}_3)$	$w(\tilde{\ell}_4)$	$w(\tilde{\ell}_5)$	$w(\tilde{\ell}_6)$	$w(\tilde{\ell}_7)$
$\tilde{\ell}_1$	(6,7)	0.8571	-0.0145	-0.0195	-0.0103	-0.0005	-0.001	0.0002
$\tilde{\ell}_2$	(33,37)	-0.0021	0.6045	0.2075	-0.0926	0.0113	0.0226	-0.0041
$\tilde{\ell}_3$	(19,34)	-0.0016	0.1193	0.3115	-0.0913	0.0126	0.0251	-0.0045
$\tilde{\ell}_4$	(38,30)	-0.0040	-0.2435	-0.4177	0.7644	-0.0471	-0.0938	0.0170
$\tilde{\ell}_5$	(23,24)	-0.0002	0.0327	0.0633	-0.0517	0.9290	-0.1414	0.0256
$\tilde{\ell}_6$	(24,72)	-0.0001	0.0163	0.0316	-0.0258	-0.0355	0.6911	0.0559
$\tilde{\ell}_7$	(70,71)	0.0001	-0.0163	-0.0316	0.0258	0.0355	0.3089	0.9441

For $\tilde{\mathcal{L}}_{(7)} = \{\tilde{\ell}_1, \tilde{\ell}_2, \cdots, \tilde{\ell}_7\}$ we compute $\underline{H}_7$ and perform the Gaussian elimination, which produces a zero diagonal element at step 5. The RRQR factorization for this matrix determines

$$
\underline{R} = \begin{bmatrix}
-0.8354 & 0.0707 & 0.0022 & -0.0061 & -0.1644 & -0.0004 & -0.0079 \\
0 & -0.4761 & -0.0043 & -0.0086 & -0.1939 & 0.0007 & -0.0117 \\
0 & 0 & 0.4698 & 0.0010 & 0.0862 & -0.0850 & 0.0786 \\
0 & 0 & 0 & 0.1425 & 0.0000 & 0.0000 & 0.0000 \\
0 & 0 & 0 & 0 & -0.0666 & 0.0000 & -0.0607 \\
0 & 0 & 0 & 0 & 0 & 0.0000 & 0.0000 \\
0 & 0 & 0 & 0 & 0 & 0 & 0.0000
\end{bmatrix}, (3.21)
$$

where the two *0* diagonal elements indicate that $\rho(7) = 2$. The corresponding $\underline{Q}_{\rho(7)}$

given by (3.16) is

$$
\underline{Q}_{\rho(7)} = \begin{bmatrix}
0.0000 & -0.0319 & -0.0319 & 0.0319 & -0.0319 & -0.7056 & -0.7056 \\
0.0000 & -0.4989 & -0.4989 & 0.4989 & -0.4989 & 0.0451 & 0.0451
\end{bmatrix}^T .(3.22)
$$

The two vectors in $\mathbb{R}^7$ given in (3.22) span $\mathfrak{N}(\underline{H}_7^T)$. We construct the transformation

matrix

$$
\underline{T} = \begin{bmatrix}
-0.4989 & -0.0319 \\
0.0451 & -0.7056
\end{bmatrix}, \tag{3.23}
$$

and obtain the transformed basis vector

$$
\begin{bmatrix} \underline{v}_1 \vdots \underline{v}_2 \end{bmatrix} = \begin{bmatrix}
0 & 1 & 1 & -1 & 1 & 0 & 0 \\
0 & 0 & 0 & 0 & 0 & 1 & 1
\end{bmatrix}^T . \tag{3.24}
$$

It follows that the zero diagonal element in the Gaussian elimination implies that the

system separates into two or more islands when all seven lines are outaged. However,

since $\rho(7) = 2$, we established that there exist two minimal cutsets in the set of $\tilde{\mathcal{L}}_{(7)}$

outaged lines.

Table 3.2 IEEE 118-Bus System: $\tilde{\mathcal{L}}_{(7)}$ **Minimal Cutset Information**

$\hat{\mathcal{L}}^i$	nodes belonging to $\mathcal{N}_a^i$	nodes belonging to $\mathcal{N}_b^i$
$\{\tilde{\ell}_2, \tilde{\ell}_3, \tilde{\ell}_4, \tilde{\ell}_5\}$	19, 23, 30, 33	24, 34, 37, 38
$\{\tilde{\ell}_6, \tilde{\ell}_7\}$	24, 70	71, 72

The components of $\underline{v}_1$ and $\underline{v}_2$ allow us to identify the members of the two minimal cutsets as shown in Table 3.2. We use the relative sign difference of the elements of $\underline{v}_1$ $(\underline{v}_2)$ to determine the nodes of the subnetworks to which the terminal nodes of the lines of in each minimal cutset belong. Thus, the Gaussian elimination and the RRQR factorization provide comprehensive information on the impacts of the outages of the seven lines for the IEEE 118-bus system case.

3.5 Summary

We develop a combined graph-theoretic-algebraic approach to detect island formation in power system networks under multiple line outages. We effectively combine the characterization of the connectivity from a graph-theoretic viewpoint with that from the circuit theoretic notions to construct the proposed approach. The approach is able to detect island formation under multiple line outages and to identify which outaged lines cause the system separation. In cases where several lines are outaged and no island formation occurs, the method can identify whether a set of candidate line outages separates the system into islands. Such identification provides the information needed for the deployment of appropriate tools for security assessment.

A salient feature of the proposed approach is its low computational requirements – a function simply of the number of outaged lines and not of the size of the system. The

approach provides an effective tool for both planning and system operations for security analysis and control. In particular, the scheme serves well in the formulation of appropriate preventive/corrective control actions in cases involving the *domino effect* of sequential multiple line outages so as to effectively mitigate the ensuing impacts.

CHAPTER 4

SIDE-BY-SIDE OPERATIONS OF THE POWER SYSTEM
AND THE ELECTRICITY MARKETS

Security management is a highly challenging task, and even more so in the more complex market environment. In fact, the tight coupling between market and system operations under restructuring requires a thorough understanding of the interdependence between the way the power systems are operated and the performance of the electricity markets. As system and market operations strongly interact, the assurance of secure power system operations impacts the economics and vice-versa. As such, the simultaneous accommodation of all the *desired* transactions of market participants for a given system snapshot of interest may not be feasible due to the constraining effects of the secure power system operations. While the nature of these interactions is well understood on a qualitative basis, the quantification of the system security impacts on the overall economics of electricity markets is, typically, not performed. The key steps in the effort for such quantification are the formulation and solution of the problem that capture the way that both the system and the markets are managed. This and the following two chapters aim to provide the formulation of this problem for different levels of detail and its appropriate solutions.

In this chapter, we explicitly consider the market and the system operations from the point of view of the IGO. We use the models developed in Chapter 2 for the security management and describe the way the IGO clears the market. While there are different

market implementations in the various jurisdictions around the world, we concentrate on the typical market structure widely adopted in North American markets with uniform price auction coexisting side-by-side with bilateral transactions. Such market implementations are consistent with the basic guidelines in FERC blueprints [1], [2] and market design proposals [49] - [51]. Actual implementations include ISO New England (ISO-NE) [97], Pennsylvania–New Jersey–Maryland ISO (PJM-ISO) [98], and New York ISO (NY-ISO) [99]. For each system snapshot used to describe the IGO decision making problem at a given point of time of the system, we formulate a security-constrained OPF (SCOPF) problem under the specified security criterion. This system snapshot SCOPF problem has the objective to maximize auction surplus under constraints that are imposed on power system and market operations. In a highly competitive market environment and a uniform price auction mechanism, the market participants tend to reveal their true marginal costs and benefits [6]. Under such conditions, the auction surplus becomes a good proxy for the social welfare and, therefore, an appropriate approximation of the economic efficiency of the markets [6]. The formulation takes explicitly into account the physics of the multiarea structure and the security criterion in force. As such, we consider the set of contingencies postulated by the criterion, as well as control actions associated with each contingency – be they corrective or preventive. The SCOPF formulation and solution serve as the tool for the quantification of the economics of secure power system operations.

This chapter contains three sections. We devote Section 4.1 to provide a brief review of the basic structure of the electricity markets for the MWh commodity. In Section 4.2, we discuss the decision making problem of the IGO and introduce the SCOPF problem

formulation and solution. We discuss the metrics of interest for use in the quantification of the impacts of secure power system operations on the performance of electricity markets. We summarize the chapter's results in Section 4.3.

4.1 The Basic Structure of Electricity Markets

In this dissertation, we adopt the timeline typically used in system and market operations analysis [66]. We consider a specific snapshot of the system state and a sequence of electricity commodity markets associated with that state. The electricity markets in this sequence are held at different points in time ranging from a year- and a month-ahead – the so-called forward markets – to a day- and hour-ahead – the so-called spot markets – and to minutes-ahead – the so-called real-time markets. We display in Figure 4.1 a possible sequence of forward, day-ahead spot and associated real-time markets for the hour h.
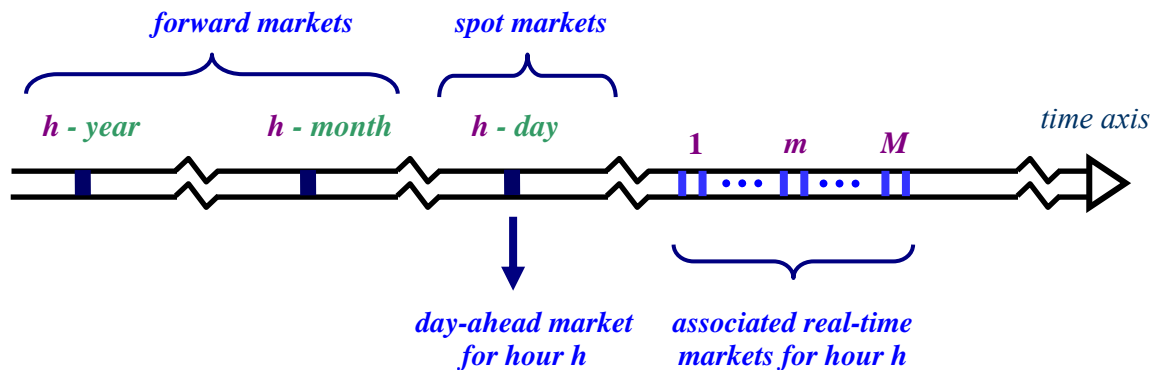

Figure 4.1 Time frame for the electricity markets

Our focus in this work is on the day-ahead spot markets and their associated real-time markets. Each market, be it a day-ahead hourly market or one of the associated real-time

markets, trades the MWh commodity at different prices that reflect the information on the system and market conditions available at the time the MWh commodity is cleared. As these conditions are subject to continuous changes in real time, real-time markets (RTMs) are cleared at a high frequency, typically every 5 min. On the other hand, markets that run ahead of real-time system operations have a lower clearing frequency, e.g., hourly clearing in the day-ahead markets (DAMs), reflecting the lower resolution of the imperfect information on the real-time conditions in the next day. The hour h DAM is cleared on the forecasts of the real-time conditions for that hour the next day. The hourly clearing influences each RTM in the near real-time during that hour. The RTM clearing determines the volume of deviations from the hour h DAM value and the associated price. Such a market design with different lead times and clearing frequencies is commonly referred to as a *multi-settlement system*. In this chapter, we focus on the clearing of a given market, and in Chapter 6 we analyze in detail the interrelated settlement of the multiple markets at different points in time.
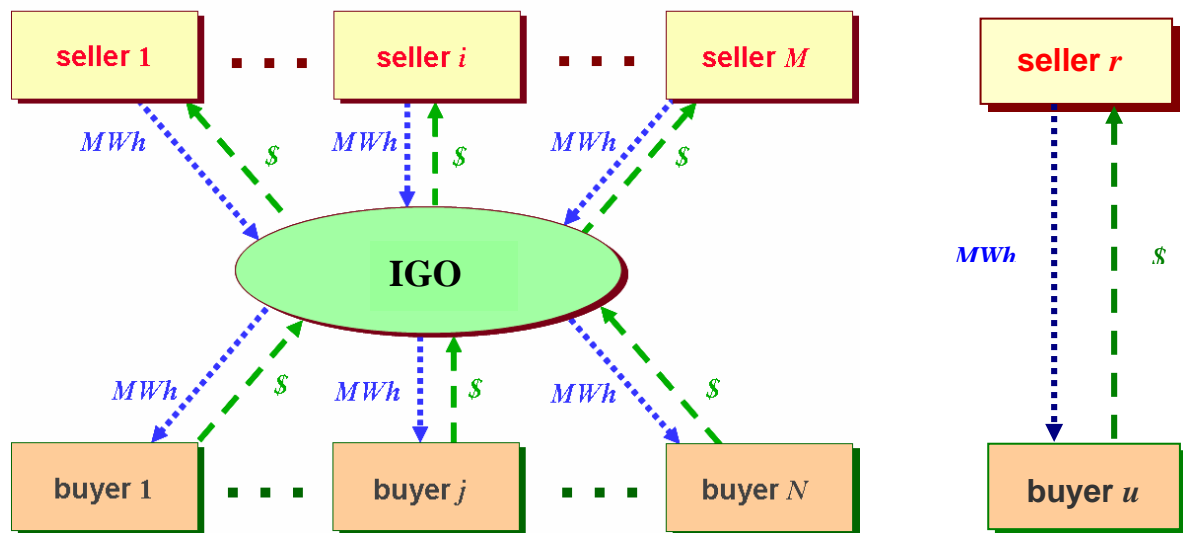

Figure 4.2 The players in the electricity markets

68

We represent the basic structure of a single market for a system snapshot in Figure 4.2. In this market, the sellers indicate their willingness to sell electricity to the IGO by submitting sealed offers specifying the quantities and prices for sale. At the same time, the pool buyers submit sealed bids to indicate their willingness to buy the electricity from the IGO. We also consider the bilateral transactions in which the electricity is traded directly between a selling entity and a buying entity. Each transaction submits a willingness to pay function, which states a willingness to pay maximum transmission usage fee for receiving the requested transmission services as a function of the transaction amount delivered. From the collection of these offers, bids, and the willingness to pay functions of the transactions, the IGO determines the market clearing that ensures feasible system operations under a specified security criterion. In the next section, we discuss the formulation of the market-system snapshot problem and provide the metrics necessary to be deployed in the quantification of the economics of secure power system operations.

4.2 Formulation of the Market-System Snapshot Problem

The IGO decision making problem for a given snapshot of the system under a specified security criterion takes explicitly into account the multiarea structure and the constraints imposed by the tie line limits. We introduce specific assumptions on unit commitment decisions, ancillary services and the market participants' behaviors. We assume that the unit commitment decisions fully reflect the requirements of the security criterion under consideration. In particular, this assumption ensures the feasibility of meeting the system fixed demands under such a criterion. As the focus of this

investigation is limited to energy-only markets, we assume that the ancillary services provision and acquisition requirements under the IGO framework do not impose any additional constraints on the system. For the purposes of this study, we furthermore assume that the bidding behavior of each market participant is independent of the security criterion in force. Since we replicate the IGO actions, we ensure compliance with the security criterion in force, but implicitly ignore the probability of any contingency in the studies.

The modeling of the large-scale interconnected system operated by the IGO requires the explicit representation of the areas that make up the system as well the tie lines that interconnect them in market and system operations. We consider a power system network consisting of K interconnected areas denoted by the set $\boldsymbol{a} \triangleq \{ \mathcal{A}^k : k=1,\ldots,K\}$ with each area $\mathcal{A}^k$ having a node set $\boldsymbol{\mathcal{N}}^k$ with N^k buses. Each area $\mathcal{A}^k \in \boldsymbol{a}$ is connected to one or more other areas via tie lines. We associate a security criterion $\mathcal{C}$ with a specific contingency list and a specified control action – preventive or corrective – for every contingency on that list.

While the interconnected system has a single market operated by the IGO, the presence of network and physical constraints necessitate that we consider the market players in each area separately. We assume without loss of generality, that at each bus $i \in \boldsymbol{\mathcal{N}}^k$ there are four market participants: a seller with a generating unit, a buyer associated with a physical load, a financial seller and a financial buyer. We denote by the sets $\mathcal{S}^{k,r}$ and $\mathcal{B}^{k,r}$ the collection of sellers with generating resources and that of buyers with physical load of the area $\mathcal{A}^k \in \boldsymbol{a}$, respectively. Similarly, we denote by the sets

$\mathscr{S}^{k,f}$ and $\mathscr{B}^{k,f}$ the collection of financial sellers and buyers of the area $\mathscr{A}^k \in \mathcal{A}$, respectively. We define the set of sellers by the collection of $\mathscr{S} \triangleq \bigcup_{k=1}^{K} \left(\mathscr{S}^{k,r} \cup \mathscr{S}^{k,f} \right)$ and the set of buyers by the collection of $\mathscr{B} \triangleq \bigcup_{k=1}^{K} \left(\mathscr{B}^{k,r} \cup \mathscr{B}^{k,f} \right)$. Each seller (buyer) submits price and quantity offer (bid) function indicating the willingness to sell (buy) the amount of energy to (from) the IGO. Bilateral transactions coexist with the IGO market operations. We represent a bilateral transaction ω_w, whose *from* node is $m_w \in \mathcal{N}^k$ of $\mathscr{A}^k$, *to* node is $n_w \in \mathcal{N}^r$ of $\mathscr{A}^r$, and desired transaction amount is $\bar{t}_w$, by the triplet $\omega_w \triangleq \{m_w, n_w, \bar{t}_w\}$. Here k and r are indices that may represent different areas. The set of bilateral transactions is $\mathcal{W} = \{\omega_1, \cdots, \omega_W\}$. Each transaction submits a willingness to pay function, which states a willingness to pay maximum transmission usage fee for receiving the requested transmission services as a function of the transaction amount delivered [66].

We define the total injection amount at bus $i \in \mathcal{N}^k$ for $\mathscr{A}^k \in \mathcal{A}$ as

$$g_i^k \triangleq \sum_{\substack{s \in \mathscr{S}^{k,r} \\ \text{at node } i \in \mathcal{N}^k}} p_s + \sum_{\substack{\tilde{s} \in \mathscr{S}^{k,f} \\ \text{at node } i \in \mathcal{N}^k}} p_{\tilde{s}} + \sum_{\substack{w \in \mathcal{W} \\ i = m_w \in \mathcal{N}^k}} t_w, \qquad (4.1)$$

and the total withdrawal amount at the same bus as

$$d_i^k \triangleq \sum_{\substack{b \in \mathscr{B}^{k,r} \\ \text{at node } i \in \mathcal{N}^k}} p_b + \sum_{\substack{\tilde{b} \in \mathscr{B}^{k,f} \\ \text{at node } i \in \mathcal{N}^k}} p_{\tilde{b}} + \sum_{\substack{w \in \mathcal{W} \\ i = n_w \in \mathcal{N}^k}} t_w. \qquad (4.2)$$

71

We use g_i^k, d_i^k and construct the areawide injection vector $\underline{g}^k$ and the areawide withdrawal vector $\underline{d}^k$, respectively. We define the vector of systemwide injection

$$\underline{g} = \left[\left(\underline{g}^1 \right)^T, \cdots, \left(\underline{g}^K \right)^T \right] \qquad \text{and} \qquad \text{the} \qquad \text{systemwide} \qquad \text{withdrawal} \qquad \text{vector}$$

$$\underline{d} = \left[\left(\underline{d}^1 \right)^T, \cdots, \left(\underline{d}^K \right)^T \right], \text{ respectively.}$$

The IGO uses the willingness to pay of the bilateral transactions along with that of the individual market participants to determine the amount of transmission service provision to each player. For this purpose for a given snapshot of the system, the IGO solves a security constrained OPF, or SCOPF, problem with the objective to maximize the auction surplus under the security criterion $\mathcal{C}$ whose contingency index set is denoted by $\mathcal{J}_c$. We state the SCOPF problem as

$$max \;\; \mathcal{S} \triangleq \sum_{k=1}^{K} \left(\sum_{b \in \mathcal{B}^k} \beta_b \left(p_b^{(0)} \right) - \sum_{s \in \mathcal{S}^k} \beta_s \left(p_s^{(0)} \right) \right) + \sum_{w \in \mathcal{W}} \alpha_w \left(t_w^{(0)} \right) \tag{4.3}$$

subject to base case constraints

$$\sum_{s \in \mathcal{S}} p_s^{(0)} - \sum_{b \in \mathcal{B}} p_b^{(0)} = 0 \qquad\qquad \leftrightarrow \lambda^{(0)} \tag{4.4}$$

$$\underline{f}^{min^{(0)}} \leq \underline{\Psi}^{(0)} \left(\underline{g}^{(0)} - \underline{d}^{(0)} \right) \leq \underline{f}^{max^{(0)}} \qquad \leftrightarrow \underline{\mu}_+^{(0)}, \underline{\mu}_-^{(0)} \tag{4.5}$$

for every $j \in \mathcal{J}_e$

$$\sum_{s \in \mathcal{S}} p_s^{(j)} - \sum_{b \in \mathcal{B}} p_b^{(j)} = 0 \qquad\qquad \leftrightarrow \lambda^{(j)} \tag{4.6}$$

$$\underline{f}^{min^{(j)}} \leq \underline{\Psi}^{(j)} \left(\underline{g}^{(j)} - \underline{d}^{(j)} \right) \leq \underline{f}^{max^{(j)}} \qquad \leftrightarrow \underline{\mu}_+^{(j)}, \underline{\mu}_-^{(j)} \tag{4.7}$$

$$\Delta p_s^{min} \leq p_s^{(j)} - p_s^{(0)} \leq \Delta p_s^{max^{(j)}} \qquad\qquad \leftrightarrow \gamma_+^{(j)}, \gamma_-^{(j)}, \forall s \in \mathcal{S} \qquad\qquad (4.8)$$

$$\Delta p_b^{min} \leq p_b^{(j)} - p_b^{(0)} \leq \Delta p_b^{max^{(j)}} \qquad\qquad \leftrightarrow \rho_+^{(j)}, \rho_-^{(j)}, \forall b \in \mathcal{B} \qquad\qquad (4.9)$$

$$\Delta t_w^{min} \leq t_w^{(j)} - t_w^{(0)} \leq \Delta t_w^{max^{(j)}} \qquad\qquad \leftrightarrow \tau_+^{(j)}, \tau_-^{(j)}, \forall w \in \mathcal{W} \qquad\qquad (4.10)$$

and for every $j \in \{0\} \cup \mathcal{J}_e$

$$p_s^{min} \leq p_s^{(j)} \leq p_s^{max} \qquad\qquad \leftrightarrow \sigma_+^{(j)}, \sigma_-^{(j)}, \forall s \in \mathcal{S} \qquad\qquad (4.11)$$

$$p_b^{min} \leq p_b^{(j)} \leq p_b^{max} \qquad\qquad \leftrightarrow \kappa_+^{(j)}, \kappa_-^{(j)}, \forall b \in \mathcal{B} \qquad\qquad (4.12)$$

$$t_w^{min} \leq t_w^{(j)} \leq t_w^{max} \qquad\qquad \leftrightarrow \upsilon_+^{(j)}, \upsilon_-^{(j)}, \forall w \in \mathcal{W} \qquad\qquad (4.13)$$

Here, we use the notation $\vartheta^{(j)}$ to denote the value of the ϑ under the contingency case j with the base case denoted by 0. The vector or the scalar associated with the right-hand side of a constraint is the dual variable of that constraint. The relations in (4.4) and (4.5) represent the operational constraints for the base case, while those in (4.6) - (4.10) represent the operational constraints for the contingency cases. The equality constraints in (4.4) and (4.6) state the nodal power balance equations for the base case and for each postulated contingency case, respectively. The base case (4.5) and contingency case (4.7) inequality constraints state the transmission system operational limits. The range of the decision variables of the security control action for each contingency $j \in \mathcal{J}_e$ is given in (4.8) - (4.10), together with the limiting values of these ranges. The preventive control actions have a zero range in contrast to the corrective actions, whose nonzero range reflects the additional flexibility to address the onset of the contingency. Note that we explicitly take into account the costs of modifying the precontingency state but ignore any costs related to the postcontingency state modification. We refer to this SCOPF

problem as the market-system snapshot problem and denote it by $\mathcal{M}\left(\mathcal{S},\mathcal{B},\mathcal{W};\mathcal{C}\right)$.

With the contingency and base case constraints considered, the market may no longer have a unique clearing price. Such a situation arises because we explicitly consider the supply-demand balance at each of the buses of the system in the equality constraints of the $\mathcal{M}\left(\mathcal{S},\mathcal{B},\mathcal{W};\mathcal{C}\right)$. We analyze the characteristics of the optimal solution of the $\mathcal{M}\left(\mathcal{S},\mathcal{B},\mathcal{W};\mathcal{C}\right)$ in Appendix B. The different locational marginal prices (LMPs) at each node of the system may be evaluated by values of the dual variables as shown in (B.33):

$$\lambda_i = \left[\lambda^{(0)} + \left(\underline{\mu}_+^{(0)} - \underline{\mu}_-^{(0)} \right)^T \underline{\psi}_i^{(0)} \right] + \sum_{j \in \mathcal{S}_c} \left[\lambda^{(j)} + \left(\underline{\mu}_+^{(j)} - \underline{\mu}_-^{(j)} \right)^T \underline{\psi}_i^{(j)} \right]. \quad (4.14)$$

We note that the last term in (4.14) explicitly illustrates the contingency case constraints impacts on the LMPs. When any of these constraints is binding, the LMPs at each node may become different. Consequently, the nonzero LMP difference is an indication of the impacts of system operational constraints. When system constraints are binding, we refer to such a situation as system congestion. The LMP differences also yield nonnegative revenue for the IGO [66]. The IGO collects these revenues, which are given by

$$\mathcal{K} = \sum_{i=0}^{N} \sum_{\substack{b \in \mathcal{B} \\ at\ node\ i}} \lambda_i \ p_b^{(0)} - \sum_{i=0}^{N} \sum_{\substack{s \in \mathcal{S} \\ at\ node\ i}} \lambda_i \ p_s^{(0)} + \sum_{w=1}^{W} \left(\lambda_{m_w} - \lambda_{n_w} \right) t_w^{(0)}. \quad (4.15)$$

Such revenues are commonly referred as congestion rents. Since the IGO does not have any "financial position" [97] - [99], the collected congestion rents will be reallocated back to market participants [66]. As the focus of this work is on energy markets, we omit the analysis of various market based mechanisms [66] for this reallocation.

We distinguish between fixed demand buyers and those with price-responsive demand. The fixed demand bid is a special case of the price sensitive bid in which a specified quantity is submitted with no price information. Such a bid indicates an unlimited willingness to pay for the electricity purchases to meet the fixed quantity bid, i.e., the buyer is willing to pay any price to obtain the electricity. There are, however, difficulties in determining the appropriate value of the benefits of the fixed demand buyers. In order to include these buyers' benefits in the $\mathcal{M}(\mathcal{S},\mathcal{B},\mathcal{W};\mathcal{C})$ problem formulation (4.3) - (4.13), we use a constant per MWh benefit value, τ, for the fixed demand.

We conceptually represent the structure of the IGO decision making problem addressing the tight coupling between market and system operations in Figure 4.3. The multiarea system layer presents the modeling of the key physical elements of the power system including the multiarea structure of the region as discussed in Chapter 2. The relationship between the generation/demand at each node and line flows in each area and the interaction of the areas by the tie line flows are established. The system security issues are explicitly addressed in this layer. The market layer presents the modeling of the electricity market in terms of the bids and offers of sellers and buyers, respectively. This layer contains the representation of the determination of the market equilibrium which provides the resulting generation/demand schedule. The interaction between the two layers is through the information flows, as indicated in Figure 5.1 on page 81. The market layer provides the *preferred* inter- and intra-area transmission schedules, including the nodal injections and withdrawals. This information flows to the network layer so as to verify the feasibility of the desired transactions.
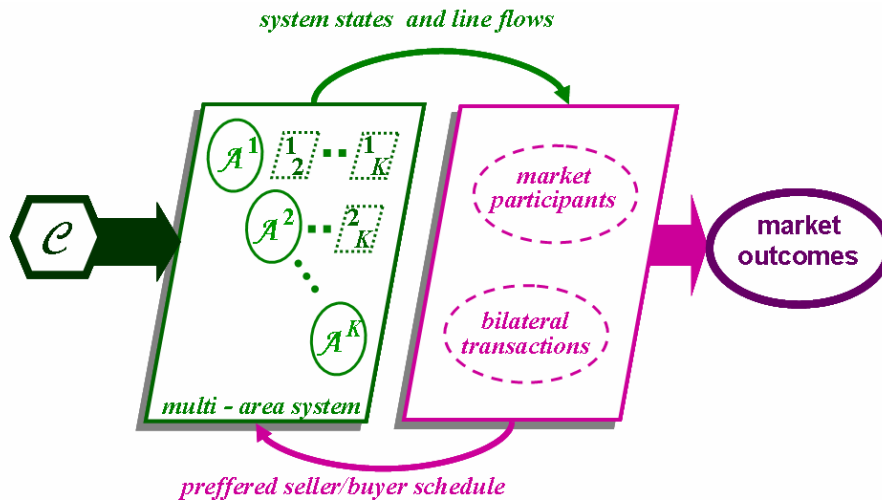
Figure 4.3 Conceptual structure for the market clearing

The market performance under the specified security criterion $\mathcal{C}$ for the snapshot system may be quantified from the market outcomes given by the solution of (4.3) - (4.13). The LMP (4.14) and congestion rent (4.15) metrics are also used for the development of additional metrics in the following two chapters in order to quantify the economics of secure power system operations.

4.3 Summary

In this chapter, we discuss the basic structure and modeling of the electricity markets and explicitly represent the tight coupling between system and market operations. We formulate the market-system snapshot problem based on the emulation of the way the IGO currently operates the market and the grid, the latter in compliance with the security criterion. The market-system snapshot problem takes into account the preferred seller/buyer schedule as well as bilateral transactions for a multiarea system as well as the postulated contingency list and control actions associated with each contingency in that list. The adopted formulation allows the representation of the constraints associated with

multiple line outage contingency cases in closed-form using the GLODF results from Chapter 2.

The market-system snapshot problem formulation serves as the basic building block in developing the quantification of the economics of secure power system operations. In Chapter 5, we develop a general approach to quantify the economic impacts of complying with a specified security criterion when the deployment of appropriate preventive and/or corrective security control actions is fully taken into account. In Chapter 6, we extend this approach to the multi-settlement environment.

CHAPTER 5

QUANTIFICATION OF MARKET PERFORMANCE AS A FUNCTION OF SYSTEM SECURITY

The system security criterion directly impacts the system operations which, in turn, affect the market outcomes. Analogously, the market operations strongly influence the ability of the IGO to ensure secure power system operations. We use the modeling results in Chapter 4 to represent this tight coupling between market and system operations in order to quantify the economics of secure power system operations. We measure the economics from the performance of the electricity markets. In this chapter, we lay out the nature of this problem and discuss the approach we develop for the evaluation of the market performance as a direct function of the system security criterion.

We use the auction surplus as the key metric for the market performance. In addition, we evaluate appropriate metrics to measure the market performance on a system- and an areawide basis, as well as the surplus of each market participant. Our approach can quantify the impacts on the market performance due to a change from the specified to another security criterion. In this way, we can quantify the economic impacts of specifying a set of different contingencies and/or associated security control actions. We extend the snapshot approach to study the impacts of diverse system and market conditions – changes in the network parameters, the set of resources and the market participants' behaviors – over a given period. The extension to construct the multiple

snapshot approach constitutes a major contribution of this dissertation since it provides, for the first time, a practical tool for use by the IGO to evaluate the interdependencies between market performance and system security over an extended period.

This chapter contains four sections. We devote Section 5.1 to quantifyig the market performance as a function of the security criterion for a single system snapshot using a set of economic and resource dispatch metrics. In Section 5.2, we focus on the DAMs in a given period and extend the snapshot assessment to cover that period. The approach is notable for its computational efficiency obtained from a sampling scheme that takes advantage of the structural characteristics of the models in the formulation. We discuss various possible applications of the multiple snapshot approach. We summarize the results of this chapter in Section 5.3.

5.1 Market Performance Assessment for a System Snapshot

The starting point in system security assessment is the snapshot analysis of the interconnected system as formulated in Chapter 2. We use the security assessment models to formulate the market-snapshot problem $\mathcal{M}(\mathcal{S},\mathcal{B},\mathcal{W};\mathcal{C})$ in Chapter 4 to represent the tight coupling between market and system operations. The market performance under the specified security criterion $\mathcal{C}$ for the snapshot system may be quantified from the market outcomes given by the solution of $\mathcal{M}(\mathcal{S},\mathcal{B},\mathcal{W};\mathcal{C})$.

We use the optimal solution of $\mathcal{M}(\mathcal{S},\mathcal{B},\mathcal{W};\mathcal{C})$ – the offer/bid functions and the optimal dispatch quantities of market participants as well as the LMP values given by Equation (4.14) – to define metrics to measure market outcomes on a system and an area

79

basis, as well as the impacts on individual player outcomes. We use the optimal value of the auction surplus $\mathcal{S}$ under $\mathcal{C}$ given by Equation (4.3) as the measure for the performance of the market as a whole. In addition, for area $\mathcal{A}^k$, we evaluate

$$\mathcal{S}^k \triangleq \left(\sum_{b \in \mathcal{B}^k} \beta_b \left(p_b^{(0)} \right) - \sum_{s \in \mathcal{S}^k} \beta_s \left(p_s^{(0)} \right) \right) \tag{5.1}$$

to determine the area $\mathcal{A}^k$ contributions to the system auction surplus. The *producer* (*consumer*) offer (bid) surplus measures the performance or the gain of each seller (buyer) for participating in the electricity market. The producer offer surplus for a seller s at node i of the area $\mathcal{A}^k$ is

$$\mathcal{S}_s \triangleq \lambda_i p_s^{(0)} - \beta_s \left(p_s^{(0)} \right), \tag{5.2}$$

and the consumer bid surplus change for a buyer b at the same node is

$$\mathcal{S}_b \triangleq \beta_b \left(p_b^{(0)} \right) - \lambda_i p_b^{(0)}, \tag{5.3}$$

where λ_i^* is the LMP at node i of the area $\mathcal{A}^k$ given by the Equation (4.14). We sum the dispatched loads to evaluate the total cleared demand P under criterion $\mathcal{C}$:

$$P \triangleq \mathbf{1}^T \underline{d}. \tag{5.4}$$

We compute the areawide net injection to indicate the amount of net power imported into an area $\mathcal{A}^k$ with

$$\Delta P^k \triangleq \mathbf{1}^T \left[\underline{g}^{(0)k} - \underline{d}_s^{(0)k} \right]. \tag{5.5}$$

The value of the metrics mentioned above is useful for the performance quantification of market for a given snapshot and constitutes the basic building of the approach. We conceptually represent this structure in Figure 5.1.
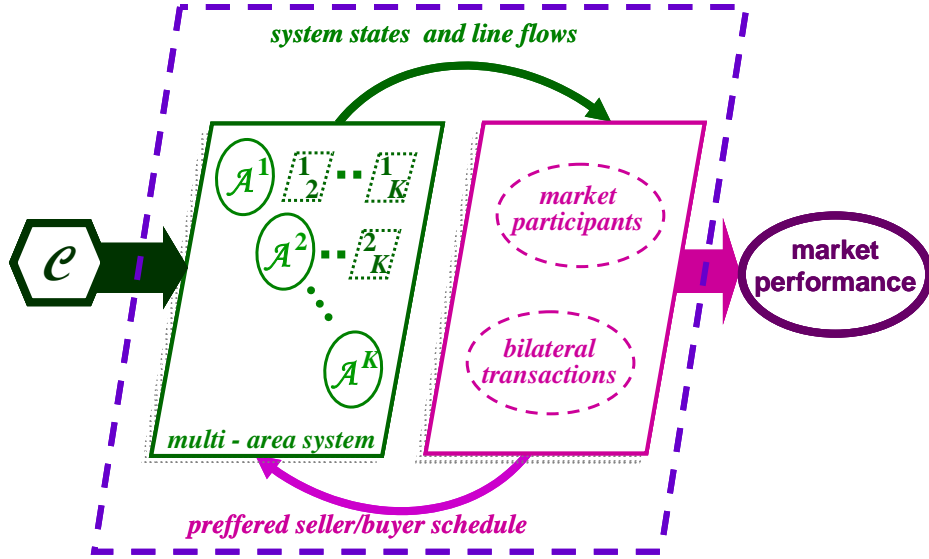
Figure 5.1 Conceptual structure for snapshot comparative assessment

For a different security criterion $\mathcal{C}'$, the IGO must solve a modified SCOPF, $\mathcal{M}(\mathcal{S},\mathcal{B},\mathcal{W};\mathcal{C}')$ in which the constraints in (4.6) - (4.10) reflect the changes in the contingency set $\mathcal{I}_{\mathcal{C}}$ and in the security control actions associated with each contingency. The relative market performance under criterion $\mathcal{C}'$ is assessed with respect to those under reference criterion $\mathcal{C}$ using the metrics provided above. The change in the auction surplus

$$\Delta \mathcal{S}_{\mathcal{C}'} = \mathcal{S}|_{\mathcal{C}'} - \mathcal{S}|_{\mathcal{C}} \tag{5.6}$$

quantifies the market efficiency change. The expression in (5.6) implicitly assumes that the benefits of the fixed demand remain equal under every security criterion.

Consequently, there is no loss of generality incurred with the assumption of constant benefits for fixed demand for the evaluation of the market efficiency changes.

We use the metrics in (5.1) - (5.5) to evaluate the relative performance impacts under a security criterion $\mathcal{C}'$ with respect to those under the reference criterion $\mathcal{C}$. These relative measures have useful interpretations. For example, the change in the contribution of an area to the auction surplus indicates how that area's market participants are impacted by a change of security criterion from the reference $\mathcal{C}$ to the criterion $\mathcal{C}'$ under consideration. We interpret in a similar fashion the changes in producer/consumer surplus, the total dispatched load change and the areawide net injection.

The feasibility set under the security criterion $\mathcal{C}$ is determined by the collection of decision variables that satisfy the constraints (4.4) - (4.10). We call the security criterion $\mathcal{C}'$ tighter than $\mathcal{C}$ if the feasibility set under $\mathcal{C}'$ is a strict subset of the feasibility set corres-ponding to the criterion $\mathcal{C}$. It follows that the optimal auction surplus under $\mathcal{C}'$ is bounded from above by that under $\mathcal{C}$. The value of the relative auction surplus metric is, therefore, non-positive and depends on, among other factors, the willingness to pay of the buyers.

Under a given security criterion, the snapshots corresponding to different system and market conditions may result in marked changes in the market performance outcomes. Such differences are caused by many factors including changes in the loads, the set of available units, and the offers/bids submitted. In turn, these changes may also result in different values of the relative performance metrics. Consequently, these assessments must be carried out over a period to correctly capture the impacts of the different

conditions that exist during that period. In the next section, we extend the snapshot approach to carry out such assessments.

5.2 Proposed Multiple-Snapshot Approach

In this section, we describe the way we extend the comparative market performance assessment over a study period and provide the multiple snapshot approach. Since the focus of this chapter is on the DAMs, we use an hourly resolution as the shortest time unit and represent the system for the hour h by its system snapshot. Conceptually, we assess the market performance assessment at each hour of a given study period. In effect, we apply the conceptual structure for snapshot comparative assessment shown in Figure 5.1 to each hour of the period for the specified security criterion. To assess the market performance impacts due to a change in the security criterion, the entire multiple snapshot procedure must be repeated for the security criterion under consideration. The hourly values of the relative performance metrics are summed to obtain the daily values which, in turn, are used to compute the relative performance metrics for the entire study period. However, for a large-scale system, such an approach may impose a large burden on computing resources. One way to deal with this complication is to perform the assessments for a smaller representative sample of the hours. For this purpose, we next develop the sampling scheme that systematically selects this smaller subset of representative hours

A key requirement for the sampling scheme is the incorporation of the unit commitment decisions which entail intertemporal effects across the hours of the commitment. To fully capture the intertemporal effects, all the hours of the unit

83

commitment period need to be considered. Since, for typical market applications, the unit commitment period is a day, this requirement shifts the selection of representative sample of hours to that of days, since all the hours of such days must be included.

A first step in the sampling scheme is the partitioning of the study period into subperiods. Since many operational studies are carried out on a monthly basis, we use a month as a subperiod. For a given month i, we determine the subset of representative days and construct the set $\mathcal{I}$. We choose the elements of $\mathcal{I}$ on the basis of the daily peak demand values. These values take into account both the fixed demands and the price sensitive quantities bid. Let $\mathcal{I} = \{d_i : i = 1, \cdots, D\}$ be the set of days in the month i. We denote the day d_i peak demand load by p_{d_i}. We reorder the set of the demand values $\{p_{d_1}, \cdots, p_{d_D}\}$ as $\{\tilde{p}_1, \cdots, \tilde{p}_D\}$ with $\tilde{p}_j \geq \tilde{p}_{j+1}$, where $\tilde{p}_j$ denotes the jth largest value of the month. We construct the ordered daily load curve using the set of points $\{(0, \tilde{p}_1), (1, \tilde{p}_2), \cdots, (D-1, \tilde{p}_D)\}$. This curve has at most D distinct load levels. We normalize the time axis using D as the base value and construct the so-called load duration curve (LDC) $\mathcal{L}(\cdot)$ as a piecewise step function using the set of points $\{(0, \tilde{p}_1), (1/D, \tilde{p}_2), \cdots, ((D-1)/D, \tilde{p}_D)\}$.

The basic idea in the construction of $\mathcal{I}$ is to use an approximation of the LDC by a curve with fewer levels of load. We construct such an approximation by maintaining the base and the peak load levels, and then selecting d days so that we replace the original LDC by at most a $(d+2)$ load level approximate LDC. We superpose the grid with k equally distributed LDC factors

$$0 = \upsilon_0 < \upsilon_1 < \cdots < \upsilon_{d+1} = 1 \qquad (5.7)$$

on the time axis. We determine the load level $\hat{p}_i = \mathcal{L}(\upsilon_i)$ for each υ_i. We choose d so

that the $(d+2)$ load values are distinct and

$$\hat{p}_0 > \hat{p}_1 > \cdots > \hat{p}_{d+1}. \qquad (5.8)$$

We use the load levels to subdivide the interval between $\hat{p}_0$ and $\hat{p}_{d+1}$ into $(d+2)$ load

tranches

$$\mathscr{P}_i = \begin{cases} \left[\hat{p}_{d+1}, \dfrac{\hat{p}_d + \hat{p}_{d+1}}{2} \right] & i = d+1 \\[3mm] \left(\dfrac{\hat{p}_{i-1} + \hat{p}_i}{2}, \dfrac{\hat{p}_i + \hat{p}_{i+1}}{2} \right] & i = 1, \cdots, d \\[3mm] \left(\dfrac{\hat{p}_0 + \hat{p}_1}{2}, \hat{p}_0 \right] & i = 0 \end{cases} \qquad (5.9)$$

and determine from the time axis the corresponding duration n_i of each tranche. Note

that n_i is an integer multiple of $1/D$ and $\displaystyle\sum_{i=0}^{d+1} n_i = 1$. We define

$$\hat{\upsilon}_i = \sum_{r=0}^{i-1} n_r , \quad i = 1, \cdots, d . \qquad (5.10)$$

We construct $\mathcal{L}^a(\cdot)$ from the $(d+2)$ load levels using the set of points

$\{(0, \hat{p}_0), (\hat{\upsilon}_0, \hat{p}_1), \cdots, (\hat{\upsilon}_k, \hat{p}_{d+1})\}$ and use it to approximate $\mathcal{L}(\cdot)$. For each load level $\hat{p}_j$

of $\mathcal{L}^a(\cdot)$, we identify the day d_i with $p_{d_i} = \hat{p}_i$. In case of two or more such days, we select the most or more recent day. We construct $\mathcal{I}$ using these $(d+2)$ selected days. We illustrate such construction in Figure 5.2.

We measure the "goodness" of the approximation in terms of an error based on the monthly energy. We define the error in the LDC approximation by

$$\varepsilon\big|_d = \int_0^1 \left| \mathcal{L}^a(x;k) - \mathcal{L}(x) \right| dx \bigg/ \int_0^1 \mathcal{L}(x)\, dx. \tag{5.11}$$

We compare the value of $\varepsilon\big|_d$ with a specified error tolerance value $\bar{\varepsilon}$. If the error fails to satisfy $\bar{\varepsilon}$, d is increased until the tolerance check is satisfied and selects the corresponding $\mathcal{D}_r^i$.
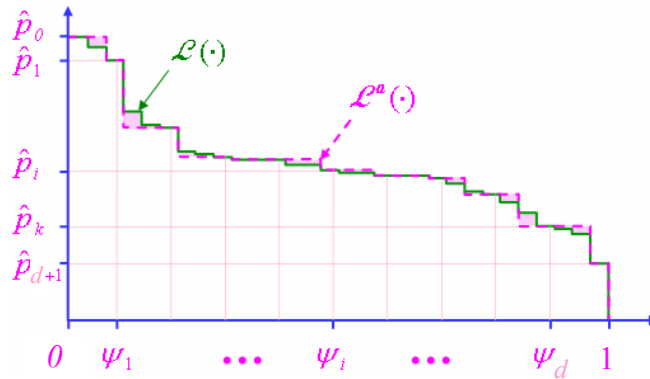
Figure 5.2 Construction of $\mathcal{L}^a(\cdot)$ from $\mathcal{L}(\cdot)$

A byproduct of the approximation is the number of days associated with each representative day in $\mathcal{I}$. We repeat the sampling scheme for each month within the study period, then construct the set of representative days $\mathcal{I}$ of the study period by the union of the monthly $\mathcal{I}$.
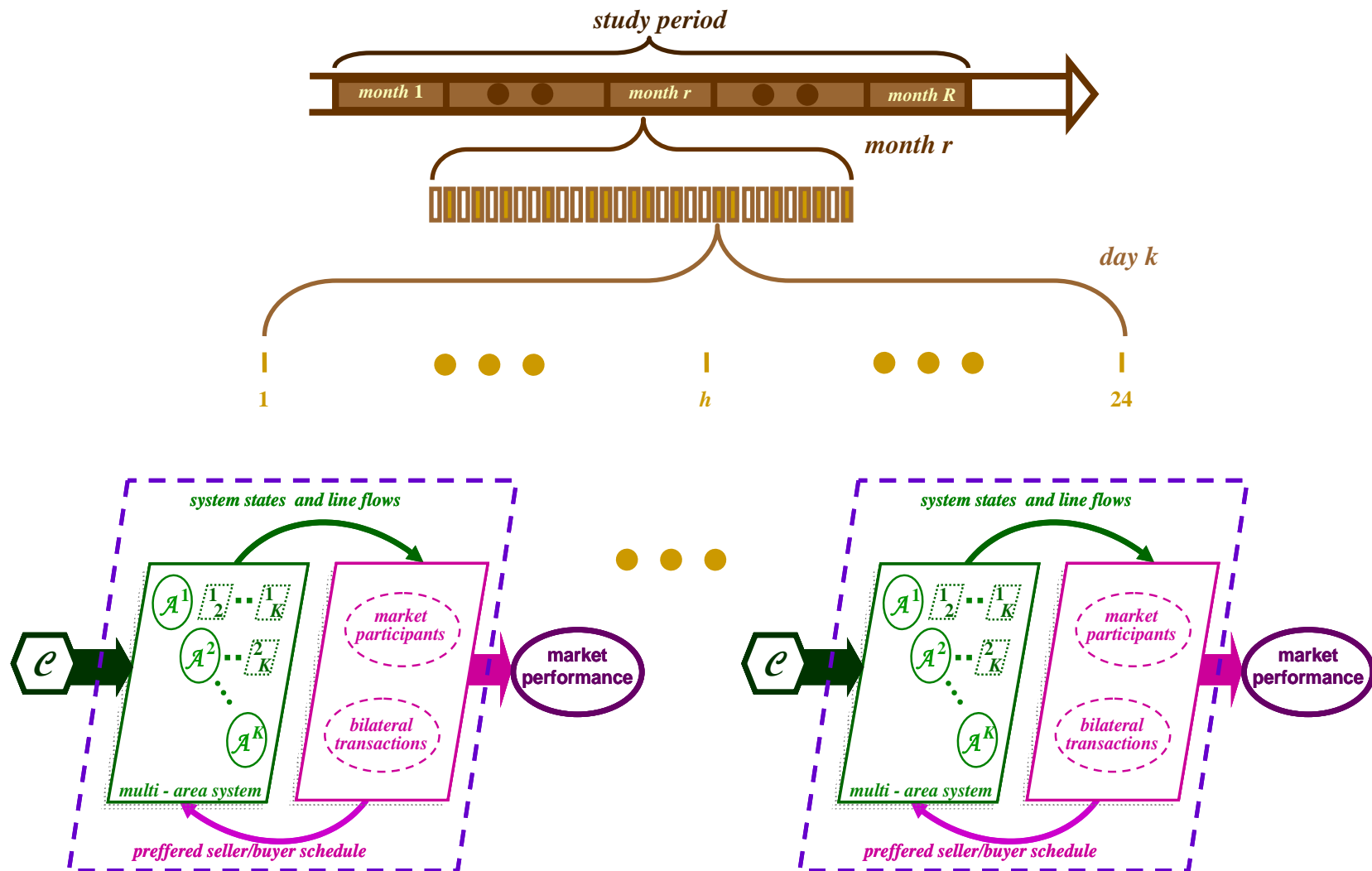
Figure 5.3 Extension of comparative assessments over a period of time

We deploy the snapshot conceptual structure shown in Figure 5.1 as the basic building block of the approach for the DAMs. We apply the structure to each hour of the days in $\mathcal{T}$. We use the snapshot market problem $\mathcal{M}(\mathcal{S}, \mathcal{B}, \mathcal{W}; \mathcal{C})$ to represent the hour h DAM complying with security criterion $\mathcal{C}$ as conceptually illustrated in Figure 5.3. Here, we explicitly take into account the existence of different sets of sellers and buyers at hour h. The solution of the $\mathcal{M}(\mathcal{S}, \mathcal{B}, \mathcal{W}; \mathcal{C})$, then, determines the market clearing of the hour h DAM. Based on the market clearing, we quantify the hourly values of market performance metrics and aggregate them for each day. We use the number of days each day in $\mathcal{T}$ represents and aggregate the daily figures to obtain monthly figures. The daily figures also serve to evaluate key statistics for each month such as mean, variance and range. The study period impacts are then aggregated form the monthly ones. Thus, we are able to quantify the system and the areawide net injection as well as dollar figures on a daily, monthly and period basis.

The proposed multiple snapshot approach has a wide range of applications including the justification by the IGO of the decision to modify the security criterion to be used and the cost/benefit analysis of network improvements to mitigate the market performance impacts of a set of specified contingencies. Additional applications are the formulation of the control actions for specific contingencies, and the assessment of specific behavioral changes of market participants under various security criteria. We illustrate an application of the proposed approach to the study of the ISO-NE DAM in Chapter 7.

5.3 Summary

In this chapter, we propose an approach for the evaluation of the market performance

under a specified security criterion for a single system snapshot. We apply this approach to quantify the market performance impacts arising from a change from a given to another security criterion. This quantification provides meaningful measures of the economic and the resource dispatch impacts on both a system and an area basis. We further extend the approach to a multiple snapshot approach to have the capability to evaluate the impacts of diverse system and market conditions for a given period of interest. The development of the multiple snapshot approach is a major contribution of this dissertation as, for the first time, the IGO has a useful tool to analyze the economics of secure power system operations.

The multiple snapshot approach has a wide range of applications in regulatory studies, longer-term planning activities and short-term activities related to the market and system operations. In fact, the tool allows the IGO to make better informed decisions. Other applications include the justification by the IGO to modify its selection of a security criterion and the cost/benefit analysis of network improvements to mitigate the market performance impacts of a set of specified contingencies. We illustrate an application of the multiple snapshot approach to the ISO-NE DAMs to analyze whether the market efficiency of the ISO-NE DAM is adversely impacted by the system operations complying with the security criterion in force at Chapter 7.

CHAPTER 6

ECONOMICS OF SYSTEM SECURITY IN MULTI-SETTLEMENT SYSTEMS

In this chapter, we extend the multiple snapshot approach developed in Chapter 5 to multi-settlement systems. We limit our focus to the hourly day-ahead markets (DAMs) and their associated real-time markets (RTMs). The basic thrusts of this chapter are to quantitatively characterize the linkages between the real-time system security and the day-ahead markets as well as to investigate the role of the financial entities in a multi-settlement system. The resulting systematic approach permits the quantification of the auction surplus attained through the multi-settlement system, and the evaluation of the impacts of the DAMs on market participants' surpluses as well as on the near-real-time secure power system operations. The multi-settlement multiple snapshot approach is an important contribution of this dissertation as it provides the methodology to quantify the auction surplus attained through a sequence of markets. The approach also constitutes a practical tool for the IGO to evaluate the impacts of financial entities on near-real-time security.

This chapter contains four additional sections. The nature of the multi-settlement problem and the market performance quantification for a DAM and its associated RTMs are described in Section 6.1. We further show that the auction surplus attained through a multi-settlement system equals the auction surplus attained in the RTMs. The multi-settlement multiple snapshot approach and the impacts of financial entities on the near-real-time system security are discussed in Section 6.2. We summarize this chapter's results in Section 6.3.

6.1 Performance Quantification of a DAM and of Its Associated RTMs

Recall from our discussions in Sections 4.1 and 5.2 that, in a multi-settlement environment, we deal with temporally interrelated electricity markets. The sequence of the markets explicitly recognizes that while the same MWh commodity is traded, the snapshots corresponding to the times the markets clears may be considerably different. In particular, the system conditions during the actual hour h may differ from those used to determine the DAM hour h outcomes. The IGO runs the RTMs, typically, every 5-10 min to ensure that the market outcomes reflect the changed system conditions, resulting in secure power system operations in near-real time. As such, we view RTMs as *balancing energy markets*. We associate with the DAM $\left.\mathcal{D}\right|_h$ for the hour h, the M RTMs $\left.\mathcal{R}\right|_{(h,1)}$, $\left.\mathcal{R}\right|_{(h,2)}$, $\cdots$, $\left.\mathcal{R}\right|_{(h,M)}$.

The DAMs are 24 separate hourly energy markets, one for each hour of the next day. We denote the DAM for the hour h by $\left.\mathcal{D}\right|_h$. The financial nature of each $\left.\mathcal{D}\right|_h$ makes possible the participation of financial entities, in addition to the players with physical resources. We use a snapshot to represent the system for the hour h DAM $\left.\mathcal{D}\right|_h$ and an "updated" snapshot for each associated RTM, which we denote by $\left.\mathcal{R}\right|_{(h,m)}$, $m = 1, \cdots, M$. In what follows, we suppress the hour h so as to simplify the notation. In addition, we consider for the purposes of development of the multi-settlement market exposition only a single area and, therefore, we also suppress the area k notation. We analyze the hour h DAM $\mathcal{D}$ operated in compliance with the security criterion $\mathcal{C}$ using $\mathcal{M}(\mathcal{S},\mathcal{B},\mathcal{W};\mathcal{C})$ in which we associate preventive control actions for each contingency case in $\mathcal{I}_e$. The problem statement explicitly takes into account all the entities that constitute the set of sellers and the set of buyers in hour h – both financial

and physical players. We use the superscript r (f) to denote the participants with physical resources (financial players). Therefore, the set of sellers $\mathscr{S}$ (buyers $\mathscr{B}$) is given by $\mathscr{S} = \mathscr{S}^r \bigcup \mathscr{S}^f$ $\left(\mathscr{B} = \mathscr{B}^r \bigcup \mathscr{B}^f\right)$. We denote the subset with nonzero cleared quantities in the DAM by $\mathscr{S}^{*r} \subseteq \mathscr{S}^r$ and the subset of transactions that receive transmission services by $\mathscr{W}^* \subseteq \mathscr{W}$. Even though a physical buyer b^r may have $p_{b^r}^* = 0$ in $\mathscr{D}$, b^r participates in the RTM to meet his fixed demand.

Each RTM is designed to be a purely physical market restricting participation to only those players with actual loads and physical generation assets who have nonzero outcomes in the DAM. For each $\mathscr{R}|_m$, the IGO uses the offers of the physical sellers in $\mathscr{S}^{*r}$, the willingness to pay of the bilateral transactions cleared in $\mathscr{W}^*$ and the real-time fixed demand of the physical buyers in $\mathscr{B}^r$. We use the identical system snapshot approach for $\mathscr{R}|_m$ and so we formulate and solve the market problem $\mathcal{M}\left(\mathscr{S}^{*r}, \mathscr{B}^r, \mathscr{W}^*; \mathcal{C}\right)$ for $\mathscr{R}|_m$.

The metrics of interest – the auction surplus, the market participant surpluses and the congestion rents collected – are evaluated using the relations in (5.1) - (5.5) for $\mathcal{M}\left(\mathscr{S}^{*r}, \mathscr{B}^r, \mathscr{W}^*; \mathcal{C}\right)$ for the subperiod m. We depict the interrelationships between $\mathscr{D}$ and an associated $\mathscr{R}|_m$ in Figure 6.1. We use the notation "^" to denote the optimal values attained in the clearing of $\mathscr{R}|_m$. The figure clearly indicates the players who participate in each market, as well as the inputs and the outcomes of these markets.
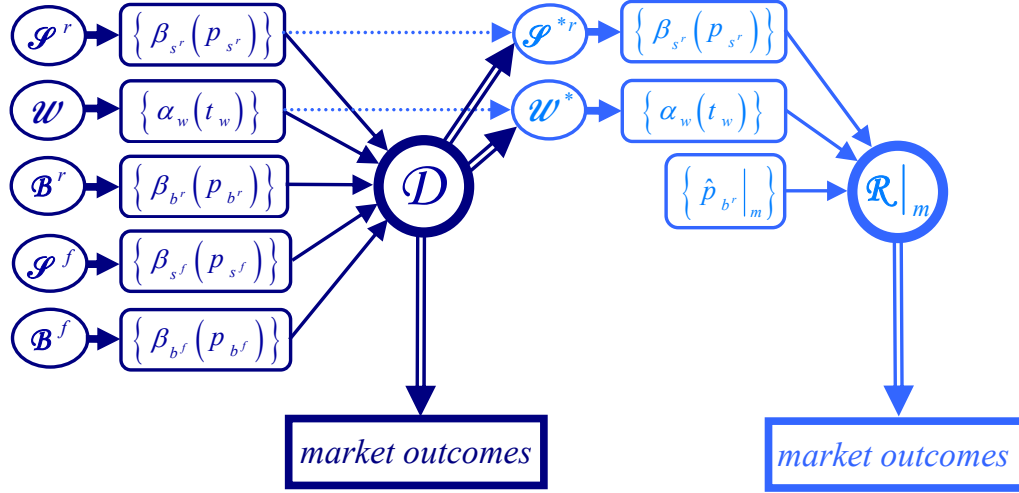
Figure 6.1 Information flow in $\mathscr{D}$ and an associated $\mathcal{R}\big|_m$

The outcomes of $\mathscr{D}$ and those of $\mathcal{R}\big|_m$ are inputs into the settlement – the mechanism that specifies the payments to or by each market participant after the fact. We consider a system where the same MWh may be sold in two different markets – $\mathscr{D}$ and a specific $\mathcal{R}\big|_m$ – and so we deal with a multi-settlement system. Each of the M subperiods of the hour h has a duration of $1/M$ of an hour and we consider the multi-settlement for such a subperiod. A physical seller $s^r \in \mathscr{S}^{*r}$, located at node i, who has cleared $p_{s^r}^*$ in $\mathscr{D}$ receives revenues of $1/M\left(\lambda_i^* p_{s^r}^*\right)$ over that subperiod. As his real-time production $\hat{p}_{s^r}\big|_m$ may deviate from $p_{s^r}^*$, there is an adjustment to account for the production deviation $1/M\left(-p_{s^r}^* + \hat{p}_{s^r}\big|_m\right)$, which is paid at the $\mathcal{R}\big|_m$ LMP $\hat{\lambda}_i\big|_m$. The subperiod m revenues of s^r are

$$\eta_{s^r}\big|_m = \frac{1}{M}\left[\lambda_i^* p_{s^r}^* + \hat{\lambda}_i\big|_m\left(-p_{s^r}^* + \hat{p}_{s^r}\big|_m\right)\right]. \tag{6.1}$$

93

We note that if the seller s^r production in real time does not deviate from its DAM value, i.e., $p^*_{s^r} = \hat{p}_{s^r}\big|_m$, then the revenues $\eta_{s^r}\big|_m$ are simply the DAM revenues. As such, the $\mathcal{R}\big|_m$ LMP $\hat{\lambda}_i\big|_m$ has no impact on the subperiod m of s^r.

A financial seller s^f, located at node i, has revenues of $1/M\left(\lambda^*_i p^*_{s^f}\right)$ for his DAM "production." As s^f cannot participate in $\mathcal{R}\big|_m$, his real-time production $\hat{p}_{s^f}\big|_m = 0$, resulting in a deviation of $-p^*_{s^f}$. As a result, the RTM produces an adjustment of $-\hat{\lambda}_i\big|_m p^*_{s^r}$ to the DAM revenues of s^f. We may view the financial seller s^f as selling $p^*_{s^f}$ in the DAM at λ^*_i and buying back the same amount in the RTM at $\hat{\lambda}_i\big|_m$. The revenues of the seller s^f in subperiod m are

$$\eta_{s^f}\big|_m = \frac{1}{M}\left[p^*_{s^r}\left(\lambda^*_i - \hat{\lambda}_i\big|_m\right)\right]. \tag{6.2}$$

We note that as long as the DAM LMP λ^*_i is above the RTM LMP $\hat{\lambda}_i\big|_m$ the financial seller s^f has positive revenues.

In an analogous manner, the physical buyer b^r located at node i makes payments in the subperiod m of

$$\gamma_{b^r}\big|_m = \frac{1}{M}\left[-\lambda^*_i p^*_{b^r} - \hat{\lambda}_i\big|_m\left(-p^*_{b^r} + \hat{p}_{b^r}\big|_m\right)\right]. \tag{6.3}$$

The buyer b^r pays λ_i^* for the portion $p_{b^r}^*$ cleared in $\mathcal{D}$ and $\hat{\lambda}_i\big|_m$ for the remainder of his

real-time demand. The payments of a financial buyer b^f in the subperiod m are

$$\gamma_{b^f}\big|_m = \frac{1}{M}\left[p_{b^f}^*\left(-\lambda_i^* + \hat{\lambda}_i\big|_m\right)\right].$$ (6.4)

We use the same reasoning to determine the payments by the bilateral transaction $w \in \mathcal{W}^*$

in the subperiod m to be

$$\gamma_w\big|_m = \frac{1}{M}\left[\left(\lambda_{m_w}^* - \lambda_{n_w}^*\right)t_w^* + \left(\hat{\lambda}_{m_w}\big|_m - \hat{\lambda}_{n_w}\big|_m\right)\left(-t_w^* + \hat{t}_w\big|_m\right)\right].$$ (6.5)

We note that if the bilateral transaction w does not deviate from the DAM clearing outcomes

in the subperiod, then its payments are independent on the RTM outcomes.

The IGO makes the payments in (6.1) and (6.2) to the sellers and receives from the buyers

and the bilateral transactions the payments in (6.3) - (6.5). The difference between these

payments is the subperiod m congestion rents collected by the IGO:

$$\mathcal{K}_\Sigma\big|_m = \frac{1}{M}\left[\sum_{b^r \in \mathcal{B}^r}\gamma_{b^r}\big|_m + \sum_{b^f \in \mathcal{B}^f}\gamma_{b^f}\big|_m + \sum_{w \in \mathcal{W}^*}\gamma_w\big|_m - \sum_{s^r \in \mathcal{S}^{*r}}\eta_{s^r}\big|_m - \sum_{s^f \in \mathcal{S}^f}\eta_{s^f}\big|_m\right].$$ (6.6)

We use the results in (6.1) - (6.6) for the quantification of the performance of the multi-

settlement system in the subperiod m. The output of the seller $s^r \in \mathcal{S}^{*r}$ is produced in real

time, i.e., in the subperiod m, and is offered for sale for $1/M\,\beta_{s^r}\left(\hat{p}_{s^r}\big|_m\right)$. The offer surplus

of the seller s^r in the subperiod m is expressed in terms of the difference between the

revenues and the offer, i.e.,

$$\mathcal{S}_{s^r}\big|_m = \eta_{s^r}\big|_m - \frac{1}{M}\,\beta_{s^r}\left(\hat{p}_{s^r}\big|_m\right). \tag{6.7}$$

The fact that the financial seller s^f has no real-time production implies that the s^f producer offer surplus equals his revenues

$$\mathcal{S}_{s^f}\big|_m = \eta_{s^f}\big|_m. \tag{6.8}$$

The physical buyer b^r consumes the energy in the subperiod, resulting in a buyer bid surplus given by the difference between the b^r willingness to pay in real time and the actual payments:

$$\mathcal{S}_{b^r}\big|_m = \frac{1}{M}\,\hat{\beta}_{b^r}\left(\hat{p}_{b^r}\big|_m\right) - \gamma_{b^r}\big|_m. \tag{6.9}$$

We note that the real-time $\hat{\beta}_{b^r}$ may differ from β_{b^r} due to the fact that the real-time demand is viewed as fixed.

The financial buyer b^f cannot consume in real time, and so has a buyer bid surplus which is

$$\mathcal{S}_{b^f}\big|_m = -\gamma_{b^f}\big|_m. \tag{6.10}$$

The bilateral transaction $w \in \mathcal{W}^*$ receives the actual transmission service in real time, resulting in a surplus of

$$\mathcal{S}_w\big|_m = \frac{1}{M}\,\alpha_w\left(\hat{t}_w\big|_m\right) - \gamma_w\big|_m\,. \tag{6.11}$$

We make use of the market participants' offer/bid surpluses, including those of the bilateral transactions and the congestion rents collected by the IGO, to evaluate the total auction surplus attained in the multi-settlement system:

$$\mathcal{S}_\Sigma\big|_m = \sum_{s^r \in \mathscr{P}^{*r}} \mathcal{S}_{s^r}\big|_m + \sum_{b^r \in \mathscr{B}^r} \mathcal{S}_{b^r}\big|_m + \sum_{s^f \in \mathscr{P}^f} \mathcal{S}_{s^f}\big|_m +$$
$$\sum_{b^f \in \mathscr{B}^f} \mathcal{S}_{b^f}\big|_m + \sum_{w \in \mathscr{W}^*} \mathcal{S}_w\big|_m + \mathcal{K}_\Sigma\big|_m \qquad . \tag{6.12}$$

We substitute (6.6) - (6.11) into (6.12) to simplify and get

$$\mathcal{S}_\Sigma\big|_m = \frac{1}{M}\left[\sum_{b^r \in \mathscr{B}^r} \hat{\beta}_{b^r}\left(\hat{p}_{b^r}\big|_m\right) - \sum_{s^r \in \mathscr{P}^{*r}} \beta_{s^r}\left(\hat{p}_{s^r}\big|_m\right)\right] + \frac{1}{M}\sum_{w \in \mathscr{W}^*} \alpha_w\left(\hat{t}_w\big|_m\right). \tag{6.13}$$

Now, the auction surplus attained in the RTM $\mathcal{R}\big|_m$ is $\hat{\mathcal{S}}\big|_m$ and its value is given by (4.3):

$$\hat{\mathcal{S}}\big|_m = \frac{1}{M}\left\{\sum_{b^r \in \mathscr{B}^r} \hat{\beta}_{b^r}\left(\hat{p}_{b^r}\big|_m\right) - \sum_{s^r \in \mathscr{P}^{*r}} \beta_{s^r}\left(\hat{p}_{s^r}\big|_m\right)\right\} + \frac{1}{M}\sum_{w \in \mathscr{W}^*} \alpha_w\left(\hat{t}_w\big|_m\right). \tag{6.14}$$

We conclude that

$$\mathcal{S}_\Sigma\big|_m = \hat{\mathcal{S}}\big|_m\,. \tag{6.15}$$

Therefore, the total auction surplus of the multi-settlement system attained in the subperiod m is precisely the auction surplus attained in $\mathcal{R}\big|_m$. We furthermore conclude that the outcomes

97

of $\mathcal{D}$ do not explicitly impact the total auction surplus $\mathcal{S}_\Sigma\big|_m$, but impact the allocation of the auction surplus among the market participants.
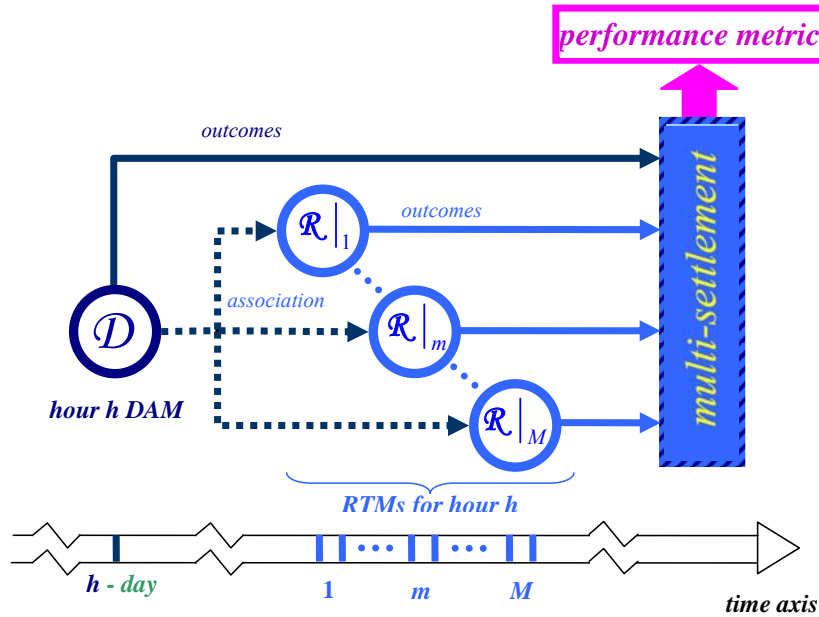

Figure 6.2 Interactions between $\mathcal{D}$ and $\mathcal{R}\big|_m$ and the performance quantification in a multi-settlement environment

The performance metrics in (6.6) - (6.13) are for the subperiod m of the hour h. We aggregate them for the M subperiods of hour h to evaluate the hourly metrics. In particular, we compute the hour h auction surplus $\mathcal{S}_\Sigma$ attained in the multi-settlement system to be

$$\mathcal{S}_\Sigma = \sum_{m=1}^{M} \mathcal{S}_\Sigma\big|_m = \sum_{m=1}^{M} \hat{\mathcal{S}}\big|_m. \tag{6.16}$$

The performance quantification of the multi-settlement system clearly makes use of the interrelationships between the DAM and its associated RTMs, as illustrated in Figure 6.2. We note the clearing of the financial entities in $\mathcal{D}$ impacts the clearing of the physical generation as well as the clearing of the physical loads. As such, the participation of the financial entities

impacts the deviations of the physical resources clearing in real time. Such deviations have implications for the market and the system operations. In particular, they impact the ability of the IGO to ensure real-time system security. In the next section, we describe the way we extend the multiple snapshot approach of Chapter 5 to quantitatively assess the impacts of operating a system under a specified criterion $\mathcal{C}$ on the market performance in a multi-settlement environment. Also, we quantify the impacts of financial entities on the ability of the IGO to meet system security $\mathcal{C}$ in near-real time.

6.2 The Multi-Settlement Multiple-Snapshot Approach

The maintenance of secure power system operations is a task that strongly depends on the outcomes of the DAMs. We may view the DAM physical generation and consumption as a rough *guess* of the actual outcomes in the associated RTMs. As the system and the market conditions in the near to real time may change from those forecast and cleared in the DAM, the RTMs are run to manage the resulting deviations.

The actual physical demand in the M RTMs gives rise to the physical demand deviation in hour *h*:

$$\delta\hat{p}_{\mathcal{B}^r} \;=\; \frac{1}{M}\left[\sum_{m=1}^{M}\left(\sum_{b^r\in\mathcal{B}^r}\hat{p}_{b^r}\Big|_m + \sum_{w\in\mathcal{W}^*}\hat{t}_w\Big|_m\right)\right] - \left[\sum_{b^r\in\mathcal{B}^r}p^*_{b^r} + \sum_{w\in\mathcal{W}^*}t^*_w\right]. \qquad (6.17)$$

Similarly, the physical generation deviation in hour *h* is

$$\delta\hat{p}_{\mathcal{S}^{*r}} \;=\; \frac{1}{M}\left[\sum_{m=1}^{M}\left(\sum_{s^r\in\mathcal{S}^{*r}}\hat{p}_{s^r}\Big|_m + \sum_{w\in\mathcal{W}^*}\hat{t}_w\Big|_m\right)\right] - \left[\sum_{s^r\in\mathcal{S}^{*r}}p^*_{s^r} + \sum_{w\in\mathcal{W}^*}t^*_w\right]. \qquad (6.18)$$

99

The participation of the financial entities in the DAM gives rise to the lack of balance between physical demand deviation $\delta\hat{p}_{\mathcal{B}^r}$ and the physical generation deviation $\delta\hat{p}_{\mathcal{S}^{*r}}$. A positive net injection of the financial participants in the DAM corresponds to $\sum_{s^f \in \mathcal{S}^f} p_{s^f}^* > \sum_{b^f \in \mathcal{B}^f} p_{b^f}^*$, which implies that $\sum_{s^r \in \mathcal{S}^{*r}} p_{s^r}^* < \sum_{b^r \in \mathcal{B}^r} p_{b^r}^*$. In this case, the physical generation deviation exceeds the physical demand deviations so that $\delta\hat{p}_{\mathcal{S}^{*r}} > \delta\hat{p}_{\mathcal{B}^r}$. Therefore, more generation is required in real time than cleared in $\mathcal{D}$ leading to the deviations in the physical sellers' outcomes. In case of $\sum_{s^f \in \mathcal{S}^f} p_{s^f}^* < \sum_{b^f \in \mathcal{B}^f} p_{b^f}^*$ – a negative net injection of the financial entities – some of the physical generation serves the demand of the financial buyers in $\mathcal{D}$ and so $\sum_{s^r \in \mathcal{S}^{*r}} p_{s^r}^* > \sum_{b^r \in \mathcal{B}^r} p_{b^r}^*$. In this case, $\delta\hat{p}_{\mathcal{S}^{*r}} < \delta\hat{p}_{\mathcal{B}^r}$.

Whenever there is zero net injection by the financial entities, the physical generation deviation and the physical demand deviation are in exact balance. The absence of financial entity participation is a special case of this zero net injection. While the injection/withdrawal deviation metrics of (6.17) and (6.18) provide systemwide aggregate measures, we can also introduce analogous metrics for zonal as well as nodal measures in order to meet the requirements at the different levels of granularity.

We use the auction surplus in (6.16), the total congestion rents (6.6) and the market participant offer/bid surplus metrics (6.7) - (6.11) to evaluate the overall economic performance of the multi-settlement system and that of each market participant, respectively. In addition, we need appropriate metrics to analyze the combined impacts of the DAM-RTM clearing outcomes.

As market and system conditions may change, the price of the MWh commodity in each $\mathcal{R}|_m$ at a specified node may deviate from that in $\mathcal{D}$. The hour h price deviation at node i is

$$\delta\lambda_i = \frac{1}{M}\sum_{m=1}^{M}\left[\lambda_i^* - \hat{\lambda}_i\Big|_m\right].$$

(6.19)

Whenever $\delta\lambda_i \neq 0$ over a nontrivial subset of hours, arbitrage opportunities exist, implying market inefficiency. A financial entity can participate in the market to take advantage of price arbitrage opportunities at such a node. As more and more financial entities eye such opportunities, leading to their participation in the markets to arbitrage the price deviation, the arbitrage opportunities begin disappearing. As such, $\delta\lambda_i \rightarrow 0$, leading to the improved economic efficiency of the markets. Thus, price convergence is a desirable outcome in multi-settlement systems.

The price deviation $\delta\lambda_i$ also impacts the offer/bid surplus of each market participant. The output of the seller $s^r \in \mathcal{S}^{*r}$, located at node i, is produced in real time. Therefore, his offer is, unlike his revenues in (6.1), independent of the $\mathcal{D}$ outcomes. Therefore, the $\mathcal{D}$ outcomes impact the offer surplus of the seller s^r in hour h. Using (6.7), the s^r offer surplus in hour h is

$$\mathcal{S}_{s^r} = \frac{1}{M}\sum_{m=1}^{M}\left[\hat{p}_{s^r}\Big|_m\,\hat{\lambda}_i\Big|_m - \beta_{s^r}\left(\hat{p}_{s^r}\Big|_m\right)\right] + \delta\mathcal{S}_{s^r}.$$

(6.20)

Here, $\delta\mathcal{S}_{s^r}$ is the physical seller offer surplus deviation metric

$$\delta \mathcal{S}_{s^r} = p^*_{s^r} \, \delta \lambda_i \qquad\qquad (6.21)$$

and quantifies the impact of the $\mathcal{D}$ outcomes on the revenues of the seller s^r. A positive

(negative) $\delta \mathcal{S}_{s^r}$ implies that s^r captures more (less) revenue for his real-time production

than those in $\mathcal{D}$. To illustrate the nature of $\delta \mathcal{S}_{s^r}$, we consider a specific case in which seller

s^r is the marginal seller in both $\mathcal{D}$ and an associated $\mathcal{R}|_m$ with $\hat{\lambda}_i\big|_m > \lambda^*_i$ and

$\hat{p}_{s^r}\big|_m > p^*_{s^r}$. While $p^*_{s^r}$ is paid at λ^*_i the $\hat{p}_{s^r}\big|_m - p^*_{s^r}$ is paid at $\hat{\lambda}_i\big|_m$. Therefore, the

portion $p^*_{s^r}$ receives less revenue per MWh than $\hat{p}_{s^r}\big|_m - p^*_{s^r}$. The fact that s^r

participates in $\mathcal{D}$ and sells $p^*_{s^r}$ implies that for this case he receives less revenue than had

he participated in only $\mathcal{R}|_m$. The negative $\delta \mathcal{S}_{s^r}$ is illustrated in Figure 6.3.
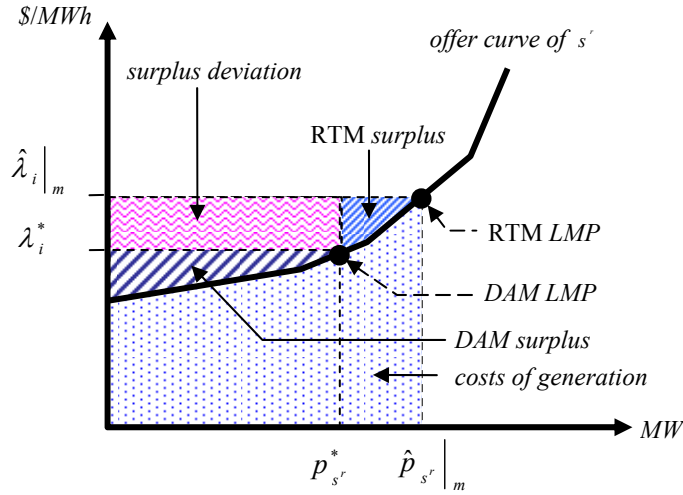

Figure 6.3 The effects of $\mathcal{D}$ and $\mathcal{R}|_m$ clearing on the surplus deviation of the physical seller s^r located at node i for the case $\hat{\lambda}_i\big|_m > \lambda^*_i$

Once we compute the individual surplus deviation of a physical seller, we can determine

the offer surplus deviation of the subset of the physical sellers using

$$\delta \mathcal{S}_{\mathcal{S}^{*r}} = \sum_{i=0}^{N} \sum_{s^r \in \mathcal{S}^{*r}} p_{s^r}^* \, \delta\lambda_i \, \varepsilon_{is^r}, \qquad \varepsilon_{is^r} = \begin{cases} 1, & s^r \text{ is at node } i \\ \\ 0, & \text{otherwise} \end{cases}. \qquad (6.22)$$

Similarly, we can evaluate the physical buyers bid surplus deviations

$$\delta \mathcal{S}_{\mathcal{B}^r} = \sum_{i=0}^{N} \sum_{b^r \in \mathcal{B}^r} p_{b^r}^* \, \delta\lambda_i \, \varepsilon_{ib^r}, \qquad \varepsilon_{ib^r} = \begin{cases} 1, & b^r \text{ is at node } i \\ \\ 0, & \text{otherwise} \end{cases}. \qquad (6.23)$$

A positive $\delta \mathcal{S}_{\mathcal{B}^r}$ implies that the physical buyers pay less for their aggregate real-time demand in $\mathcal{D}$ than in the associated RTMs. This happens because the physical buyers benefit from the lower DAM prices that they pay for the portion of the demand cleared in the DAM.

The MW deviation metrics along with the price and the offer/bid surplus deviation metrics capture important aspects of system and market operations in a multi-settlement environment. The physical generation and demand deviation metrics quantify how "close" the real-time system conditions are to those forecasted in the clearing of the DAM. Smaller magnitude deviations imply improved "forecasts" of the system conditions in the DAM, which, in turn, result in the improved ability of the IGO to ensure real-time system security. Therefore, the DAM clearing is strongly interrelated with the real-time system operations. The price and the physical participants' offer/bid surplus deviation metrics, on the other hand, quantify the impacts of the DAM outcomes on the market participants' surpluses. As price deviations increase, the financial entity participation becomes more pronounced in the DAMs. Such participation leads to changes in the DAM outcomes, which, in turn, impact

how the real-time system conditions are forecasted in the DAM. Therefore, these metrics capture the strong interrelationships between system and market operations in the multi-settlement environment.

Each MW or surplus deviation metric given in (6.17) - (6.23) depends on the specified security criterion $\mathcal{C}$. Under a different security criterion $\mathcal{C}'$, the IGO explicitly considers the solution of the problem $\mathcal{M}(\mathcal{S}, \mathcal{B}, \mathcal{W}; \mathcal{C}')$ at each system snapshot, be it a DAM or an RTM. We measure the impacts on market performance due to the change in the security criterion from $\mathcal{C}$ to $\mathcal{C}'$ by the change in each metric of interest from one criterion to the other. For example, the change in the auction surplus metric is given by

$$\Delta \mathcal{S}_\Sigma \big|_{\mathcal{C} \to \mathcal{C}'} = \mathcal{S}_\Sigma \big|_{\mathcal{C}'} - \mathcal{S}_\Sigma \big|_{\mathcal{C}} \tag{6.24}$$

and measures the change in the economic efficiency of the markets in a multi-settlement environment due to a change in the security criterion from $\mathcal{C}$ to $\mathcal{C}'$. We deploy analogous expressions for each metric in (6.6) - (6.23) to measure the relative change in response to the security criterion change from $\mathcal{C}$ to $\mathcal{C}'$. The changes in the producer/consumer offer/bid surpluses, the total dispatched load and the multi-settlement system deviation metrics are all of interest in our assessment. We also need the changes in the physical demand and generation deviation to quantify the impacts on the ability of the IGO to meet system security in real time. For example, to evaluate the impacts on the physical generation deviation, we use

$$\Delta \delta_{\mathcal{G}^{*r}} \big|_{\mathcal{C} \to \mathcal{C}'} = \delta \hat{p}_{\mathcal{G}^{*r}} \big|_{\mathcal{C}'} - \delta \hat{p}_{\mathcal{G}^{*r}} \big|_{\mathcal{C}}. \tag{6.25}$$

These metrics effectively capture the multi-settlement system performance for the security criterion change from $\mathcal{C}$ to $\mathcal{C}'$ for a given hour h $\mathcal{D}$ and each associated $\mathcal{R}|_m$, $m = 1,...,M$.

Under a specified security criterion, the hourly snapshots corresponding to different system and market conditions may result in markedly different market performance outcomes as discussed in Chapter 5. We use the sampling scheme introduced in Chapter 5 to construct a set of representative days for a given period of interest. We then assess the market performance of the DAM and the associated RTMs at each hour of the set of representative days. The needs are similar in assessing the market performance impacts due to a change in the security criterion. The quantification of the multi-settlement system performance based on the selected representative snapshots constitutes the extended multiple snapshot approach for evaluating the impacts of a security criterion or in its change on a multi-settlement system, as well as to quantify the impacts of financial entity participation on the ability of the IGO to ensure real-time system security.

6.3 Summary

In this chapter, we extend the multiple-snapshot analysis and approach to the study of multi-settlement systems. The construction of the extended approach makes use of the proof of the fact that the auction surplus attained through the multi-settlement system equals that attained in the RTMs. As such, the RTMs determine the auction surplus, which is independent of the DAMs. Therefore, the DAMs' outcomes represent the surplus transfers among market participants for the information available at the times those markets are cleared. These surplus transfers are readily quantified and their implications on real-time system security can be evaluated using the multi-settlement multiple-snapshot approach. The

extended approach provides a useful tool to the IGO to analyze the interdependence between market performance and system security in a multi-settlement environment. The ability to quantify the economic impacts of compliance with a specified security criterion makes the approach highly useful in regulatory proceedings, as well as in longer-term planning and short-term market and system operational studies with the explicit representation of both the financial and the physical asset owning players.

CHAPTER 7

APPLICATION STUDIES: THE ISO NEW ENGLAND

We devote this entire chapter to present a set of applications to the large-scale ISO New England (ISO-NE) of the various schemes developed in Chapters 3, 5 and 6. The studies described in this chapter are the identification of island formation under multiple line outages and the quantification of the economics of secure power system operations for the ISO-NE markets for the case of DAMs only and for the multi-settlement system. The reported studies serve to illustrate the capabilities of the proposed approaches to determine practical solutions to a wide range of problems in the various applications.

We analyze a 2200-bus portion of the large Northeast Power Coordinating Council (NPCC) network that corresponds to the ISO-NE system and study the impacts of multiple line outages. We apply the island detection method described in Chapter 3 to evaluate conditions under which the selected subnetwork is separated into two or more islands. This realistic-sized system study takes fully into account the system operational practices by explicitly representing the scheduled transmission maintenance activities, real-time switching actions and the impacts of forced outages. The study makes clear the computational efficiency of the proposed scheme.

We next focus on the studies to quantify the economics of secure power system operations in the ISO-NE system and DAMs in the 2005 - 2006 period. We quantify the impacts of the security criterion in force on the market performance using the actual day-ahead data – the system model and the bids/offers submitted – with the actual market clearing methodology.

The results of this study serve as the reference case, with respect to which we compare the impacts of a tightened and a relaxed security criterio on the market performance. The use of the multiple snapshot approach in this comparative study provides the result that when a power system is operated under a stricter criterion, the economic efficiency of the electricity markets need not decrease as long as there is price-responsive demand.

We discuss a set of parallel studies on the economic impacts of complying with the security criterion in the multi-settlement environment. In addition to study of the economic efficiency of the ISO-NE multi-settlement as a function of the security criterion in force, we also evaluate the economic and the system operational impacts of the financial entity participation. The results of these studies vividly show that financial entity participation not only leads to price convergence but also improves real-time system security. The results of another study reinforce the findings of the DAM investigation that the relaxation of the security criterion in force has insignificant impacts on market performance in the multi-settlement environment.

This chapter contains five sections. We provide in Section 7.1 a brief description of the multiarea structure of the ISO-NE system and state the current ISO-NE security criterion. In Section 7.2, we illustrate the application of the detection of island formation scheme to study the multiple line outage impacts on the NPCC subnetwork corresponding to ISO-NE system. We report in Section 7.3 the results of the ISO-NE DAM comparative study and those of the set of studies for the multi-settlement system in Section 7.4. We provide concluding remarks in Section 7.5.

7.1 Description of the ISO-NE Multiarea System and Security Criterion

The ISO-NE is the regional transmission organization serving the states of Connecticut, Maine, Massachusetts, New Hampshire, Rhode Island and Vermont. The ISO-NE is a member of the Northeast Power Coordinating Council (NPCC) and is part of the Eastern Interconnection. An important characteristic of the ISO-NE system is its multiarea structure. Such a structure has major implications for the way the system operations comply with the security criterion.

Each area of the ISO-NE multiarea network is characterized as being either an import or an export area. We depict conceptually the multiarea structure of the ISO-NE in Figure 7.1. The import areas [100] are

- $\mathcal{A}^1$: Boston / NE Massachusetts

- $\mathcal{A}^2$: Connecticut

- $\mathcal{A}^3$: SW Connecticut
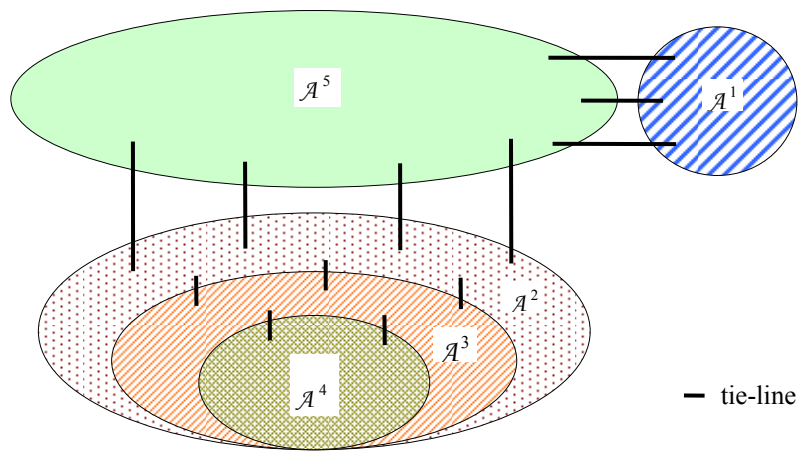
- $\mathcal{A}^4$: Norwalk/Stamford

Figure 7.1 Multiarea structure of the ISO-NE system

We treat the rest of the system as a single export area and denote it by $\mathcal{A}^5$. A salient feature is the nested structure of the areas $\mathcal{A}^4 \subset \mathcal{A}^3 \subset \mathcal{A}^2$. From the physical and the economic point of view, the generation of the export area is required to meet the load of the import areas.

The ISO-NE system security criterion takes into account this multiarea structure. This is a modified $(n - 2)$ security criterion. We denote this security criterion by $\mathcal{C}_0$, whose contingency list is

$$\mathcal{I}_{\mathcal{C}_0} = \mathcal{I}_{n\text{-}1} \cup \left(\bigcup_{k=1}^{4} \mathcal{M}^k \right). \tag{7.1}$$

Here, $\mathcal{I}_{n\text{-}1}$ is the set of single element contingencies considered by the ISO-NE and $\mathcal{M}^k$ is the set of double tie line contingencies specified for each import area $\mathcal{A}^k \in \mathcal{a}$, $k=1,..,4$. Each selected tie line pair interconnects the import area $\mathcal{A}^k$ to any other area of the system. The set of control actions for the security criterion consists of preventive control actions which are associated with the elements of $\mathcal{I}_{n\text{-}1}$, and corrective control actions which are associated with the double element tie-line contingencies of $\bigcup_{k=1}^{4} \mathcal{M}^k$. A detailed discussion is given in [100] and particulars of system operations are discussed in [97].

We use the ISO-NE in all the case studies presented in this chapter since it provides a good, realistic-sized system that is large enough to effectively illustrate the capabilities of the proposed methodologies.

7.2 Detection of Island Formation under Multiple Line Outages

We illustrate the application of the island detection method introduced in Chapter 3 for a

2200-bus portion of the large-scale NPCC network corresponding to the ISO-NE system. This study specifically considers the system operational practices by taking into account scheduled transmission maintenance activities, real-time switching actions and forced outages.

Table 7.1 The Outaged Lines and Line Definitions

scheduled maintenance	$\tilde{\ell}_1 = (3108,3118)$, $\tilde{\ell}_2 = (1796,2929)$, $\tilde{\ell}_3 = (1790,2694)$, $\tilde{\ell}_4 = (2727,2764)$, $\tilde{\ell}_5 = (2718,2721)$.	$\left.\begin{array}{c} \\ \\ \\ \\ \\ \end{array}\right\} \tilde{\mathcal{L}}_{(9)}$
switched outages	$\tilde{\ell}_6 = (486,2927)$, $\tilde{\ell}_7 = (3106,3113)$, $\tilde{\ell}_8 = (2716,2765)$, $\tilde{\ell}_9 = (2718,2769)$.	
unplanned outages	$\tilde{\ell}_{10} = (90,2693)$, $\tilde{\ell}_{11} = (2925,2926)$, $\tilde{\ell}_{12} = (2691,2693)$, $\tilde{\ell}_{13} = (2693,2694)$, $\tilde{\ell}_{14} = (2926,2927)$, $\tilde{\ell}_{15} = (2924,2926)$.	

For the island detection study, we consider the set of outaged lines given in Table 7.1. We denote the set of outaged lines corresponding to the scheduled maintenance and the switching actions by $\tilde{\mathcal{L}}_{(9)}$ and consider the network with the elements of $\tilde{\mathcal{L}}_{(9)}$ outaged. We analyze the impacts of the six unplanned line outages listed in Table 7.1 on the system connectivity for this network in terms of the so-called updated PTDFs. For this purpose we use (3.11) and construct

$$(\underline{H}_6)^{\tilde{\mathcal{L}}_{(9)}} = \begin{bmatrix} 0.5349 & 0.0000 & -0.4222 & 0.1127 & 0.0000 & 0.0000 \\ 0.0000 & 0.1556 & 0.0000 & 0.0000 & 0.0000 & -0.1556 \\ -0.1146 & 0.0000 & 0.3011 & 0.1865 & 0.0000 & 0.0000 \\ 0.0466 & 0.0000 & 0.2841 & 0.3307 & 0.0000 & 0.0000 \\ 0.0000 & 0.0000 & 0.0000 & 0.0000 & 0.0000 & 0.0000 \\ 0.0000 & -0.1950 & 0.0000 & 0.0000 & 0.0000 & 0.1950 \end{bmatrix}. \tag{7.2}$$

The zero diagonal element in (7.2) implies the singularity of $(\underline{\boldsymbol{H}}_6)^{\tilde{\mathcal{L}}_{(9)}}$. Hence, in this case we detect island formation simply by inspection.

For the identification of the minimal cutset elements, we consider all the outaged lines, denoted by the set $\tilde{\mathcal{L}}_{(15)}$, and construct $\underline{\boldsymbol{H}}_{15}$. The RRQR factorization as described in Chapter 3 results in three zero-diagonal elements in $\underline{\boldsymbol{R}}$, so that $\rho(15) = 3$. We evaluate the three basis vectors $[\underline{\boldsymbol{v}}_1 \vdots \underline{\boldsymbol{v}}_2 \vdots \underline{\boldsymbol{v}}_3]$ spanning $\mathfrak{N}(\underline{\boldsymbol{H}}_{15}^T)$ using $\underline{\boldsymbol{Q}}_{\rho(15)}$:

$$
[\underline{\boldsymbol{v}}_1 \vdots \underline{\boldsymbol{v}}_2 \vdots \underline{\boldsymbol{v}}_3] =
\begin{bmatrix}
0 & 0 & 0 \\
0 & 0 & 0 \\
1 & 0 & 0 \\
-1 & 0 & 0 \\
-1 & 0 & 0 \\
0 & 1 & 0 \\
0 & 0 & 0 \\
-1 & 0 & 0 \\
-1 & 0 & 0 \\
-1 & 0 & 0 \\
0 & 0 & 1 \\
-1 & 0 & 0 \\
1 & 0 & 0 \\
0 & 1 & -1 \\
0 & 0 & 1
\end{bmatrix},
\quad
\underline{\boldsymbol{Q}}_{\rho(15)} =
\begin{bmatrix}
0.0000 & 0.0000 & 0.0000 \\
0.0000 & 0.0000 & 0.0000 \\
-0.0440 & 0.3505 & -0.0134 \\
0.0440 & -0.3505 & 0.0134 \\
0.0440 & -0.3505 & 0.0134 \\
0.0595 & 0.0370 & 0.7714 \\
0.0000 & 0.0000 & 0.0000 \\
0.0440 & -0.3505 & 0.0134 \\
0.0440 & -0.3505 & 0.0134 \\
0.0440 & -0.3505 & 0.0134 \\
0.5909 & 0.0823 & 0.2097 \\
0.0440 & -0.3505 & 0.0134 \\
-0.0440 & 0.3505 & -0.0134 \\
-0.5314 & -0.0452 & 0.5617 \\
0.5909 & 0.0823 & 0.2097
\end{bmatrix}.
$$

$$(7.3)$$

The value 3 of $\rho(15)$ indicates the existence of 3 minimal cutsets in $\tilde{\mathcal{L}}_{(15)}$. The components of $\underline{\boldsymbol{v}}_1, \underline{\boldsymbol{v}}_2$ and $\underline{\boldsymbol{v}}_3$ allow us to identify the members of these three minimal cutsets and the corresponding subnetworks associated with the terminal nodes of each minimal cutset. The identification results are summarized in Table 7.2.

Table 7.2 Large-Scale Network: $\tilde{\mathcal{L}}_{(15)}$ **Minimal Cutset Information**

$\hat{\mathcal{L}}^i$	nodes belonging to $\mathcal{N}_a^i$	nodes belonging to $\mathcal{N}_b^i$
$\{\tilde{\ell}_3, \tilde{\ell}_4, \tilde{\ell}_5, \tilde{\ell}_8,$ $\tilde{\ell}_9, \tilde{\ell}_{10}, \tilde{\ell}_{12}, \tilde{\ell}_{13}\}$	1790, 2764, 2721, 2765, 2769, 2693	2694, 2727, 2718, 2716, 90, 2691
$\{\tilde{\ell}_6, \tilde{\ell}_{14}\}$	486, 2926	2927
$\{\tilde{\ell}_{11}, \tilde{\ell}_{14}, \tilde{\ell}_{15}\}$	2925, 2927, 2924	2926

The proposed approach is flexible and does not require the updated PTDFs. In fact, to study system connectivity, we first investigate the impacts of the outages of the elements of $\tilde{\mathcal{L}}_{(9)}$. We construct the corresponding $\underline{H}_9$ and perform the Gaussian elimination on $\underline{H}_9$. We determine that the outages of the lines in $\tilde{\mathcal{L}}_{(9)}$ do not form islands. We next focus on the impacts of the unplanned outages of the lines using the sequence given in Table 7.4. For the first outage in this sequence, we augment $\underline{H}_9$ by adding a row and a column to form $\underline{H}_{10}$. We perform the Gaussian elimination on $\underline{H}_{10}$ using the factors of $\underline{H}_9$. Since no islanding results, for the second unplanned outage, we again augment $\underline{H}_{10}$ by adding a row and a column, and perform the Gaussian elimination of the resulting $\underline{H}_{11}$ using the factors of $\underline{H}_{10}$. This process continues until either we detect a zero diagonal element in the Gaussian elimination of each augmented matrix in the sequence or we complete the Gaussian elimination of $\underline{H}_{15}$. We can similarly analyze the impacts of any subset of additional outages by using the factors of the unaugmented matrix in the Gaussian elimination step of the augmented matrix.

The ISO-NE application study illustrates the capability of the island detection approach for large-scale power system networks. In fact, the size of the network is unimportant as the computations are carried out on matrices whose dimension is the number of outaged lines. These computations take advantage of the structural characteristics of the method whereby a set of k-line outages serves to establish the results of any larger set of outaged lines containing this k-line set as a subset. In this way, we can directly pinpoint the impact of the interactions between the additional line outage and the k-line outages as a causal factor for island formation. For this reason, the proposed method is particularly useful in the analysis of appropriate preventive/corrective control actions in cases involving the *domino effect* of multiple line outages to effectively mitigate the impacts of such a sequence of outages.

7.3 Quantification of the ISO-NE DAM Performance as a Function of Security Criterion

The objective of this study is to analyze whether the economic efficiency of the ISO-NE DAM is adversely impacted by the system operations complying with the security criterion in force. For this purpose, we quantify the market performance as a function of three security criteria and perform comparative assessments. We measure the changes with respect to the outcomes under the current ISO-NE security criterion.

We use the system and market data from the year 2005 and utilize the actual market clearing software used for the ISO-NE DAM. We start out with a discussion of important aspects of the study period and then discuss the selection of the representative days for that period. We next describe the two other security criteria considered for the comparative studies. We then summarize and interpret the study results.

The study is performed for the second half of the year 2005 and the first half of the year 2006. This study period was chosen to allow the use of market and system data that reflects the most up-to-date ISO-NE procedures and rules. The analysis of the load in the selected period shows that the demand levels in the summer months, July and August, are significantly higher than those in the *nonsummer* months. Furthermore, the range of daily peak demands in the summer months is considerably larger than that in the nonsummer months. Due to the maintenance scheduling, the sets of available resources in summer months are different than those in the other months. In addition, the ratings of the system components in each summer month differ from those in the other months.

The period under study is further characterized by the existence of two distinct regimes $\mathcal{R}_1$ and $\mathcal{R}_2$ – pre- and post-October 9, 2005, respectively. The ratio of the hourly price-sensitive bid amounts to the total hourly demand changes markedly from a small value under the regime $\mathcal{R}_1$, to a sizable fraction under the regime $\mathcal{R}_2$. The hourly loads in these two regimes are further distinguished in terms of their peak, base and average values. We present the load characteristics of the regimes $\mathcal{R}_1$ and $\mathcal{R}_2$ in Figures 7.2 and 7.3. The significant increase in the fraction of price-sensitive demand is due to the bidding behavior change of the large buying entity whose demand corresponds to approximately 25% of the total system demand. This buyer submits, on the average, only 10% of his demand as price sensitive under the regime $\mathcal{R}_1$. However, the buyer has no fixed demand under regime $\mathcal{R}_2$ as all of the buyer's bids become price sensitive, as shown in Figure 7.4. Due to the size of the buyer's demand, the marked change in his bidding behavior results in a significant portion of the total system demand that is price responsive under the regime $\mathcal{R}_2$.
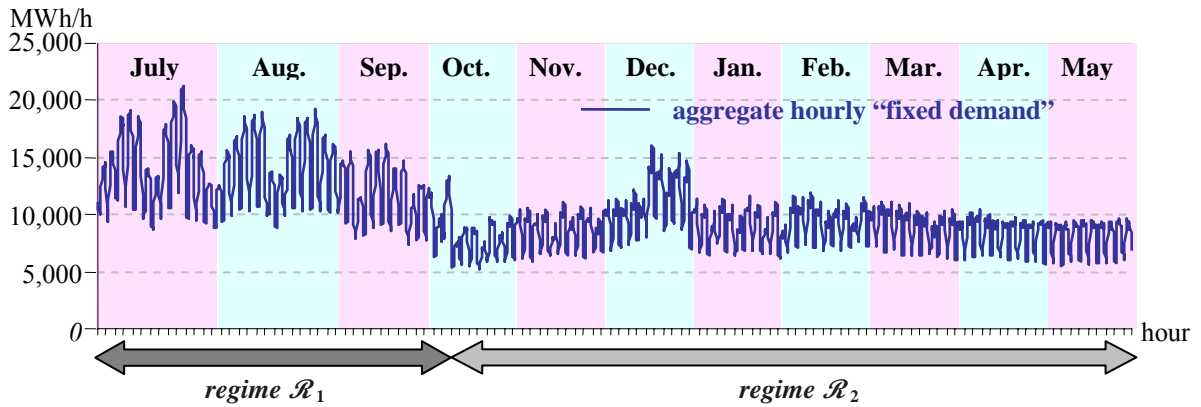
115

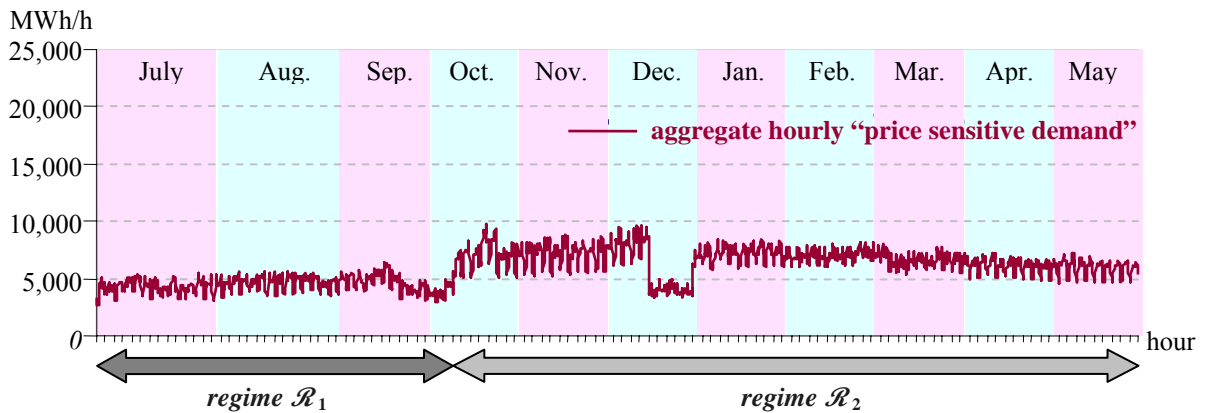*Figure 7.2 Aggregate hourly "fixed demand"*

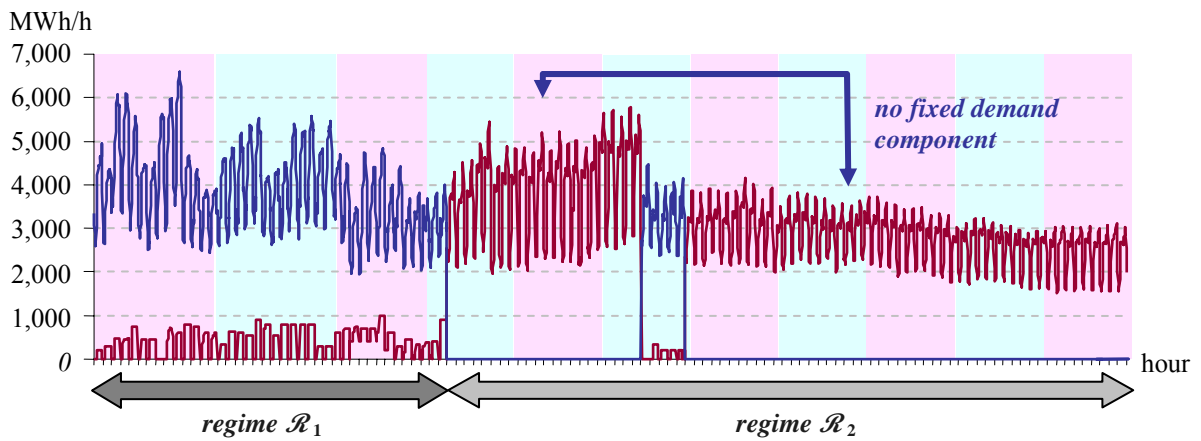*Figure 7.3 Aggregate hourly "price sensitive demand"*

Figure 7.4 The bidding pattern of the single large buying entity

We select the representative days from each month using the sampling scheme provided in Chapter 5. We construct the LDC approximation for each summer and nonsummer month by

14 and 10 representative days, respectively. Since these approximations provide acceptably small errors, we determine the elements of each $\mathcal{T}_r$.

Table 7.3 Total Hourly Dispatched Loads and Range of Impacts

metric	regime	range (MW)	average (MW)
P_{e_0}	$\mathcal{R}_1$	(9,177 , 25,638)	16,967
	$\mathcal{R}_2$	(8,733 , 23,281)	15,421
ΔP_{e_1}	$\mathcal{R}_1$	(-646 , 961)	141
	$\mathcal{R}_2$	(-485 , 913)	8
ΔP_{e_2}	$\mathcal{R}_1$	(-836 , 868)	-184
	$\mathcal{R}_2$	(-694 , 714)	-42

We select the criterion $\mathcal{C}_0$ as the reference criterion and consider two specific criteria $\mathcal{C}_1$, a modified $(n-1)$ security, and $\mathcal{C}_2$, a modified $(n-2)$ security. For the criterion $\mathcal{C}_1$, the contingency list $\mathcal{J}_{e_1} = \mathcal{J}_{n-1}$, and preventive control action is deployed for each contingency in $\mathcal{J}_{e_1}$. For the criterion $\mathcal{C}_2$, the contingency list $\mathcal{J}_{e_2} = \mathcal{J}_{e_0}$, but we replace the corrective control actions by the preventive control actions for the contingencies in $\bigcup_{k=1}^{4} \mathcal{M}^k$. We next discuss the market performance impacts of the change of $\mathcal{C}_0$ to each of the criteria considered and distinguish those impacts under the two regimes $\mathcal{R}_1$ and $\mathcal{R}_2$.

We first focus on the MW impacts. For the reference criterion $\mathcal{C}_0$, we obtain the range and the average values of the total hourly dispatched load P_e under the regimes $\mathcal{R}_1$ and $\mathcal{R}_2$. We compute the changes from the P_e values under the two security criteria and present the results in Table 7.3. We observe that the price responsive demand plays an important role in the DAM. For each security criterion, the changes under the regime $\mathcal{R}_2$ are considerably lower than those under the regime $\mathcal{R}_1$. In fact, the changes are attenuated to a greater extent

for the change of the security criterion from $\mathcal{C}_0$ to $\mathcal{C}_1$ than from $\mathcal{C}_0$ to $\mathcal{C}_2$. We hypothesize that the factors that contribute to such outcomes are due to system structure, the effectiveness of the security control actions and the nature of the constraints imposed on the system operations.

The change from the current security criterion to either of the two criteria studied impacts the value of the system transfer capability. The change in the value of the system transfer capability, in turn, affects the ability of the import areas to bring in energy from the export area. In fact, the analysis of the ISO-NE system during the study period indicates that the replacement of the security criterion $\mathcal{C}_0$ by the criterion $\mathcal{C}_1$ results in the increased import capabilities of the import areas for each hour. But the increased capability may not be utilized in every hour. For example, the stand-alone area $\mathcal{A}^1$ buyers increase their imports from the export area, thereby decreasing their dependence on the less economic $\mathcal{A}^1$ resources. On the other hand, the imports of the nested area $\mathcal{A}^2$, due to the physical constraints of the $\mathcal{A}^2$ network, may not utilize such increased capability in every hour. We measure the changes in the utilization of the increased import capabilities using the areawide net injection changes. We illustrate the results for the import areas $\mathcal{A}^1$ and $\mathcal{A}^2$, and the export area $\mathcal{A}^5$ for a sample of 14 days from both regimes in Figure 7.5. These plots indicate the changing nature of the import area $\mathcal{A}^1$. In particular, the constraints due to the contingencies in $\mathcal{M}^1$ are binding in regime $\mathcal{R}_1$ under criterion $\mathcal{C}_0$, but not necessarily in $\mathcal{R}_2$. As such, the import area $\mathcal{A}^1$ behaves similarly to the export area. On the other hand, the constraints due to the contingencies in $\mathcal{M}^2$ are binding throughout the study period. The results are typical for the study period, particularly in terms of the more pronounced impacts in the daily peak hours.
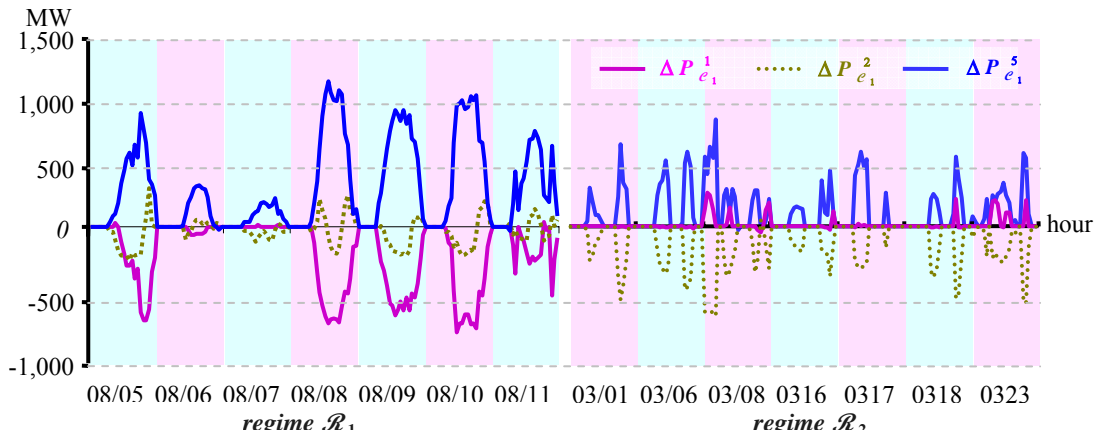
Figure 7.5 Areawide net injection impacts: $\mathcal{C}_0$ wrt. $\mathcal{C}_1$

Due to the fact that the system operations under the criterion $\mathcal{C}_2$ are more constraining than those under the criterion $\mathcal{C}_0$, the security change from $\mathcal{C}_0$ to $\mathcal{C}_2$ results in decreased import capabilities of the import areas for every hour of the study period. In fact, the impacts on the imports of the stand-alone area $\mathcal{A}^1$ are exactly in the opposite direction to those under the criterion change from $\mathcal{C}_0$ to $\mathcal{C}_1$. On the other hand, the imports of the nested area $\mathcal{A}^2$ exhibit results similar to those under the criterion change from $\mathcal{C}_0$ to $\mathcal{C}_1$. We plot these outcomes for the same days in Figure 7.6.
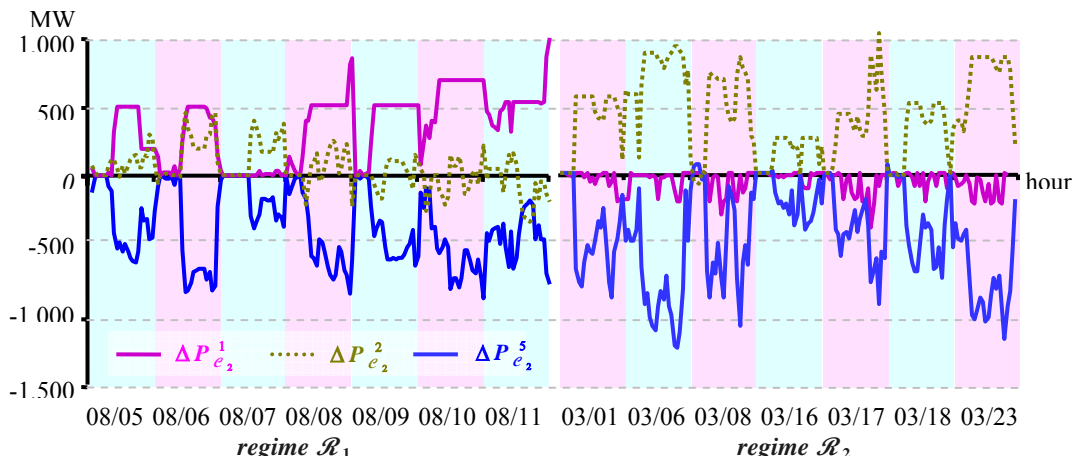

Figure 7.6 Areawide net injection impacts: $\mathcal{C}_0$ wrt. $\mathcal{C}_2$

119

We next examine the monetary impacts of the changes in the security criterion. We use the daily auction surplus as the basic metric in this investigation. We first normalize the daily auction surplus values using the average value of the daily auction surplus under the reference criterion $\mathcal{C}_0$ as a base value. Such normalization is needed to facilitate effective comparison of the monetary impacts. We first consider the economic repercussions of the increased import capabilities arising from the relaxation of the security criterion from $\mathcal{C}_0$ to $\mathcal{C}_1$. Throughout the study period, the increased import capabilities are utilized, leading to higher market efficiencies. We may view these improvements as a measure of the "costs" of not violating the constraints due to the double element contingencies in the reference criterion. On the other hand, the decreased import capabilities arising from changing the criterion from $\mathcal{C}_0$ to $\mathcal{C}_2$ may lower the market efficiencies. Indeed, such reductions are present throughout the study period. We may interpret these reductions to be a measure of the "costs" of replacing corrective for preventive control actions. The plot of the normalized daily auction surplus values under the reference criterion $\mathcal{C}_0$ is given in Figure 7.7 for the set of representative days.
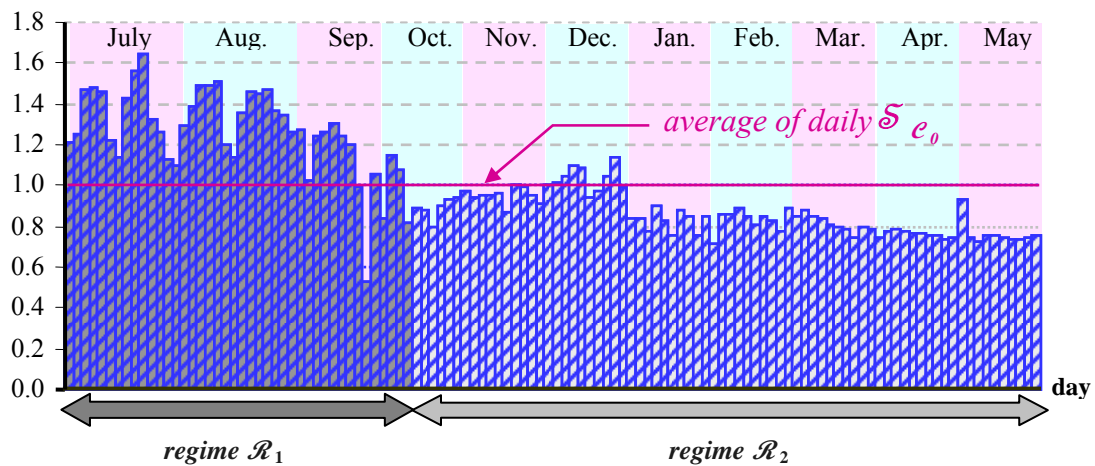

Figure 7.7 Daily auction surplus under criterion $\mathcal{C}_0$

The plots of the changes of the market efficiency arising from a change of the security criterion are shown in Figure 7.8. We provide some of the statistics related to the maximum, the mean and the standard deviation of the market efficiency impacts under the regimes $\mathcal{R}_1$ and $\mathcal{R}_2$ for each security criterion change in Table 7.4.
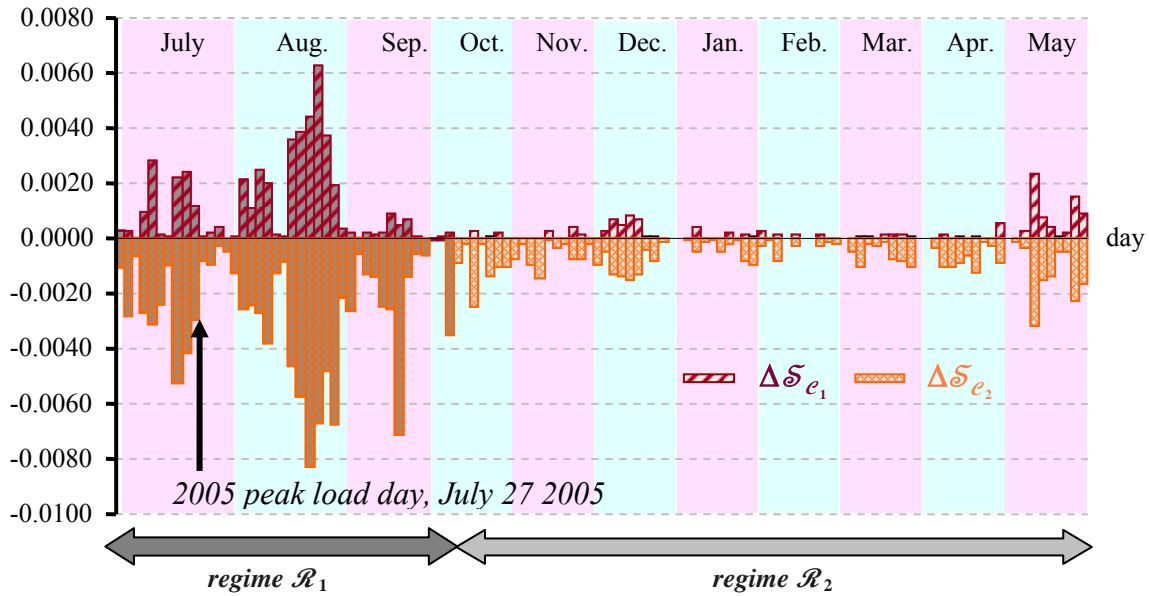

Figure 7.8 Daily market efficiency impacts

Table 7.4 Statistical Analysis of Market Efficiency Change Impacts under the Regimes $\mathcal{R}_1$ and $\mathcal{R}_2$ (Basis is $\mathcal{C}_0$)

criterion	regime	maximum	mean	standard deviation
$\mathcal{C}_1$	$\mathcal{R}_1$	0.0506	0.0091	0.0122
	$\mathcal{R}_2$	0.0065	0.0011	0.0004
$\mathcal{C}_2$	$\mathcal{R}_1$	-0.0670	-0.0210	0.0170
	$\mathcal{R}_2$	-0.0201	-0.0063	0.0048

We obtain some insights by studying the disaggregation of the metric $\Delta\mathcal{S}_{\mathcal{C}_1}$ and $\Delta\mathcal{S}_{\mathcal{C}_2}$ by each area. The area by area contribution is in line with the changes in the utilization of the

modified import and export capabilities. We plot the changes of the import areas $\mathcal{A}^1$ and $\mathcal{A}^2$, and the export area $\mathcal{A}^5$, contribution to the auction surplus in Figure 7.9 (7.10) corresponding to shifting the security criterion from $\mathcal{C}_0$ to $\mathcal{C}_1$ ($\mathcal{C}_2$).
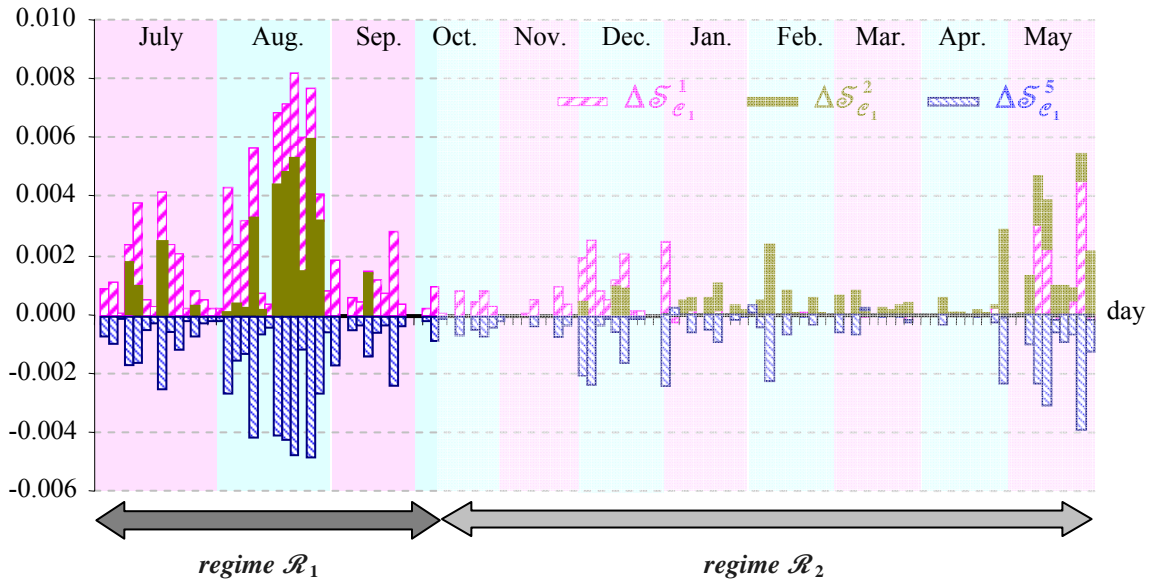

Figure 7.9 Changes in the area's contributions to auction surplus: $\mathcal{C}_0$ wrt. $\mathcal{C}_1$
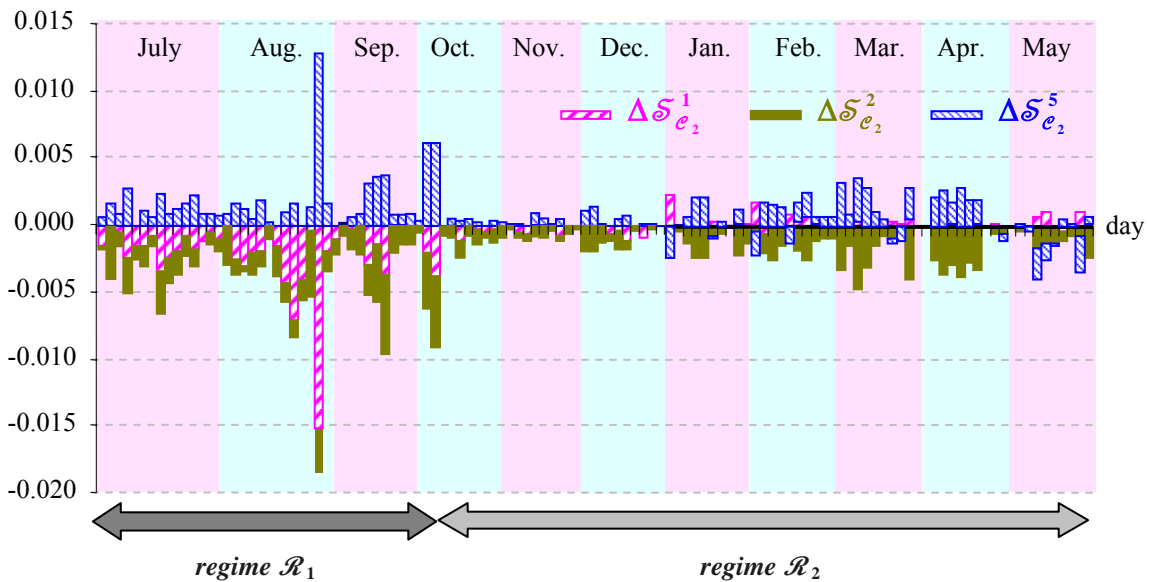
Figure 7.10 Changes in the area's contributions to auction surplus: $\mathcal{C}_0$ wrt. $\mathcal{C}_2$

We note from the plots in Figures 7.8 – 7.10 that the price responsive regime $\mathscr{R}_2$ leads to a strong attenuation of the economic impacts of changing the security criterion to either $\mathscr{C}_1$ or $\mathscr{C}_2$. Moreover, the relaxation of the security criterion from $\mathscr{C}_0$ to $\mathscr{C}_1$, i.e., not taking into account the double element contingencies, results in an insignificantly small dollar gain under the regime $\mathscr{R}_2$. It is, therefore, questionable whether such a relaxation is worthwhile given the meager impacts. The tightening of the security criterion from $\mathscr{C}_0$ to $\mathscr{C}_2$ by replacing the corrective by preventive actions leads to dollar losses. These findings of the comparative assessment lead us to conclude that the reference criterion $\mathscr{C}_0$ is, for all intents and purposes, more appropriate for the ISO-NE DAM than either of the two security criteria considered. Through this study, we also gain important insights on the role of price-responsive demand and the selected security control action. In fact, a key finding of the ISO-NE study is that the economic efficiency of the electricity markets need not decrease when a power system is operated under a stricter criterion as long as there is price-responsive demand. The proposed approach provides good insights into the ramification of changing the security criterion on both qualitative and quantitative bases.

As the real-time energy markets, or RTM, become more prominent, the comparative assessments of a security criterion change have to be broadened to include the impacts on RTM. To be able to accomplish this broadened scope, the incorporation of a multi-settlement system [1], [87] - [90] involving the DAM and the RTM is required. The studies extending the proposed approach to incorporate the multi-settlement system are reported in the next section.

7.4 The ISO-NE Multi-Settlement System Performance Quantification

We illustrate the application of the proposed approach to the study of the ISO-NE system and markets. The objectives of our studies are to quantify the economic efficiency of the ISO-NE multi-settlement markets as a function of the security criterion in force, to investigate the impacts of the financial entity participation on the ISO-NE system and markets and to quantify the impacts on the ISO-NE market performance of a security criterion change from the criterion in force to a modified $(n-1)$ security. We apply the proposed approach to quantitatively analyze the ISO-NE multi-settlement system performance. We assess the impacts of the participation of financial entities in the DAMs by performing a side-by-side comparison of the outcomes of the DAMs and the associated RTMs without and with such players. A particularly insightful aspect of the comparison is the set of values for the deviation metrics of the physical entities. In the following study, we quantify the impacts of a change in the security criterion from the current security criterion in force to a modified $(n-1)$ security criterion and compare the observed impacts under the two criteria.

We select 40 representative days from 2005 and 2006 to study the DAMs and their associated RTMs. For the discussion in this study, we focus specifically on the four contiguous peak demand hours of each selected day and analyze the values of metrics of interest for those 160 hours. We start out with the evaluation of the ISO-NE multi-settlement system performance under the security criterion in force to determine the values of the metrics for the reference case for the study.

We perform market clearing for the DAMs and their associated RTMs for the selected 160

hours and quantify the market performance metrics under the security criterion $\mathcal{C}_0$. We first focus on the DAM-RTM MW deviations. As the real-time demand in each RTM is considered to be fixed, the cleared demand values are not a function of the security criterion per se, as long as the security-constrained market problem is feasible. We compare the fixed real-time demand in each of the M RTMs associated with the demand cleared in a DAM to evaluate the deviation metrics. We plot in Figure 7.11 the demand values in the DAMs and in their associated RTMs for the selected 160 hours. We note that the real-time demand values exceed the DAM demand for the selected 160 hours. As these hours are representative of the ISO-NE system past behavior, they correctly indicate that the RTM demands typically exceed the DAM demands.
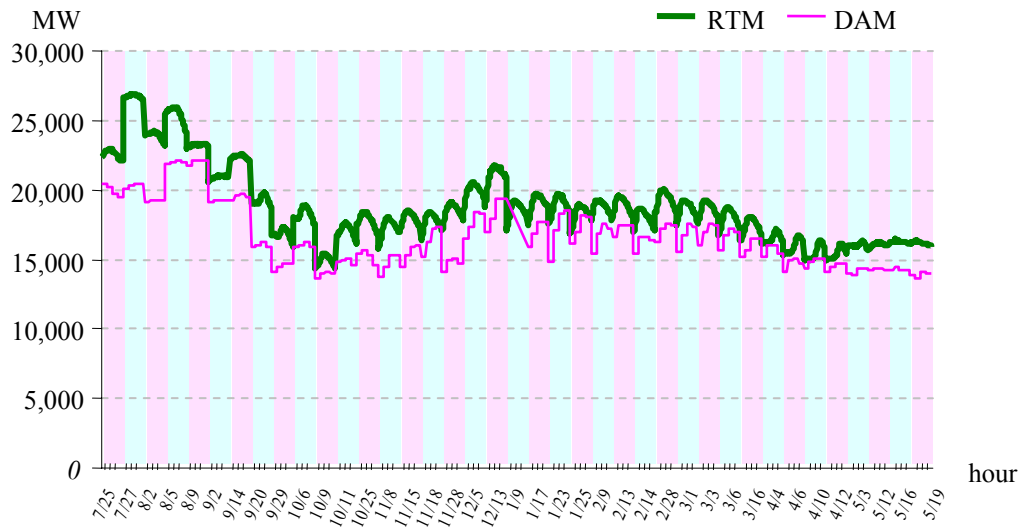

*Figure 7.11 Cleared demand in the **DAM**s and in the associated **RTM**s for the selected 160 hours*

We examine the physical demand and generation deviations and use the plots in Figure 7.12 to gain insights into their nature. These plots indicate that both the physical demand and the generation deviations are positive for the hours under consideration. Also, the positive values indicate that as much as 75% of the real-time demand and generation are cleared in

the DAM. The plot of the net differences between the generation and the load deviations, also given in Figure 7.12, indicates the impacts of the net positions of the financial players in the DAMs. While there are daily variations in the financial entities' net positions, their range is up to 10 % of the real-time demand, with the more pronounced impact in the higher demand days.
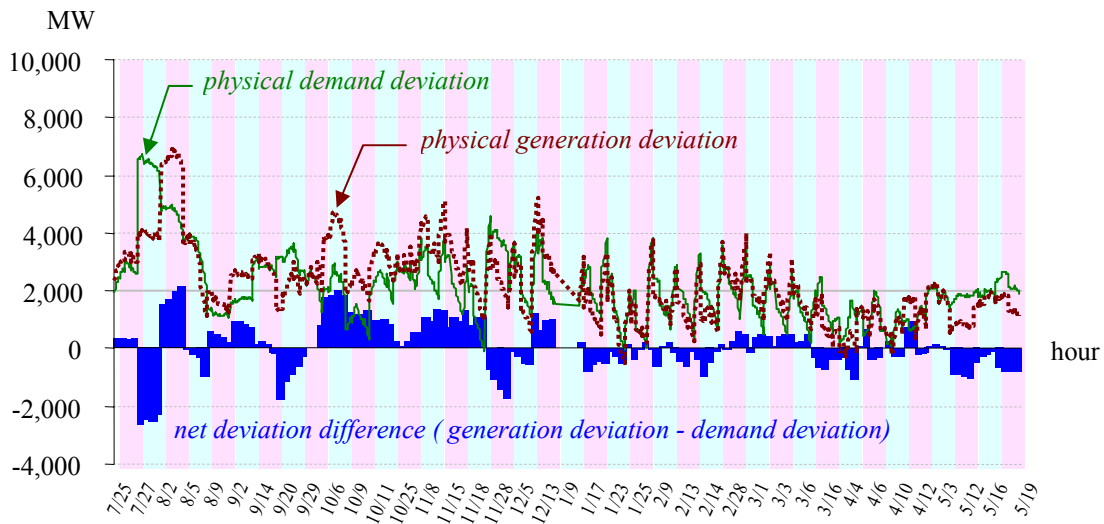

Figure 7.12 Deviation in the physical demand and the generation for the selected 160 hours

We now discuss the financial aspects of the secure operations of the power system. Analysis of the DAM-RTM price deviation metric indicates that, on average, the prices are higher in the DAM*s* than in their associated RTMs. Such results are clearly visible in the plots of the price deviation duration curves of the import areas $\mathcal{A}^1$, $\mathcal{A}^2$ and the export area $\mathcal{A}^5$, shown in Figure 7.13. The areawide price deviation measure of an area is evaluated using the load-weighted average of the prices in the area for a snapshot system. We observe that the price deviations are more pronounced for the import areas $\mathcal{A}^1$ and $\mathcal{A}^2$ than for the export area $\mathcal{A}^5$. For the study hours selected, the area $\mathcal{A}^2$ price deviations are larger than those of any other area, indicating that congestion has more pronounced impacts on this area than other

126

areas. The price deviation results also indicate that the physical sellers in the import areas capture more revenues for their real-time production in the 160 hours of the study period. Under these conditions, financial entities have more incentives to be sellers in the import area $\mathcal{A}^2$ than in any other area. Given the nature of the physical generation and the demand deviations, we conjecture that financial entities may expect higher price deviations in the peak-demand periods and therefore they may adjust their bidding behaviors to clear more quantities in the DAMs in which they participate.
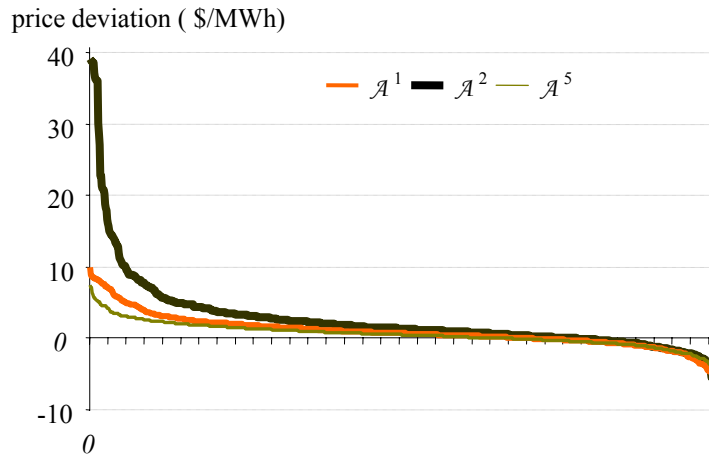

Figure 7.13 Price deviation duration curves for the areas $\mathcal{A}^1$, $\mathcal{A}^2$ and $\mathcal{A}^5$

Next, we turn our attention to assessing the auction surplus of multi-settlement markets. We use the value of $\tau = 1000$ \$/MWh for the fixed demand. We choose this value on the basis that it is the authorized bid/offer price cap in the ISO-NE markets and it is a reasonable proxy of the willingness to pay of the buyers with fixed demands. We evaluate using τ the auction surplus for the DAMs and the associated RTMs. We summarize the results in the plots given in Figure 7.14 of the normalized auction surplus values for the 160 hours in the study period. We normalize the auction surplus values using the average RTM auction

surplus value so as to provide a meaningful comparison of the observed results. The positive

load deviations and the fact that they represent fixed demands imply that the auction surplus

outcomes are higher in the RTMs than in the DAMs. We next examine the individual

components of the deviations of the auction surplus in the DAMs and their associated RTMs.

Figure 7.14 The normalized auction surplus attained in the DAMs and the associated RTMs for the 160 hours of the study period

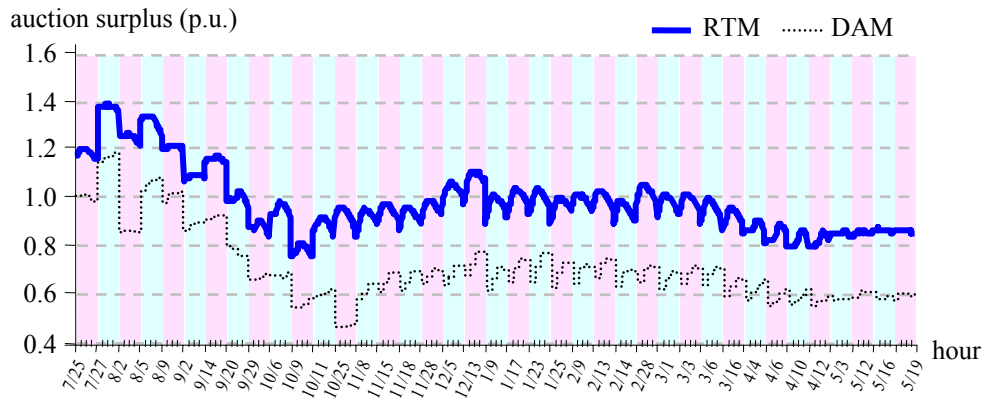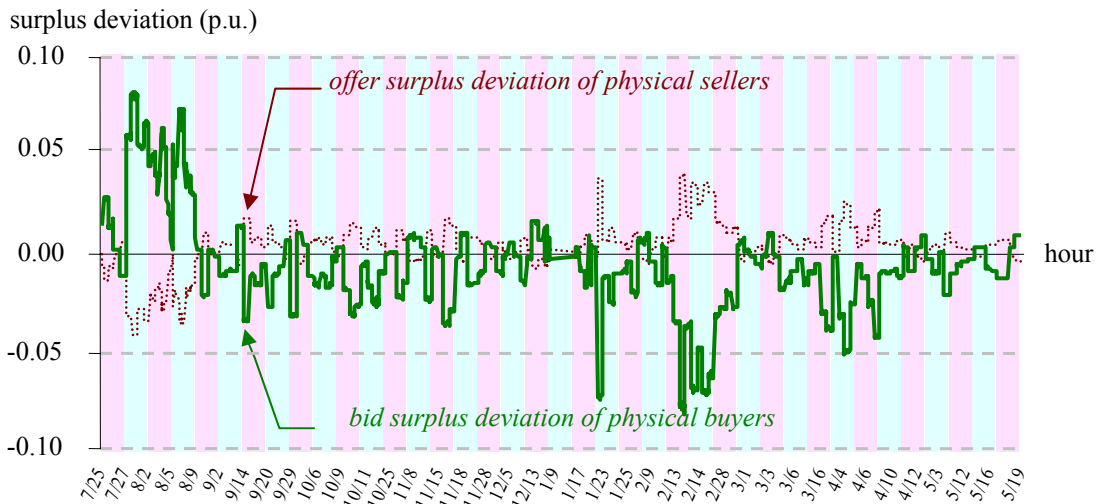*Figure 7.15 The normalized auction surplus attained in the DAMs and the associated RTMs for the 160 hours of the study period*

We investigate the deviations in the offer/bid surpluses of the physical market participants

using their normalized values, with the base value being the RTM auction surplus. We

128

provide the plots of the physical buyers and sellers in Figure 7.15. We note that the physical sellers capture additional revenue for their real-time production for the majority of the hours in the simulation period. Therefore, the physical buyers pay a "premium" for that portion of their real-time demand needs that is cleared in the DAM. The plots clearly demonstrate that the sum of the bid/offer surplus deviations is not equal to zero, due to the financial entity participation, the bilateral transactions and the congestion rents. The metrics in (6.6)-(6.23) serve to provide the quantification of the multi-settlement system performance for the 160 hours of the study period under the reference criterion $\mathcal{C}_0$. We use these results as the reference basis for the comparative studies which we discuss next.

We examine the impacts that the financial players have on the market performance under the ISO-NE security criterion $\mathcal{C}_0$ in force. We first evaluate the impacts by considering the market operations without and with the participation of the financial entities in the DAMs. The difference between the two cases quantifies the contribution of the financial players in the multi-settlement environment. We evaluate the physical demand deviations, as well as the price deviations observed for the two cases.

Without financial entities in the DAM, lower physical demand is cleared in the DAM than in the case with the financial entity participation. Therefore, more generation is required in real time to compensate for the lower demand in order to ensure near-real-time system security. In fact, the ISO-NE study indicates that, on average, 700 MW additional output is required in real time without financial entity participation. Such an increase clearly indicates that the absence of financial entity participation makes the task of operating securely the near-real-time ISO-NE system more difficult. The plots of the cleared DAM demand without

and with financial entity participation together with the real-time demand needs for the 160 hours in the study period are given in Figure 7.16.
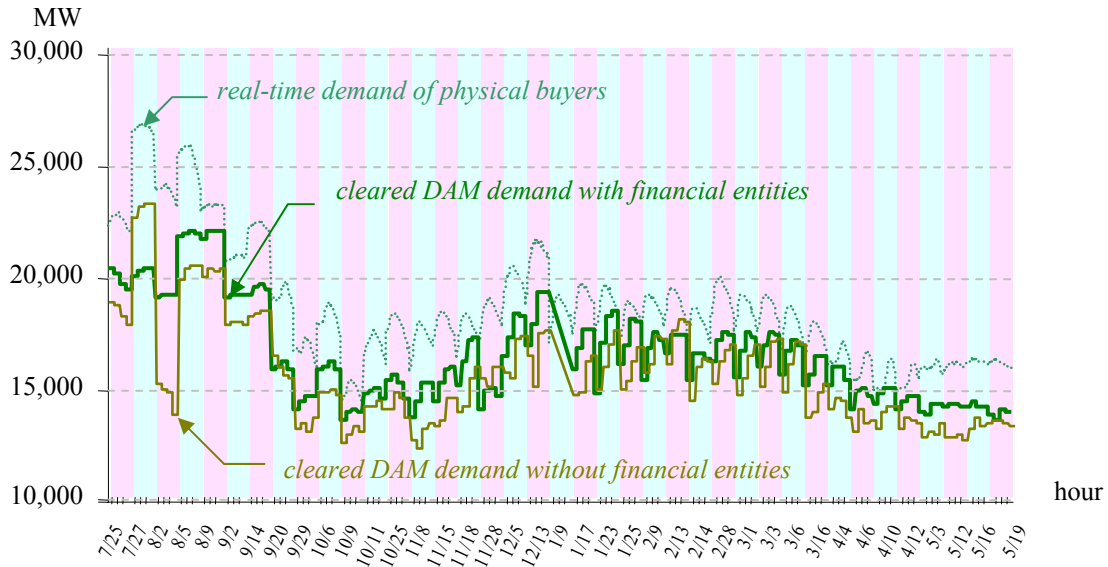
Figure 7.16 Comparison of the cleared demands in the DAMs without and with financial entities

The most striking fact about financial entity participation can be discerned from examining the DAM-RTM price deviation results without and with financial entities. We superimpose in Figure 7.17 the price deviation duration curves for the areas $\mathcal{A}^1$, $\mathcal{A}^2$ and $\mathcal{A}^5$ without the financial entity participation on those with their participation shown in Figure 7.16. The financial entity participation markedly reduces the deviation values for the areas $\mathcal{A}^1$ and $\mathcal{A}^2$. Since such a decrease corresponds to the desirable price convergence, its impact is very significant and attains the desired objective of price convergence.

This side-by-side comparison results indicate very clearly the important role that financial entities play in electricity markets. Their participation decreases the magnitude of the physical demand deviations. In turn, these lower deviations make the management of near-

real-time operations easier and, moreover, improve near-real-time system security. In terms of market performance, the participation of financial entities decreases the magnitude of the price deviations.
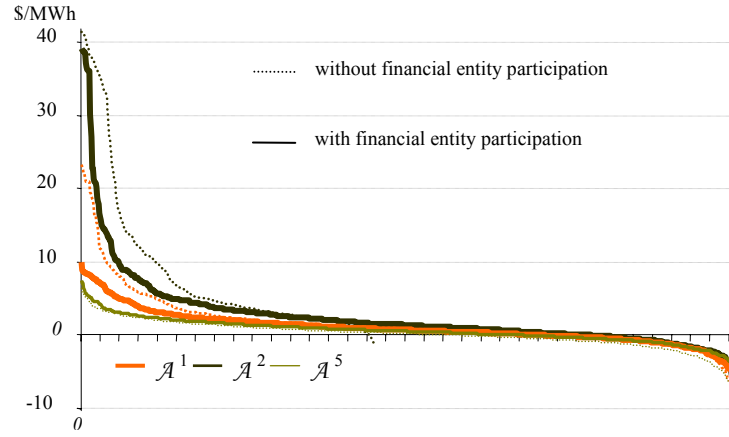
Figure 7.17 Price deviation duration curves for the areas $\mathcal{A}^1$, $\mathcal{A}^2$ and $\mathcal{A}^5$ with and without financial entities

We next study the impacts on the multi-settlement performance of a security criterion change from the reference criterion $\mathcal{C}_0$ to a modified $(n - 1)$ security criterion $\mathcal{C}_1$. The contingency set $\mathcal{I}_{e_1}$ consists of the single element contingencies in $\mathcal{I}_{e_0}$. For the security criterion $\mathcal{C}_1$, we perform market clearing of the DAMs and their associated RTMs for the selected hours in the study period and evaluate the market performance metrics. We compare the values of the metrics of interest with respect to those under the reference criterion $\mathcal{C}_0$.

We compute the hourly auction surplus under the security criterion $\mathcal{C}_1$ and normalize these values using the average value of the hourly auction surplus under the reference criterion $\mathcal{C}_0$ as the base. The change from the security criterion $\mathcal{C}_0$ to $\mathcal{C}_1$ impacts the values of the system transfer capability, which, in turn, affects the ability of the import areas to

bring in energy from the export area. Indeed, the analysis of the ISO-NE system during this study period indicates that the change from the security criterion $\mathcal{C}_0$ to the criterion $\mathcal{C}_1$ results in the increased import capabilities of the import areas for each hour of the study period as discussed in Section 7.2. We note that the utilization of the increased import capabilities leads to increased auction surplus. We may view such an improvement as a measure of the "costs" of not violating the constraints associated with the double element contingencies in $\mathcal{G}_{e_0}$. There are also a number of hours during which the change in security criterion from $\mathcal{C}_0$ to $\mathcal{C}_1$ has no impacts on the auction surplus. For such hours, the double element contingencies have zero economic impact. We plot the changes in the normalized auction surplus values corresponding to the security criterion change in Figure 7.18.
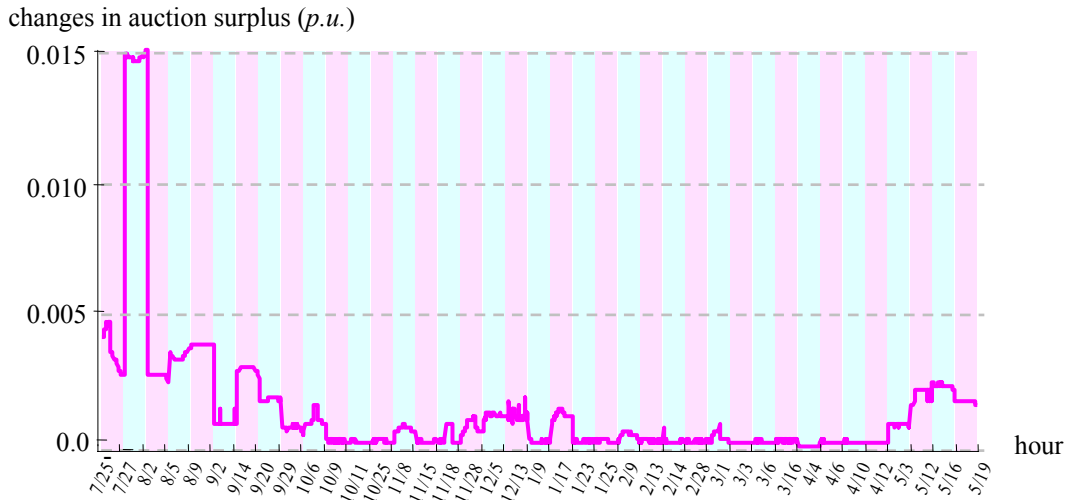

changes in auction surplus (*p.u.*)

Figure 7.18 Auction surplus change due to the security criterion change from $\mathcal{C}_0$ to $\mathcal{C}_1$

We next discuss the impacts of the change of security criterion from $\mathcal{C}_0$ to $\mathcal{C}_1$ on the market participants' surpluses. The change of security criterion from $\mathcal{C}_0$ to $\mathcal{C}_1$ has widely

132

varying impacts on the different market participants within the different areas. For illustration purposes, we consider five specific days to discuss the impacts. The security criterion change results in greater utilization of the export area sellers and, therefore, in decreased production of the import area physical sellers. Such a change leads to a corresponding change in the surpluses of the players in the various areas. In Figure 7.19, we plot changes in the physical sellers' surpluses in areas $\mathcal{A}^1$, $\mathcal{A}^2$ and $\mathcal{A}^5$ for the five selected days.

Figure 7.19 Changes of the physical sellers' offer surpluses in response to the criterion change from $\mathcal{C}_0$ to $\mathcal{C}_1$

The impacts have almost the opposite effects on the surpluses of the physical buyers: while the surpluses of the export area physical buyers are decreasing, those in the import areas are increasing. The physical buyers within the import areas are able to meet their demand using more economic resources from the export area $\mathcal{A}^5$ to take advantage of the increased transfer capabilities, thereby decreasing their payments. In fact, the changes in the surpluses are particularly more pronounced for the import area $\mathcal{A}^2$ physical buyers than other areas'

physical buyers as shown in Figure 7.20.

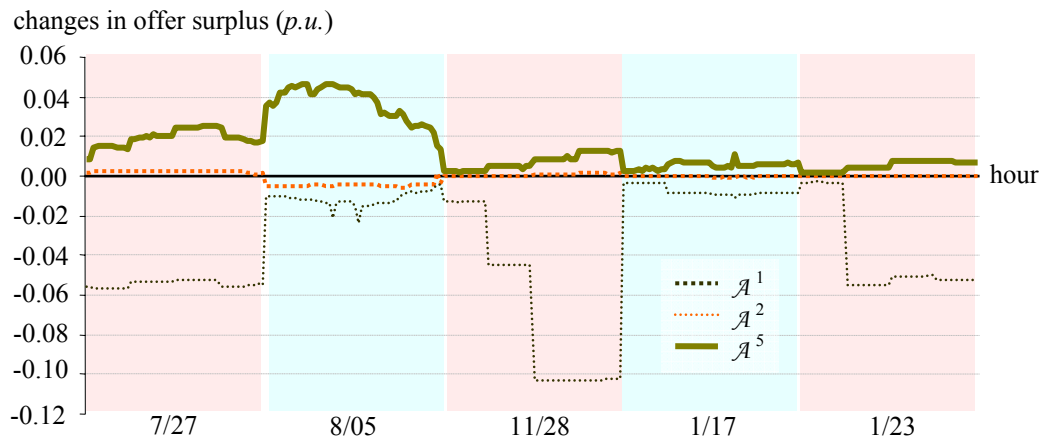changes in bid surplus (*p.u.*)
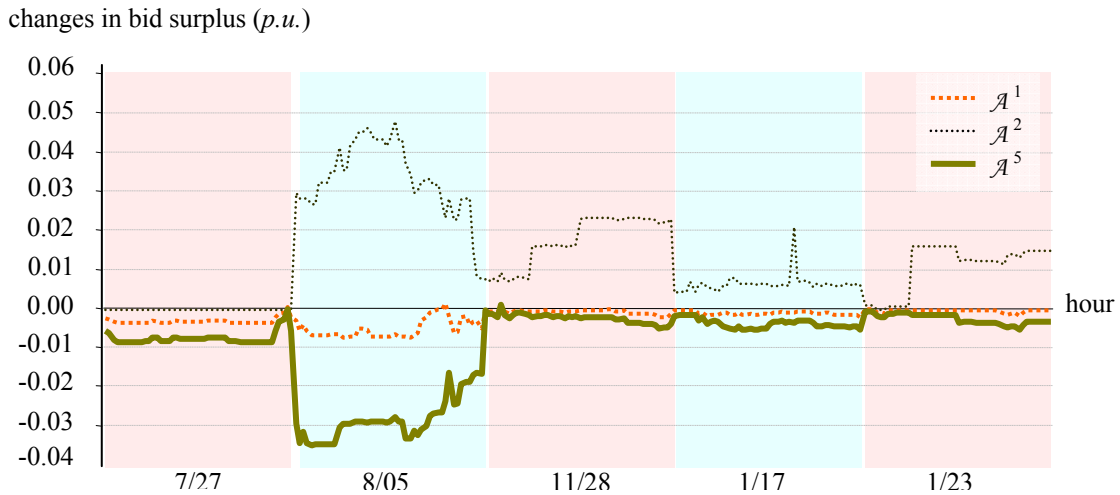
Figure 7.20 Changes of the physical buyers' bid surpluses in response to the criterion change from $\mathcal{C}_0$ to $\mathcal{C}_1$

The impacts of changing the security criterion on the surpluses of the financial entities are minor and of little significance compared to those impacts on the players with physical assets for a change in the security criterion. Overall, the relatively small dollar impacts due to the change of the security criterion from $\mathcal{C}_0$ to $\mathcal{C}_1$, as evident from the Figures 7.18 - 7.20, furthermore justify that the current security criterion in force, $\mathcal{C}_0$, is appropriate for the ISO-NE markets.

Through the ISO-NE study, we gain important insights into the system security and its economics in a multi-settlement environment. The multi-settlement, multiple-snapshot approach effectively captures the impacts of the DAM clearing on the market participant offer/bid surpluses. Furthermore, the price signals, provided by the multi-settlement system, encourage financial entity participation, which in turn leads not only to improvements in the overall market performance but also in the ability of the IGO to ensure near-real-time system

security.

7.5 Concluding Remarks

In this chapter, we present a set of applications of the proposed methodologies developed in this dissertation to various studies on the large-scale ISO-NE system and markets. These studies effectively illustrate the capabilities of the island detection scheme, multiple snapshot approach and its extension to the multi-settlement environment. The application of the island detection method study makes clear that it is a very useful tool to effectively deal with the complications in large-scale system separations due to its ability to rapidly detect islands formed and to identify the lines whose outages are the causal factors. The market performance quantification applications provide important insights into the implications of complying with a specified security criterion, as well as the prominent role of demand responsiveness and financial entity participation in electricity markets. Indeed, a key finding of the DAM comparative study is that the economic efficiency of electricity markets does not necessarily need to be adversely impacted under a tightened security criterion as long as there is effective price responsiveness. Such results are further corroborated by the multi-settlement environment studies. These studies, moreover, indicate that financial entity participation not only leads to convergence of the prices in the DAMs and their associated RTMs, but also improves near-real-time secure system operations.

CHAPTER 8

CONCLUSIONS

In this chapter, we summarize the work presented in this dissertation and discuss some problems that are logical extensions of the reported research results together with some possible directions for future research.

8.1 Summary

In this dissertation, we construct models for security assessment studies to develop practical methodologies to assess the security and to quantify the economics of secure power system operations. The modeling and scheme development work explicitly represents the impacts of the physical transmission network in describing the interactions between system operations and electricity markets. We present a set of applications to the large-scale ISO-NE of the schemes developed in this dissertation. These studies serve to illustrate the capabilities of the proposed approaches to determine practical solutions to a wide range of problems in the various applications. The chapters of this dissertation provide detailed descriptions of the models and each of the proposed approaches for the island detection scheme, multiple snapshot approach and its extension to the multi-settlement environment. In this section, we restate the key developments reported and the major findings in the illustrative studies presented.

Following the description of, the motivation for and the nature of the problems tackled in this dissertation, we discus in Chapter 2 the modeling aspects of the multiarea network in the

security analysis framework and the effective representation of the operational constraints for use in system security assessments. We develop appropriate models for evaluating the impacts of multiple line and cascading outages. A key contribution of this dissertation is the development of an analytic expression for the GLODFs, which we use to assess whether the postoutage flows violate any line flow limits under such conditions. Salient characteristics of the GLODFs include their analytic expressions in terms of the preoutage network parameters and the low computing requirements for their evaluation. We make extensive use of the GLODF-based models in the analysis of system security in the subsequent chapters.

The GLODFs play an important role in the construction of the combined graph-theoretic-algebraic approach to detect island formation in power system networks under multiple line outages. We develop such a scheme in Chapter 3 by marrying the connectivity characterization in graph theory with the algebraic expressions for the GLODFs. A noteworthy aspect of the approach is its computational efficiency due to its low computational requirements – a function simply of the number of outaged lines and not of the size of the system. The approach provides an effective tool for security assessment studies in both planning and operating environment. We apply the island detection method in Section 7.2 to investigate the impacts of multiple line outages on a part of the NPCC subnetwork corresponding to ISO-NE system. The study illustrates that the computationally efficient scheme is effective in the formulation of appropriate preventive/corrective control actions in multiple line outage cases that involve the *domino effect* of cascading outages.

We discuss in Chapter 4 the basic structure and modeling of the electricity markets. We use the models developed for security assessment in Chapter 2 and formulate the market-

system snapshot problem based on the emulation of the way the IGO currently operates the market and the grid. The market-system snapshot problem formulation uses the GLODF-based expressions to represent the constraints associated with multiple line outage contingency cases and takes into account the tight coupling between market and system operations. We use in Chapter 5 the market-system snapshot problem formulation and solution to construct the scheme for the quantification of the DAM performance under a specified security criterion. This quantification provides meaningful measures of the economics in terms of the auction surplus and the resource dispatch impacts on both a system and an area basis. We apply the snapshot quantification approach to evaluate the market performance impacts arising from the change from a given to a different security criterion. Our generalization of the single snapshot quantification to that of multiple snapshots provides the capability to evaluate the impacts of changing system and market conditions during a given period. We further extend the multiple snapshot approach to the multi-settlement environment in Chapter 6 in order to capture the interactions among the sequence of the markets − in particular, the DAMs and their associated RTMs. The representation of the multi-settlement environment is needed to allow the more realistic quantification of the market performance by including the effects of operational decisions on real-time markets. The set of schemes for single snapshot quantification and its generalization to multiple-snapshot approach as well as its extension to the multi-settlement environment, constitute significant contributions of this dissertation. These tools give the IGO, for the first time, the capability to quantify the economics of secure power system operations.

The multiple snapshot approach as well as its extension to the multi-settlement environment have a wide range of applications in regulatory studies, longer-term planning

and short-term operational studies. Additional applications include the justification by the IGO of a security criterion in economic terms and the cost/benefit analysis of network improvements to mitigate the market performance impacts of a set of specified contingencies.

The application studies on the ISO-NE DAMs and multi-settlement system in Sections 7.3 and 7.4, respectively, provide useful insights into the economics of secure power system operations. An important finding of the DAM studies is that the economic efficiency of electricity markets need not decrease when the power systems are operated under a stricter criterion when price responsive demand is present and appropriate control actions are effectively deployed. The multi-settlement system studies clearly indicate the prominent role of financial entities on market performance as well as in the assurance of real-time secure operations. A key finding of these studies is that the financial entity participation not only leads to DAM-RTM price convergence but also produces DAM dispatch outcomes that are "closer" to those of the RTMs.

The GLODF-based models for security assessment and the quantification approaches for measuring market performance as a function of the system security criterion constitute practical tools for the study of system security and its economic implications. The tools are highly appropriate for handling large-scale systems as evidenced by the useful results in the ISO-NE studies presented in this dissertation. These studies provide practical insights into the multifaceted problems that arise in the today's tightly coupled market and system operations.

8.2 Possible Future Research Directions

While the development of the models and the proposed approaches provide tools that heretofore did not exist, there are numerous modifications and/or enhancements that can be introduced to overcome certain identifiable shortcomings and to extend the capabilities of the analysis and the tools. These modifications/additions fall into two major areas: the incorporation of additional levels of detail into the models, and the construction of more comprehensive schemes through the integration of additional temporal and ancillary service markets.

We use a simplified representation of the power system in the approaches proposed and the approaches presented in this dissertation. The principal simplification stems from the use of the DC power flow representation with the losslessness assumption. This simplified model renders the approaches computationally tractable. However, the explicit representation of losses, reactive power support and voltage constraints, is important in the study of actual markets, especially those we refer to as real-time markets. The ability to incorporate these considerations requires a more detailed representation that is closer to the nonlinear AC power flow model. While, conceptually, the incorporation of AC models is relatively straightforward, the principal issue to resolve is the computational tractability of AC-power-flow-based models for large-scale system applications, particularly in the deployment of the multiple-snapshot approaches. The incorporation of more detailed models can provide tools with added capabilities for the more comprehensive investigation of the problems discussed in this dissertation. In addition, the cost/benefit analysis of reactive power support equipment investments and the investigation of their impacts on market performance can be carried out

with the quantification approach using AC-power-flow-based-models. However, serious efforts are required to develop numerically efficient algorithmic improvements in the solution approach to handle nonlinearities arising from the incorporation of AC models.

In the area for extension of GLODF work, we foresee limited scope for future developments. However, in the AC power flow representation of power system networks, a useful extension of GLODF work may entail the development of loss sensitivity factors under multiple line outages. Such sensitivity factors may be used to compute the impacts of multiple line outages on system losses without the need to re-solve AC power flows for the postoutage networks.

We included in this dissertation the consideration of the mutli-settlement environment that consists of the DAMs and their associated RTMs. However, for comprehensiveness, there is a need to include additional electricity markets – both of a temporal nature and also of the interrelated ancillary service type – and perform the necessary extensions to the multi-settlement multiple-snasphot approach we described in Chapter 6. The integration of the additional markets, such as year-, month- and hour-ahead markets, can provide the capability to account for the impacts of the security management in this more complex environment by explicitly representing the forward propogation of the security constraint enforcement through the intertemporal relationships in all the markets in the time sequence. The representation of additional markets adds to the realism of the multi-settlement analysis and the extended multi-setllement approach becomes a more useful tool. In addition to the representation of these energy commodity markets, the incorporation of the capacity- and the energy-based ancillary service markets is needed to provide the capability to perform a

detailed analysis of the actual multi-settlement system. In this way, the interrelationships between the energy commodity and the ancillary service markets are explicitly represented. The efforts to represent the additional markets and the extension of the multiple snapshot multi-settlement-system approach to models incorporating the more realistic and comprehensive multi-settlement environment are important developments to improve the tools' abilities to capture all the interrelationships between the markets.

We have so far limited the scope of our discussions to a purely deterministic setting. However, for longer-term planning as well as certain shorter-term operational studies, the explicit representation of uncertainty in the models and the incorporation into the proposed approaches can provide the ability to bring about better informed decisions. As the future holds multiple sources of uncertainty, from the availability of network components to the modifications in system topology, and from the nodal loads to each market participant's behavior, the development of models and approaches that appropriately capture such inherent uncertaintites constitutes an important extension. The growth in the use of renewable resources that have highly intermittent generation patterns results in additional complications for secure power system operations, particularly in the absence of major storage capability. The extension of the proposed quantification approaches to explicitly represent the uncertainty effects in the power system can provide tools that allow the evaluation of the expected economic costs of the secure power system operations.

In terms of risk management, there is yet another type of markets that of the financial transmission rights (FTR). The FTR markets are, essentially, orthogonal to the energy-only and ancillary services markets, and provide means to the holders to get reimbursement for the

congestion costs incurred to implement the transactions undertaken based on the energy-only markets. The added representation of the FTR markets provides capabilities to study the impacts of the interrelationships among all the markets. With the extended tool, it becomes possible to quantify the impacts of changing security criteria on the performance of the comprehensive set of interrelated markets. As we can effectively capture the interrelationships among the energy-only and the FTR markets, a very useful application study is to evaluate the economic impacts of the short-term transmission/unit outage scheduling decisions of the IGO on the value of a set of FTR products that span off- and on-peak hours. Such a study can provide useful insights into the impacts of system operational decisions on FTR markets and may be effective in developing better-informed outage scheduling approaches.

The suggested topics in this section provide some fruitful directions for future research in extending the current analysis and tools so as to develop additional capabilities for more comprehensive assessments.

APPENDIX A

PROOFS OF THE THEOREMS IN CHAPTER 3

A.1 Proof of Theorem 3.1

Theorem 3.1

Let $\mathcal{G} = (\mathcal{N}, \mathcal{L})$ be a connected power system network. The minimal cutset $\hat{\mathcal{L}}_{(\beta)} = \{\hat{\ell}_1, \cdots, \hat{\ell}_\beta\}$ partitions $\mathcal{G}$ into two subnetworks $\mathcal{G}_a = (\mathcal{N}_a, \mathcal{L}_a)$ and $\mathcal{G}_b = (\mathcal{N}_b, \mathcal{L}_b)$. Each line $\hat{\ell}_k = (\hat{i}_k, \hat{j}_k) \in \hat{\mathcal{L}}$ has $\hat{i}_k \in \mathcal{N}_a$ and $\hat{j}_k \in \mathcal{N}_b$. Then,

$$(i) \qquad \varphi_{\hat{\ell}_k}^{w(\hat{\ell}_m)} > 0 \qquad\qquad \hat{\ell}_m, \hat{\ell}_k \in \hat{\mathcal{L}} \qquad (A.1)$$

$$(ii) \qquad \sum_{\hat{\ell}_k \in \hat{\mathcal{L}}} \varphi_{\hat{\ell}_k}^{\{i,j,t\}} = \begin{cases} 1 & i \in \mathcal{N}_a, j \in \mathcal{N}_b \\ -1 & i \in \mathcal{N}_b, j \in \mathcal{N}_a \end{cases} \qquad (A.2)$$

$$(iii) \qquad \sum_{\hat{\ell}_k \in \hat{\mathcal{L}}} \varphi_{\hat{\ell}_k}^{\{i,j,t\}} = 0 \quad i, j \in \mathcal{N}_a \quad \text{or} \quad i, j \in \mathcal{N}_b. \qquad (A.3)$$

∎

Proof: We use an inductive approach to prove part (i). We first illustrate that the statement is true for a minimal cutset which has a single element. Consider the network in which $\beta - 1$ elements of the set $\hat{\mathcal{L}}_{(\beta)}$ are outaged. There are β possible outage permutations, which we denote by $\hat{\mathcal{L}}_{(\beta-1)}^j = \hat{\mathcal{L}}_{(\beta)} \setminus \{\hat{\ell}_j\}$, $j = 1, \cdots, \beta$. In each outaged network, $\{\hat{\ell}_j\} \notin \hat{\mathcal{L}}_{(\beta-1)}^j$ constitutes a minimal cutset, and from (5.4)

$$\left(\varphi_{\hat{\ell}_j}^{w(\hat{\ell}_k)}\right)^{\tilde{\mathcal{L}}_{(\beta-1)}^j} = 1, \quad \hat{\ell}_j \in \hat{\mathcal{L}}_{(\beta)}, \quad \hat{\ell}_k \in \hat{\mathcal{L}}_{(\beta)} \setminus \{\hat{\ell}_j\}. \tag{A.4}$$

Next, we assume that the statement is true for the minimal cutset constituted by a set of $\beta - 1$ elements, and prove its veracity for a set of β elements. Assume $\left(\varphi_{\hat{\ell}_j}^{w(\hat{\ell}_k)}\right)^{(\hat{\ell}_k)} > 0$ holds $j \neq k$, $\hat{\ell}_j, \hat{\ell}_k \in \hat{\mathcal{L}}_{(\beta)}$. By (A.4), we can state that

$$
\begin{aligned}
\left(\varphi_{\hat{\ell}_j}^{w(\hat{\ell}_k)}\right)^{(\hat{\ell}_k)} &= \varphi_{\tilde{\ell}_j}^{w(\hat{\ell}_k)} + \varsigma_{\tilde{\ell}_j}^{(\hat{\ell}_k)} \varphi_{\tilde{\ell}_k}^{w(\hat{\ell}_k)} \\
&= \varphi_{\tilde{\ell}_j}^{w(\hat{\ell}_k)} \left(1 + \frac{\varphi_{\tilde{\ell}_k}^{w(\hat{\ell}_k)}}{1 - \varphi_{\tilde{\ell}_k}^{w(\hat{\ell}_k)}}\right), \quad \hat{\ell}_j, \hat{\ell}_k \in \hat{\mathcal{L}}_{(\beta)}, \quad j \neq k.
\end{aligned}
\tag{A.5}
$$

It follows from (3.13) that $\varphi_{\tilde{\ell}_k}^{w(\tilde{\ell}_k)} > 0$, hence (A.5) implies that

$$\varphi_{\tilde{\ell}_j}^{w(\tilde{\ell}_k)} > 0, \quad \hat{\ell}_j, \hat{\ell}_k \in \hat{\mathcal{L}}_{(\beta)}, \quad j \neq k. \tag{A.6}$$

Since any transaction between the subnetworks $\mathcal{G}_a$ and $\mathcal{G}_b$ must flow over the minimal cutset elements, the proof of (ii) follows from the results in part (i) and (3.6).

For the proof of (iii), let $w^a = \{\hat{i}_m, \hat{i}_k, t\}$ be an intra-sub-network transaction in $\mathcal{N}_a$. For an inter-sub-network transaction $w' = \{\hat{i}_m, \hat{j}_k, t\}$, $\hat{j}_k \in \mathcal{N}_b$, from part (ii),

$$\sum_{\hat{\ell}_k \in \hat{\mathcal{L}}} \varphi_{\hat{\ell}_k}^{w'} = 1. \tag{A.7}$$

Similarly, for the inter-sub-network transaction $w'' = \{\hat{j}_k, \hat{i}_k, t\}$,

$$\sum_{\hat{\ell}_k \in \hat{\boldsymbol{\mathcal{L}}}} \varphi_{\hat{\ell}_k}^{w''} = -1. \tag{A.8}$$

Note that w^a is equivalent to the two transactions w' and w'' and due to linearity

$$\sum_{\hat{\ell}_k \in \hat{\boldsymbol{\mathcal{L}}}} \varphi_{\hat{\ell}_k}^{w^a} = \sum_{\hat{\ell}_k \in \hat{\boldsymbol{\mathcal{L}}}} \varphi_{\hat{\ell}_k}^{w'} + \sum_{\hat{\ell}_k \in \hat{\boldsymbol{\mathcal{L}}}} \varphi_{\hat{\ell}_k}^{w''} = 0. \tag{A.9}$$

A similar argument holds for an arbitrary intra-sub-network where terminal node pairs are in

$\mathcal{N}_b$.

∎

A.2 Proof of Theorem 3.2

Theorem 3.2

Let $\mathcal{G} = (\mathcal{N}, \mathcal{L})$ be a connected power system network. For a set of α outaged lines

$\tilde{\boldsymbol{\mathcal{L}}}_{(\alpha)} = \{\tilde{\ell}_1, \tilde{\ell}_2, \cdots, \tilde{\ell}_\alpha\}$:

$\underline{\boldsymbol{H}}_\alpha$ *is singular* ⟺ $\tilde{\boldsymbol{\mathcal{L}}}_{(\alpha)}$ *contains one or more minimal cutsets*

∎

Proof: We prove the necessary condition by contradiction. Let $\underline{\boldsymbol{H}}_\alpha$ be singular and assume

$\tilde{\boldsymbol{\mathcal{L}}}_{(\alpha)}$ does not contain a minimal cutset. We perform the Gaussian elimination on $\underline{\boldsymbol{H}}_\alpha$ and

compute, at step k, $k = 1, \cdots, \alpha$, $i = k, \cdots, \alpha$

$$h_{i,i}^{(k)} = h_{i,i}^{(k-1)} - \frac{h_{i,k-1}^{(k-1)}}{h_{k-1,k-1}^{(k-1)}} h_{k-1,i}^{(k-1)} = 1 - \left(\varphi_{\tilde{\ell}_i}^{w(\tilde{\ell}_i)} \right)^{\tilde{\mathcal{L}}_{(k-1)}}, \tag{A.10}$$

where we use the relation given in (A.4). The Gaussian elimination of the singular matrix $\underline{H}_\alpha$ results in a zero pivot at some elimination step $m \leq \alpha$ [96], which can only happen if $\left(\varphi_{\tilde{\ell}_m}^{w(\tilde{\ell}_m)} \right)^{\tilde{\mathcal{L}}_{(m-1)}} = 1$. By (3.3), $\{\tilde{\ell}_m\}$ constitutes a minimal cutset of the network in which the first $m-1$ lines of $\tilde{\mathcal{L}}_{(\alpha)}$ are outaged. Thus $\{\tilde{\ell}_1, \tilde{\ell}_2, \cdots, \tilde{\ell}_m\} \subseteq \tilde{\mathcal{L}}$ contains a minimal cutset, which is a contradiction of the original problem.

For the sufficiency condition, let $\hat{\mathcal{L}} \subseteq \tilde{\mathcal{L}}$ be a minimal cutset with $\hat{\mathcal{L}} = \tilde{\mathcal{L}}_{(m)} = \{\tilde{\ell}_1, \cdots, \tilde{\ell}_m\}$, $1 \leq m \leq \alpha$. We partition $\underline{H}_\alpha$:

$$\underline{H}_\alpha = \begin{bmatrix} \underline{H}_m & \underline{C} \\ \underline{B} & \underline{D} \end{bmatrix}. \tag{A.11}$$

Since $\underline{H}_\alpha$ satisfies (3.14), so does $\underline{H}_m$. We construct the diagonal $\underline{U} = diag\{u_1, \cdots, u_m\}$ with $u_i u_j = sign\{-h_{i,j}\}$, $|u_i| = 1$ and $i \neq j$. Thus, $u_i u_j h_{i,j} = -|h_{i,j}| = -\left| \varphi_{\tilde{\ell}_i}^{w(\tilde{\ell}_j)} \right| < 0$, $i, j = 1, \cdots, m$, $i \neq j$. The diagonal elements of $\underline{H}_m^\dagger = \underline{U} \underline{H}_m \underline{U}$ are given by $u_i^2 h_{i,i} = 1 - \varphi_{\tilde{\ell}_i}^{w(\tilde{\ell}_i)} > 0$. The algebraic sum of column j is

$$\sum_{i=1}^{m} u_i u_j h_{i,j} = -\sum_{i=1, i \neq j}^{m} \left| \varphi_{\tilde{\ell}_i}^{w(\tilde{\ell}_j)} \right| + 1 - \varphi_{\tilde{\ell}_j}^{w(\tilde{\ell}_j)} = -\sum_{i=1}^{m} \left| \varphi_{\tilde{\ell}_i}^{w(\tilde{\ell}_j)} \right| + 1 = 0, \tag{A.12}$$

and so $\left(\underline{1}^m \right)^T \underline{H}_m^\dagger = \left(\underline{0}^m \right)^T$. Also the components of $\underline{U} \underline{C}$ are given by $u_i h_{i,k}$,

147

$k = m+1, \cdots, \alpha \quad i = 1, \cdots, m$. Theorem 1 implies that $\sum_{i=1}^{m} u_i\, h_{i,k} = 0$ and so

$(\underline{\mathbf{1}}^m)^T \underline{U}\, \underline{C} = (\underline{\mathbf{0}}^m)^T$. Consider $\underline{H}_\alpha^\dagger = \tilde{\underline{U}}\, \underline{H}_\alpha\, \tilde{\underline{U}}$ with $\tilde{\underline{U}} = diag\{\underline{U}, \underline{I}^{\alpha-k}\}$. Then

$\tilde{\underline{v}}^T \underline{H}_\alpha^\dagger = (\underline{\mathbf{0}}^\alpha)^T$ for the vector $\tilde{\underline{v}} = \left[(\underline{\mathbf{1}}^m)^T \; (\underline{\mathbf{0}}^{\alpha-m})^T \right]^T$.

In words, we construct a vector $\tilde{\underline{v}} \neq \underline{\mathbf{0}}$ and $\tilde{\underline{v}} \in \mathfrak{N}\left(\underline{H}_\alpha^T\right)$. The rows of $\underline{H}_\alpha^\dagger$ form a

linearly dependent set, indicating that $\underline{H}_\alpha^\dagger$ is singular. Therefore, $\underline{H}_\alpha = \tilde{\underline{U}}^{-1} \underline{H}_\alpha^\dagger \tilde{\underline{U}}^{-1}$ is also

singular. Furthermore, $\underline{v} = \tilde{\underline{U}}^{-1} \tilde{\underline{v}} \neq \underline{\mathbf{0}}^\alpha$ and $\underline{v}^T \underline{H}_\alpha = (\underline{\mathbf{0}}^\alpha)^T$. Because

$|v_i| = \left| (u_i)^{-1} \tilde{v}_i \right| = |\tilde{v}_i|$, using the statement of $\underline{H}_\alpha$ gives

$$|v_i| = \begin{cases} 1, & \forall \tilde{\ell}_i \in \hat{\mathcal{L}} \\ 0, & \forall \tilde{\ell}_i \notin \hat{\mathcal{L}} \end{cases} . \tag{A.13}$$

∎

APPENDIX B

CHARACTERIZATION OF THE OPTIMAL SOLUTION OF THE $\mathcal{M}\left(\mathcal{S},\mathcal{B},\mathcal{W};\mathcal{C}\right)$ PROBLEM

We analyze the characteristics of the optimal solution of the $\mathcal{M}\left(\mathcal{S},\mathcal{B},\mathcal{W};\mathcal{C}\right)$ using the Lagrange multiplier theory. We associate Lagrange multipliers with the optimal solution of the programming problem of the $\mathcal{M}\left(\mathcal{S},\mathcal{B},\mathcal{W};\mathcal{C}\right)$ and interpret them in the context of the markets. We may rewrite the $\mathcal{M}\left(\mathcal{S},\mathcal{B},\mathcal{W};\mathcal{C}\right)$ problem as a minimization problem:

$$min\left\{-\mathcal{S}\right\} = -\sum_{k=1}^{K}\left(\sum_{b\in\mathcal{B}^{k}}\beta_{b}\left(p_{b}^{(0)}\right)-\sum_{s\in\mathcal{S}^{k}}\beta_{s}\left(p_{s}^{(0)}\right)\right)-\sum_{w\in\mathcal{W}}\alpha_{w}\left(t_{w}^{(0)}\right) \qquad (B.1)$$

subject to base case constraints

$$\sum_{b\in\mathcal{B}}p_{b}^{(0)}-\sum_{s\in\mathcal{S}}p_{s}^{(0)}=0 \qquad\qquad \leftrightarrow \lambda^{(0)} \qquad (B.2)$$

$$\underline{f}^{\,min^{(0)}} \le \underline{\Psi}^{(0)}\left(\underline{g}^{(0)}-\underline{d}^{(0)}\right) \le \underline{f}^{\,max^{(0)}} \qquad \leftrightarrow \underline{\mu}_{+}^{(0)},\underline{\mu}_{-}^{(0)} \qquad (B.3)$$

for every $j\in\mathcal{J}_{c}$

$$\sum_{b\in\mathcal{B}}p_{b}^{(j)}-\sum_{s\in\mathcal{S}}p_{s}^{(j)}=0 \qquad\qquad \leftrightarrow \lambda^{(j)} \qquad (B.4)$$

$$\underline{f}^{\,min^{(j)}} \le \underline{\Psi}^{(j)}\left(\underline{g}^{(j)}-\underline{d}^{(j)}\right) \le \underline{f}^{\,max^{(j)}} \qquad \leftrightarrow \underline{\mu}_{+}^{(j)},\underline{\mu}_{-}^{(j)} \qquad (B.5)$$

$$\Delta p_s^{min} \leq p_s^{(j)} - p_s^{(0)} \leq \Delta p_s^{max^{(j)}} \qquad\qquad \leftrightarrow \gamma_+^{(j)}, \gamma_-^{(j)}, \forall s \in \mathscr{S} \qquad\qquad \text{(B.6)}$$

$$\Delta p_b^{min} \leq p_b^{(j)} - p_b^{(0)} \leq \Delta p_b^{max^{(j)}} \qquad\qquad \leftrightarrow \rho_+^{(j)}, \rho_-^{(j)}, \forall b \in \mathscr{B} \qquad\qquad \text{(B.7)}$$

$$\Delta t_w^{min} \leq t_w^{(j)} - t_w^{(0)} \leq \Delta t_w^{max^{(j)}} \qquad\qquad \leftrightarrow \tau_+^{(j)}, \tau_-^{(j)}, \forall w \in \mathscr{W} \qquad\qquad \text{(B.8)}$$

and for every $j \in \{0\} \cup \mathscr{J}_e$

$$p_s^{min} \leq p_s^{(j)} \leq p_s^{max} \qquad\qquad \leftrightarrow \sigma_+^{(j)}, \sigma_-^{(j)}, \forall s \in \mathscr{S} \qquad\qquad \text{(B.9)}$$

$$p_b^{min} \leq p_b^{(j)} \leq p_b^{max} \qquad\qquad \leftrightarrow \kappa_+^{(j)}, \kappa_-^{(j)}, \forall b \in \mathscr{B} \qquad\qquad \text{(B.10)}$$

$$t_w^{min} \leq t_w^{(j)} \leq t_w^{max} \qquad\qquad \leftrightarrow \upsilon_+^{(j)}, \upsilon_-^{(j)}, \forall w \in \mathscr{W} \qquad . \qquad \text{(B.11)}$$

The Lagrange multipliers variables associated with the constraints (B.1)-(B.11) are given in the right-hand side of the respective constraint. We suppress the notation indicating the optimal solution and provide the Lagrangian of the $\mathcal{M}(\mathscr{S}, \mathscr{B}, \mathscr{W}; \mathcal{C})$ and indicate the cardinality of the set $\mathscr{J}_e$ by J:

$$\mathcal{L} = -\mathcal{S} + \sum_{j=0}^{J} \lambda^{(j)} \left(\sum_{b \in \mathscr{B}} p_b^{(j)} - \sum_{s \in \mathscr{S}} p_s^{(j)} \right)$$

$$+ \sum_{j=0}^{J} \left[\left(\boldsymbol{\mu}_+^{(j)} \right)^T \left(\underline{\boldsymbol{\Psi}}^{(j)} \left(\underline{\boldsymbol{g}}^{(j)} - \underline{\boldsymbol{d}}^{(j)} \right) - \underline{\boldsymbol{f}}^{max^{(j)}} \right) - \left(\boldsymbol{\mu}_-^{(j)} \right)^T \left(\underline{\boldsymbol{\Psi}}^{(j)} \left(\underline{\boldsymbol{g}}^{(j)} - \underline{\boldsymbol{d}}^{(j)} \right) - \underline{\boldsymbol{f}}^{min^{(j)}} \right) \right] \text{ (B.12)}$$

$$+ \sum_{j=1}^{J} \sum_{s \in \mathscr{S}} \left[\gamma_+^{(j)} \left(p_s^{(j)} - p_s^{(0)} - \Delta p_s^{max^{(j)}} \right) - \gamma_-^{(j)} \left(p_s^{(j)} - p_s^{(0)} - \Delta p_s^{min^{(j)}} \right) \right]$$

$$+\sum_{j=1}^{J}\sum_{b\in\mathcal{B}}\left[\rho_{+}^{(j)}\left(p_{b}^{(j)}-p_{b}^{(0)}-\Delta p_{b}^{max(j)}\right)\ -\ \rho_{-}^{(j)}\left(p_{b}^{(j)}-p_{b}^{(0)}-\Delta p_{b}^{min(j)}\right)\right]$$

$$+\sum_{j=1}^{J}\sum_{w\in\mathcal{W}}\left[\tau_{+}^{(j)}\left(t_{w}^{(j)}-t_{w}^{(0)}-\Delta t_{w}^{max(j)}\right)\ -\ \tau_{-}^{(j)}\left(t_{w}^{(j)}-t_{w}^{(0)}-\Delta t_{w}^{min(j)}\right)\right]$$

$$+\sum_{j=1}^{J}\sum_{s\in\mathcal{S}}\left[\sigma_{+}^{(j)}\left(p_{s}^{(j)}-p_{s}^{max}\right)\ -\ \sigma_{-}^{(j)}\left(p_{s}^{(j)}-p_{s}^{min}\right)\right] \tag{B.12}$$

$$+\sum_{j=1}^{J}\sum_{b\in\mathcal{B}}\left[\kappa_{+}^{(j)}\left(p_{b}^{(j)}-p_{b}^{max}\right)\ -\ \kappa_{-}^{(j)}\left(p_{b}^{(j)}-p_{b}^{min}\right)\right]$$

$$+\sum_{j=1}^{J}\sum_{w\in\mathcal{W}}\left[\upsilon_{+}^{(j)}\left(t_{w}^{(j)}-t_{w}^{max}\right)\ -\ \upsilon_{-}^{(j)}\left(t_{w}^{(j)}-t_{w}^{min}\right)\right] \qquad .$$

The Kuhn-Tucker conditions for the base case of this problem are

$$\frac{\partial \mathcal{L}}{\partial p_{s}^{(0)}}=-\frac{\partial \mathcal{S}}{\partial p_{s}^{(0)}}+\left[\lambda^{(0)}+\left(\underline{\mu}_{+}^{(0)}-\underline{\mu}_{-}^{(0)}\right)^{T}\underline{\psi}_{i}^{(0)}+\sigma_{+}^{(0)}-\sigma_{+}^{(0)}\right]-\sum_{j=1}^{J}\left[\gamma_{+}^{(j)}-\gamma_{-}^{(j)}\right]=0 \tag{B.13}$$

for a seller s at node i,

$$\frac{\partial \mathcal{L}}{\partial p_{b}^{(0)}}=-\frac{\partial \mathcal{S}}{\partial p_{b}^{(0)}}+\left[\lambda^{(0)}+\left(\underline{\mu}_{+}^{(0)}-\underline{\mu}_{-}^{(0)}\right)^{T}\underline{\psi}_{i}^{(0)}+\kappa_{+}^{(0)}-\kappa_{+}^{(0)}\right]-\sum_{j=1}^{J}\left[\rho_{+}^{(j)}-\rho_{-}^{(j)}\right]=0 \tag{B.14}$$

for a buyer b at node i, and

$$\frac{\partial \mathcal{L}}{\partial t_{w}^{(0)}}=-\frac{\partial \mathcal{S}}{\partial t_{w}^{(0)}}+\left[\left(\underline{\mu}_{+}^{(0)}-\underline{\mu}_{-}^{(0)}\right)^{T}\left(\underline{\psi}_{m_{w}}^{(0)}-\underline{\psi}_{n_{w}}^{(0)}\right)+\upsilon_{+}^{(0)}-\upsilon_{+}^{(0)}\right]-\sum_{j=1}^{J}\left[\tau_{+}^{(j)}-\tau_{-}^{(j)}\right]=0 \tag{B.15}$$

for a transaction $\omega_{w}=\{m_{w},n_{w},\bar{t}_{w}\}$.

For the contingency case $j\in\mathcal{J}_{c}$, the Kuhn-Tucker conditions are

$$\frac{\partial \mathcal{L}}{\partial p_s^{(j)}} = \left[\lambda^{(j)} + \left(\underline{\mu}_+ - \underline{\mu}_- \right)^T \underline{\psi}_i^{(j)} + \gamma_-^{(j)} - \gamma_+^{(j)} + \sigma_+^{(j)} - \sigma_-^{(j)} \right] = 0 \qquad \text{(B.16)}$$

for a seller s at node i,

$$\frac{\partial \mathcal{L}}{\partial p_b^{(j)}} = \left[-\lambda^{(j)} - \left(\underline{\mu}_+ - \underline{\mu}_- \right)^T \underline{\psi}_i^{(j)} + \rho_-^{(j)} - \rho_+^{(j)} + \kappa_+^{(j)} - \kappa_-^{(j)} \right] = 0 \qquad \text{(B.17)}$$

for a buyer b at node i, and

$$\frac{\partial \mathcal{L}}{\partial t_w^{(j)}} = \left[\left(\underline{\mu}_+ - \underline{\mu}_- \right)^T \left(\underline{\psi}_{m_w}^{(j)} - \underline{\psi}_{n_w}^{(j)} \right) + \tau_-^{(j)} - \tau_+^{(j)} + \upsilon_+^{(j)} - \upsilon_-^{(j)} \right] = 0 \qquad \text{(B.18)}$$

for a transaction $\omega_w = \{m_w, n_w, \bar{t}_w\}$.

Furthermore, the complementarity-slackness condition imply

$$\sum_{b \in \mathcal{B}} p_b^{(j)} - \sum_{s \in \mathcal{S}} p_s^{(j)} = 0 , \ \forall j \in \{0\} \cup \mathcal{J}_e \qquad \text{(B.19)}$$

$$\left(\underline{\mu}_+^{(j)} \right)^T \left(\underline{\Psi}^{(j)} \left(\underline{g}^{(j)} - \underline{d}^{(j)} \right) - \underline{f}^{max^{(j)}} \right) = 0 , \ \forall j \in \{0\} \cup \mathcal{J}_e \qquad \text{(B.20)}$$

$$\left(\underline{\mu}_-^{(j)} \right)^T \left(\underline{\Psi}^{(j)} \left(\underline{g}^{(j)} - \underline{d}^{(j)} \right) - \underline{f}^{min^{(j)}} \right) = 0 , \ \forall j \in \{0\} \cup \mathcal{J}_e \qquad \text{(B.21)}$$

$$\sigma_+^{(j)} \left(p_s^{(j)} - p_s^{max} \right) = 0 , \ \forall s \in \mathcal{S} \qquad \text{(B.22)}$$

$$\sigma_-^{(j)} \left(p_s^{(j)} - p_s^{min} \right) = 0 , \ \forall s \in \mathcal{S} \qquad \text{(B.23)}$$

$$\kappa_+^{(j)} \left(p_b^{(j)} - p_b^{max} \right) = 0 , \ \forall b \in \mathcal{B} \qquad \text{(B.24)}$$

$$\kappa_-^{(j)}\left(p_b^{(j)} - p_b^{min}\right) = 0, \ \forall b \in \mathcal{B} \tag{B.25}$$

$$\upsilon_+^{(j)}\left(t_w^{(j)} - t_w^{max}\right) = 0, \forall w \in \mathcal{W} \tag{B.26}$$

$$\upsilon_-^{(j)}\left(t_w^{(j)} - t_w^{min}\right) = 0, \ \forall w \in \mathcal{W} \tag{B.27}$$

$$\gamma_+^{(j)}\left(p_s^{(j)} - p_s^{(0)} - \Delta p_s^{max^{(j)}}\right) = 0, \ \forall s \in \mathcal{S}, \forall j \in \mathcal{J}_e \tag{B.28}$$

$$\gamma_-^{(j)}\left(p_s^{(j)} - p_s^{(0)} - \Delta p_s^{min^{(j)}}\right) = 0, \ \forall s \in \mathcal{S}, \forall j \in \mathcal{J}_e \tag{B.29}$$

$$\rho_+^{(j)}\left(p_b^{(j)} - p_b^{(0)} - \Delta p_b^{max^{(j)}}\right) = 0, \ \forall b \in \mathcal{B}, \forall j \in \mathcal{J}_e \tag{B.30}$$

$$\rho_-^{(j)}\left(p_b^{(j)} - p_b^{(0)} - \Delta p_b^{min^{(j)}}\right) = 0, \ \forall b \in \mathcal{B}, \forall j \in \mathcal{J}_e \tag{B.31}$$

$$\tau_+^{(j)}\left(t_w^{(j)} - t_w^{(0)} - \Delta t_w^{max^{(j)}}\right) = 0, \ \forall w \in \mathcal{W}, \forall j \in \mathcal{J}_e \tag{B.32}$$

$$\tau_-^{(j)}\left(t_w^{(j)} - t_w^{(0)} - \Delta t_w^{min^{(j)}}\right) = 0, \ \forall w \in \mathcal{W}, \forall j \in \mathcal{J}_e \tag{B.33}$$

The LMP λ_i at node i is given by

$$\lambda_i = -\frac{\partial \mathcal{S}}{\partial p_b^{(0)}} \ . \tag{B.34}$$

where buyer b is at node i. We assume that $\kappa_+^{(j)} = \kappa_+^{(j)} = 0$, so from (B.14)

$$\lambda_i = \left[\lambda^{(0)} + \left(\underline{\mu}_+^{(0)} - \underline{\mu}_-^{(0)} \right)^T \underline{\psi}_i^{(0)} \right] + \sum_{j=1}^{J} \left[\rho_+^{(j)} - \rho_-^{(j)} \right]. \tag{B.35}$$

Since from (B.17)

$$\rho_+^{(j)} - \rho_-^{(j)} = \lambda^{(j)} + \left(\underline{\mu}_+ - \underline{\mu}_- \right)^T \underline{\psi}_i^{(j)} \tag{B.36}$$

holds, then

$$\lambda_i = \left[\lambda^{(0)} + \left(\underline{\mu}_+^{(0)} - \underline{\mu}_-^{(0)} \right)^T \underline{\psi}_i^{(0)} \right] + \sum_{j=1}^{J} \left[\lambda^{(j)} + \left(\underline{\mu}_+^{(j)} - \underline{\mu}_-^{(j)} \right)^T \underline{\psi}_i^{(j)} \right]. \tag{B.37}$$

REFERENCES

[1] FERC, "Remedying undue discrimination through open access transmission service and standard electricity market design," Docket No: RM01-12-000, Jan. 2003.

[2] The Electric Energy Market Competition Task Force, "Report to Congress on competition in the wholesale and retail markets for electric energy," Docket No: AD05-17-000, May 2006.

[3] T. E. Dy Liacco, "The adaptive reliability control system," *IEEE Transactions on Power Apparatus and Systems*, vol. PAS-86, pp. 517-531, May 1967.

[4] F. D. Galiana, A. L. Motto, and F. Bouffard, "Reconciling social welfare, agent profits, and consumer payments in electricity pools," *IEEE Transactions on Power Systems*, vol. 18, pp. 452-459, May 2003.

[5] J. Bulow, J. Levin, and P. Milgrom, "Winning play in spectrum auction," NBER Working Paper No. 14765, issued in Mar. 2009, [Online]. Available: http://www.nber.org/papers/w14765.

[6] P. Klemperer, *Auctions: Theory and Practice*. Princeton, NJ: Princeton University Press, 2004.

[7] P. I. Caro-Ochoa, "Evaluation of transmission congestion impacts on electricity markets," M.S. thesis, University of Illinois at Urbana-Champaign, 2003.

[8] ISO-NE, "The multi-settlement system," Aug. 2006. [Online]. Available: http://www.iso-ne.com/ nwsiss/grid_mkts /how_mkts_wrk /multi_settle/index.html.

[9] D. S. Kirschen and G. Strbac, *Fundamentals of Power System Economics*. New York, NY: John Wiley & Sons Ltd., 2004.

[10] J. Endrenyi, *Reliability Modeling in Electric Power Systems*. New York, NY: John Wiley & Sons, 1978.

[11] R. L. Sullivan, *Power System Planning*. New York, NY: McGraw-Hill, 1977.

[12] Power Systems Engineering Committee, "Reliability indices for use in bulk power supply adequacy evaluation," *IEEE Transactions on Power Apparatus and Systems*, vol. 97, pp. 1097-1103, July 1978.

[13] D. S. Kirschen, "Power system security," *Power Engineer*, vol. 16, pp. 241-248, Oct. 2002.

[14] U. G. Knight, *Power Systems in Emergencies: From Contingency Planning to Crisis Management*. England: John Wiley & Sons, 2000.

[15]   NERC, "Reliability standards," Jan. 2003. [Online]. Available: http://www.nerc.com /~filez/standards/Reliability_Standards.html.

[16]   K. Morison, "Power system security in the new market environment: Future directions," in *Proceedings IEEE PES Summer Meeting,* July 2000, pp. 1416-1417.

[17]   C. W. Taylor, "The future in on-line security assessment and wide area stability control," in *Proceedings IEEE PES Winter Meeting,* Jan. 2000, pp. 78-83.

[18]   A. Wood and B. Wollenberg, *Power Generation Operation and Control*, 2nd ed. New York, NY: John Wiley & Sons, 1996.

[19]   W. F. Tinney, V. Brandwajn, and S. M. Chan, "Sparse vector methods," *IEEE Transactions on Power Apparatus and Systems*, vol. 104, pp. 295-301, Feb. 1985.

[20]   A. Monticelli, *State Estimation in Electric Power System: A Generalized Approach*. Boston, MA: Kluwer Academic Publishers, 1999.

[21]   W. Y. Ng, "Generalized generation distribution factors for power system security evaluation," *IEEE Transactions on Power Apparatus and Systems*, vol. 100, pp. 1001-1005, Mar. 1981.

[22]   P. W. Sauer, "On the formulation of power distribution factors for linear load flow methods," *IEEE Transactions on Power Apparatus and Systems*, vol. 100, pp. 764-770, Feb. 1981.

[23]   P. W. Sauer, K. E. Reinhard, and T. J. Overbye, "Extended factors for linear contingency analysis," in *Proceedings of the 34th Annual Hawaii International Conference on System Sciences*, Hawaii, Jan. 2001, pp. 697-703.

[24]   M. Liu and G. Gross, "Effectiveness of the distribution factor approximations used in congestion modeling," in *Proceedings of the 14th Power Systems Computation Conference*, Seville, Spain, June 2002, pp. 802-810.

[25]   R. Baldick, "Variation of distribution factors with loading," *IEEE Transactions on Power Systems*, vol. 18, pp. 1316-1323, Nov. 2003.

[26]   M. Liu and G. Gross, "Role of distribution factors in congestion revenue rights applications," *IEEE Transactions on Power Systems*, vol. 19, pp. 802-810, May 2004.

[27]   S. Suryanarayanan, G. T. Heydt, R. G. Farmer, and S. Chakka, "An estimation technique to assign contribution factors for loop flows in an interconnected power system," *Electric Power Components and Systems*, vol. 32, pp. 813-826, Aug. 2004.

[28]   M. D. Ilic, Y. T. Yoon, and A. Zobian, "Available transmission capacity (ATC) and its value under open access," *IEEE Transactions on Power Systems*, vol. 12, pp. 636-645, May 1997.

[29]   NERC, "Available transfer capability definitions and determination," Sep. 2003 [Online]. Available: ftp://ftp.nerc.com/pub/sys/allupdl/docs/pubs/atcfinal.pdf.

[30]   S. Grijalva, P. W. Sauer, and J. D. Weber, "Enhancement of linear ATC calculations by the incorporation of reactive power flows," *IEEE Transactions on Power Systems*, vol. 18, pp. 619-624, May 2003.

[31]   T. J. Overbye, X. Cheng, and Y. Sun, "A comparison of the AC and DC power flow models for LMP calculations," in *Proceedings of the 37th Annual Hawaii International Conference on System Sciences*, Hawaii, Jan. 2004, pp. 1-9.

[32]   M. Montagna and G. P. Granelli, "Detecting of Jacobian singularity and network islanding in power flow computations," *IEE Proceedings Generation Transmission and Distribution*, vol. 142, pp. 589-594, Nov. 1995.

[33]   B. Stott, O. Alsaç, and A. J. Monticelli, "Security analysis and optimization," *IEEE Proceedings*, vol. 75, pp.1623-1644, Dec. 1987.

[34]   M. Begovic, D. Novosel, D. Karlsson, C. Henville, and G. Michel, "Wide-area protection and emergency control," *IEEE Proceedings*, vol. 93, pp. 876-891, May 2005.

[35]   A. S. Meliopoulos, S. C. Cheng and F. Xia, "Performance evaluation of static security analysis methods," *IEEE Transactions on Power System*, vol. 9, pp. 1441-1449, Aug. 1994.

[36]   O. Alsaç, J. Bright, M. Prais, and B. Stott, "Further developments in LP-based optimal power flow," *IEEE Transactions on Power System*, vol. 5, pp. 697-711, Aug. 1990.

[37]   N. Amjady and M. Esmaili, "Application of a new sensitivity analysis framework for voltage contingency ranking," *IEEE Transactions on Power Systems*, vol. 20, pp. 973-983, May 2005.

[38]   A. M. Sasson, S. T. Ehrmann, P. Lynch, and L. S. VanSlyck, "Automatic power system network topology determination," *IEEE Transactions on Power Apparatus and Systems*, vol. PAS-92, pp. 610-618, Mar. 1973.

[39]   T. E. Dy Liacco and T. J. Kraynak, "Processing by logic programming of circuit-breaker and protective-relaying information," *IEEE Transactions Power Apparatus and Systems*, vol. PAS-88, pp. 171-175, Feb. 1969.

[40]   F. Goderya, A. A. Metwally, and O. Mansour, "Fast detection and identification of islands in power Networks," *IEEE Transactions on Power Apparatus and Systems*, vol. PAS-99, pp. 217-221, Feb. 1980.

[41]   V. Donde, V. Lopez, B. Lesieutre, A. Pinar, C. Yang, and J. Meza, "Identification of severe multiple contingencies in electric power networks," in *Proceedings of the North American Power Conference*, Ames, IA, Oct. 2005, pp. 59-66.

[42]   J. Thorp and H. Wang, "Computer simulation of cascading disturbances in electric power systems," PSERC, Tempe, AZ, Publication 01-01, May 2001. [Online]. Available: http://www.pserc.wisc.edu/ecow/get/publicatio/reports/2001report/Thorp FinalReport.pdf.

[43]   M. Bertran and X. Corbella, "On the validation and analysis of a new method for power network connectivity determination," *IEEE Transactions on Power Apparatus and Systems*, vol. PAS-101, pp. 316-324, Feb. 1982.

[44]   M. S. Tsai, "Development of islanding early warning mechanism for power systems," in *Proceedings of the IEEE PES Summer Meeting*, July 2000, vol. 1, pp. 22-26.

[45]   N. Deo, *Graph Theory with Applications to Engineering and Computer Science*. Englewood, NJ: Prentice-Hall, 1974.

[46]   R. Karp and R. Tarjan, "Linear expected time for connectivity problems," *Journal of Algorithms*, vol. 1, pp. 274-393, Sep. 1980.

[47]   H. Varian, *Intermediate Microeconomics: A Modern Approach*, 2nd ed. New York, NY: W. W. Norton & Company, 1990.

[48]   F. Schweppe, M. Caramanis, R. Tabors, and R. Bohn, *Spot Pricing of Electricity*. Boston, MA: Kluwer Academic Publishers, 1988.

[49]   R. Wilson, "Architecture of power markets," *Econometrica*, vol. 70, pp. 1299-1340, July 2002.

[50]   W. Hogan, "Contract networks for electric power transmission," *Journal of Regulatory Economics*, vol. 4, pp. 211-242, Sep. 1992.

[51]   H. Chao and S. Peck, "A market mechanism for electric power transmission," *Journal of Regulatory Economics*, vol. 10, pp. 25-59, July 1996.

[52]   S. Stoft, *Power System Economics: Designing Markets for Electricity*. New York, NY: Wiley-IEEE Press, 2002.

[53]   P. L. Joskow and J. Tirole, "Transmission rights and market power on electric power networks," *RAND Journal of Economics*, vol. 31, pp. 450-487, Sep. 2000.

[54]   E. Bompard, P. Correia, G. Gross, and M. Amelin, "Congestion-management schemes: A comparative analysis under a unified framework," *IEEE Transactions on Power Systems*, vol. 18, pp. 346-352, Feb. 2003.

[55] H. P. A. Knops, L. J. deVries, and R. A. Hakvoort, "Congestion management in the European electricity systems: An evaluation of the alternatives," *Journal of Network Industry*, vol. 2, pp. 311-351, 2001.

[56] H. Singh, H. Shangyou, and A. Papalexopoulos, "Transmission congestion management in competitive electricity markets," *IEEE Transactions on Power Systems*, vol. 13, pp. 672-680, May 1998.

[57] Y. T. Yoon, J. R. Arce, K. K. Collison, and M. D. Ilic, "Implementation of cluster-based congestion management systems," Energy Laboratory, Massachusetts Institute of Technology, May 2002. [Online]. Available: http://lfee.mit.edu /publications/PDF/el00-001wp.pdf.

[58] J. L. Seelke, "Flow-based pricing of inter-regional power transfers," *The Electricity Journal*, vol. 16, pp. 47-54, Jan. 2003.

[59] A. Kumar, S. C. Srivastava, and S. N. Singh, "A zonal congestion management approach using real and reactive power rescheduling," *IEEE Transactions on Power Systems*, vol. 19, pp. 554-562, Feb. 2004.

[60] P. Gribik, G. A. Angelidis, and R. R. Kovacs, "Transmission access and pricing with multiple separate energy forward markets," *IEEE Transactions on Power Systems*, vol. 14, pp. 865-876, Aug. 1999.

[61] F. A. Wolak and R. H. Patrick, "The impact of market rules and market structure on the price determination process in the England and Wales electricity market," University of California Energy Institute, Berkeley, CA. POWER Report PWP-047, Feb. 1997. [Online]. Available: http://www.nber.org /papers /w8248.pdf.

[62] R. Rajaraman and F. L. Alvarado, "Inefficiencies of NERC's transmission loading relief procedure," *The Electricity Journal*, pp. 47-54, Oct. 1998.

[63] R. D. Christie, B. F. Wollenberg and I. Wangensteen, "Transmission management in the deregulated environment," *IEEE Proceedings*, vol. 88, pp. 170-195, Feb. 2000.

[64] T. Alvey, D. Goodwin, X. Ma, D. Streiffert and D. Sun, "A security-constrained bid-clearing system for the New Zealand wholesale electricity market," *IEEE Transactions on Power Systems*, vol. 13, pp. 340-346, May 1998.

[65] A. L. Motto, F. D. Galiana, A. J. Conejo, and J. M. Arroyo, "Network-constrained multiperiod auction for a pool-based electricity market," *IEEE Transactions on Power Systems*, vol. 17, pp. 646-653, Aug. 2002.

[66] M. Liu and G. Gross, "Congestion rents and FTR evaluations in mixed pool-bilateral systems," *International Journal of Electrical Power and Energy Systems*, vol. 30, pp. 447-454, Oct. 2008.

[67] A. L. Ott, "Experience with PJM market operation, system design and implementation," *IEEE Transactions on Power Systems*, vol. 18, pp. 528-534, May 2003.

[68] W. Hogan, "Getting the prices right in PJM: What the data teaches us," *The Electricity Journal*, vol. 11, pp. 61-67, Aug. 1998.

[69] R. Green and D. M. Newbery, "Competition in the British electric spot market," *Journal of Political Economy*, vol. 100, pp. 929-953, Oct. 1992.

[70] C. D. Wolfram, "Strategic bidding in a multi-unit auction: an empirical analysis of bids to supply electricity in England and Wales," *Rand Journal of Economics*, vol. 29, pp. 703-725, Jan. 1998.

[71] E. T. Mansur, "Pricing behavior in the initial summer of the restructured PJM wholesale electricity market," University of California Energy Institute, Berkeley, CA, Paper 083, Apr. 2001.

[72] S. Borenstein, J. B. Bushnell, and F. A. Wolak, "Measuring market inefficiencies in California's restructured wholesale electricity market," *The American Economic Review*, vol. 92, pp. 1376-1405, Dec. 2002.

[73] S. de la Torre, A. J. Conejo, and J. Contreras, "Simulating olIGOpolistic pool-based electricity markets: A multi-period approach," *IEEE Transactions on Power Systems*, vol. 18, pp. 1547-1555, Nov. 2003.

[74] R. Baldick, R. Grant, and E. Kahn, "Theory and application of linear supply function equilibrium in electricity markets," *Journal of Regulatory Economics*, vol. 25, pp. 143-167, Mar. 2004.

[75] F. Longsta and A. Wang, "Electricity forward prices: A high-frequency empirical analysis," *Journal of Finance*, vol. 59, pp. 1877-1900, Aug. 2004.

[76] R. J. Kaye, F. F.Wu and P. Varaiya, "Pricing for system security," *IEEE Transactions on Power Systems*, vol. 10, pp. 575-583, May 1995.

[77] H. Singh and A. D. Papalexopoulos, "Competitive procurement of ancillary services by an independent system operator," *IEEE Transactions on Power Systems*, vol. 14, pp. 498-504, May 1999.

[78] W. Tong, M. Rothleder, Z. Alaywan, and A. D. Papalexopoulos, "Pricing energy and ancillary services in integrated market systems by an optimal power flow," *IEEE Transactions on Power Systems*, vol. 19, pp. 339-347, Feb. 2004.

[79] J. M. Arroyo and F. D. Galiana, "Energy and reserve pricing in security and network-constrained electricity markets," *IEEE Transactions on Power Systems*, vol. 20, pp. 634-643, May 2005.

[80] S. Grijalva and A. M. Visnesky, "The effect of generation on network security: Spatial representation, metrics and policy" *IEEE Transactions on Power Systems*, vol. 21, pp. 1388-1395, Aug. 2006.

[81] F. Alvarado, Y. Hu, D. Ray, R. Stevenson, and E. Cashman, "Engineering foundations for the determination of security costs," *IEEE Transactions on Power Systems*, vol. 6, pp. 1175-1182, Aug. 1991.

[82] D. S. Kirchen, K. R. W. Bell, D. P. Nedic, D. Jayaweera, and R. N. Allan, "Computing the value of security," *IEE Proceedings of Generation, Transmission and Distribution*, vol. 150, pp. 673-678, Nov. 2003.

[83] G. Strbac, S. Ahmed, D. Kirschen, and R. Allan, "A method for computing the value of corrective security," *IEEE Transactions on Power Systems*, vol. 13, pp. 1096-1102, Aug. 1998.

[84] S. Burns and G. Gross, "Value of service reliability," *IEEE Transactions on Power Systems*, vol. 5, pp. 825-834, May 1990.

[85] P. Nitu and G. Gross, "Evaluation of reliability in power system operational planning," in *Proceeding Power System Computation Conference*, pp. 355-362, 1993.

[86] X. Ma and D. Sun, "Key elements of a successful market design," in *Proceedings of the IEEE PES Transmission Distribution and Exhibition*.: Asia and Pacific, Dalian, China, Dec. 2005, pp. 1-6.

[87] R. Kamat and S. S. Oren, "Multi-settlement systems for electricity markets: Zonal aggregation under network uncertainty and market power," in *Proceedings of the 35th Annual Hawaii International Conference on System Sciences*, Hawaii, Jan. 2002, pp. 739-748.

[88] R. Kamat and S. S. Oren, "Two-settlement systems for electricity markets under network uncertainty and market power," *Journal of Regulatory Economics*, vol. 25, pp. 5-37, Jan. 2004.

[89] I. Arciniegas, C. Barrett, and A. Marathe, "Assessing the efficiency of US electricity markets," *Utilities Policy*, vol. 11, pp. 75-86, Jan. 2003.

[90] S. Borenstein, J. Bushnell, C. R. Knittel, and C. Wolfram, "Inefficiencies and market power in financial arbitrage: A study of California's electricity markets," University of California Energy Institute, Berkeley, CA, Paper 138, 2004.

[91] ISO-NE, "Impact of Virtual Transactions on New England's Energy Market", Nov. 2004. [Online]. Available: www.iso-ne.com/pub/spcl_rpts/2004/virtual_transactions_ report .pdf.

[92] C. Saravia, "Speculative trading and market performance: the effect of arbitrageurs on efficiency and market power in the New York electricity market," University of California Energy Institute, Berkeley, California, Paper -121, 2003.

[93]   A. Isomenger, "The benefits and risks of virtual bidding in multi-settlement markets," *The Electricity Journal*, vol. 19, pp. 26-36, Nov. 2006.

[94]   G. H. Golub and C. F. Van Loan, *Matrix Computations*. Baltimore, MA: The John Hopkins University Press, 1989.

[95]   C. H. Bischof and G. Quintana-Orti, "Computing rank-revealing QR factorizations of dense matrices," *ACM Transactions on Mathematical Software*, vol. 24, pp. 226-253, June 1998.

[96]   Y. P. Hong and C. T. Pan, "Rank-revealing QR factorizations and the singular value decomposition," *Mathematics of Computation,* vol. 58, pp. 213-232, Jan. 1992.

[97]   http://www.iso-ne.com.

[98]   http://www.pjm.com.

[99]   http://www.nyiso.com.

[100]   ISO-NE, "Operating reserves white paper," June 2006. [Online]. Available: http://www.iso-ne.com/pubs/whtpprs/operating_reserves_white_paper.pdf.

AUTHOR'S BIOGRAPHY

Teoman Guler was born in Samsun, Turkey, on November 14, 1976. He received his bachelor of science degree in electrical and electronics engineering for Bogazici University in July 1999 and master of science degree in electric power engineering from Rensselaer Polytechnic Institute in June 2001. He was a research assistant at the University of Illinois at Urbana-Champaign from January 2003 through May 2007. His research interests include analysis, operations and control of power systems and electricity markets. He is a member of the Institute of Electrical and Electronics Engineers.